Novel dual setting approaches for mechanically reinforced mineral biocements

Dissertation zur Erlangung des naturwissenschaftlichen Doktorgrades der

Julius-Maximilians-Universität Würzburg

vorgelegt von

Dipl.-Ing. Martha Schamel geb. Geffers

aus Chemnitz

Würzburg 2016

Eingereicht bei der Fakultät für Chemie und Pharmazie am

01.07.2016

Gutachter der schriftlichen Arbeit

1. Gutachter: Prof. Dr. rer. nat. Jürgen Groll

2. Gutachter: Prof. Dr. rer. nat. Matthias Lehmann

Prüfer des öffentlichen Promotionskolloquiums

1. Prüfer : Prof. Dr. rer. nat. Jürgen Groll

2. Prüfer : Prof. Dr. rer. nat. Matthias Lehmann

3. Prüfer : Prof. Dr. rer. nat. Uwe Gbureck

Datum des öffentlichen Promotionskolloquiums

Doktorurkunde ausgehändigt am

“The whole is greater than the sum of its parts”

- Aristotle

Summary

Calcium phosphate biocements are inherently brittle materials due to their ceramic nature. Hence, currently applied cement formulations are only indicated for non-load bearing application sites. An approach to reduce cement brittleness is based on the use of cement – polymer composites, which combine the flexibility of a polymeric phase with the hardness and compression strength of a cement matrix. Here, a relatively new strategy is the use of “dual-setting” cements, in which the polymeric phase is simultaneously build up from monomers or prepolymers during cement setting. This approach largely maintains basic properties of the fresh paste such as rheology or setting time. Previous works on such dual setting cements were dealing with a radical polymerization reaction to create the polymeric network. This type of reaction requires the addition of a suitable initiator system (e.g. a tertiary amine in conjunction with ammonium peroxosulfate), which are often cytotoxic and may interfere with the cement setting conditions. The current thesis dealt with alternative strategies, in which the cross-linking and gelation of the second (polymeric or inorganic) cement phase is initiated by the chemical conditions of the setting reaction such that no additional initiator has to be added to the cement paste.

In a first approach a six armed star molecule functionalized with isocyanate groups as reactive termini (NCO–sP(EO-*stat*-PO)) was used to build up a hydrogel matrix, which was then subsequently mineralized with hydroxyapatite nanocrystals following the hydrolysis of incorporated α-tricalcium phosphate particles. The stimulus to initiate hydrogel cross-linking are water molecules, which subsequently hydrolyzed isocyanate groups to amines, which then cross-linked with unreacted isocyanate to form urea-bonds. Here, it was possible to show the advantages features of a dual setting system in comparison to the simple combination of hydrogels with unreactive filler particles. By the formation of the cement matrix within the hydrogel a strength improvement by the factor of 30 could be observed. Furthermore, by applying a dual setting system higher mineral concentrations are realizable. The mechanical properties such as elasticity, compression strength and E-modulus of a composite with 30 wt% NCO–sP(EO-*stat*-PO) were found to be similar to the properties of cancellous bone.

Summary

With the motivation to develop a dual setting and resorbable cement, a brushite ($CaHPO_4 \cdot 2H_2O$) forming cement was modified with a second inorganic silica based precursor. The latter was obtained by pre-hydrolysing tetraethyl orthosilicate (TEOS) under acidic conditions. This silica precursor was mixed with a cement powder composed of ß-tricalcium phosphate and monocalcium phosphate, whereas cement setting occurred by a dissolution–precipitation process to form a matrix of brushite. Simultaneously, the increase of the pH during setting from initially ~1-2 to values > 4 initiated the condensation reaction of the hydrolysed TEOS. This resulted in an interpenetrating phase composite material in which the micropores of the cement were filled with the nanoporous silica gel. This resulted in a higher density and a compressive strength of ~24 MPa, which is approximately 5-10 times higher than the CPC reference at the same powder to liquid ratio. The microporous character of the composites also altered the release of vancomycin as a model drug, whereby in contrast to the quantitative release from the CPC reference, approx. 25 % of the immobilised drug remained in the composite matrix. It was also observed, that a variation of the TEOS content in the composite enabled a control over cement phase composition to form either brushite, anhydrous monetite or a biphasic mixture of both. Cytocompatibility tests revealed that composites with the highest silicate content showed an increased cell proliferation compared to the silica-free brushite reference. Proliferation was found to be similar to a hydroxyapatite reference with a significant higher activity per cell. Mechanistically, the improved biological response could not be attributed to the released silicate ions, but to a decreased release of phosphate and adsorption of magnesium ions from the cell culture medium.

Finally, an investigated dual setting cement system was based on the combination of a brushite forming cement powder with an aqueous silk fibroin solution. Here, changes of both ion concentration and pH during cement setting were shown to build up an interpenetrating fibroin – brushite composite with combined properties of the elastic polymer and the rigid cement. Mechanistically, the low pH of the cement paste (~2) as well as the free Ca^{2+} ions during setting resulted in a conformation change of the dissolved fibroin from random coil to ß-sheet structure. This leads to a rapid gelation and contraction of the fibroin phase with a self-densifying effect on the cement paste. The set composites showed typical ductile fracture behavior under dry testing conditions and a high elasticity under wet conditions with a mechanical strength nearly an order of magnitude higher than the fibroin free cement reference.

Cell number and activity against MG63 cells were strongly increased on silk fibroin cement composite surfaces at later time points, which could be again attributed to a decreased ion release and adsorption compared to the fibroin free cements. This in turn slowed down the in vitro degradation of the CPC phase in such composites.

Zusammenfassung

Calciumphosphat-Knochenzemente sind auf Grund ihrer keramischen Struktur inhärent spröde Werkstoffe, weswegen sie gegenwärtig nur für nicht-kraftbelastete Anwendungsbereiche verwendet werden. Ein Ansatz zur Verringerung des spröden Verhaltens basiert auf der Verwendung von Zement – Polymer Kompositen, welche die Flexibilität der Polymerphase mit der hohen Härte und Druckfestigkeit des Zements vereinen. Eine relativ neue Strategie sind dabei sogenannte dual-härtende Zemente, in denen die Polymerphase aus Monomeren bzw. Präpolymeren simultan zur Abbindereaktion des Zements aufgebaut wird. Dieser Ansatz ist insofern vorteilhaft, als dass die grundlegenden Eigenschaften der Zementpaste, wie etwa deren Rheologie oder Abbindedauer, hierbei weitgehend erhalten bleiben. In frühere Arbeiten zu dual-härtenden Knochenzementen wurden die Monomere radikalisch vernetzt. Die dabei notwendigen Initiatorsysteme (z.B. tertiäres Amin und Ammoniumperoxosulfat) sind jedoch zytotoxisch und können zudem mit der Zementreaktion nachteilig interferieren. Die vorliegende Arbeit beschäftigt sich deshalb mit alternativen Lösungstrategien, bei denen die Vernetzung der sekundären (organischen oder anorganischen) Zementphase durch die Reaktionsbedingungen der Zementpaste initiiert wird, sodass kein zusätzlicher Initiator der Paste zugesetzt werden muss.

In einem ersten Ansatz wurden Isocanat-modifizierte, sternförmige Präpolymere (NCO–sP(EO-*stat*-PO)) zum Aufbau der Hydrogelmatrix durch Hydrolyse von zugesetzten α-Tricalciumphosphat Partikeln schrittweise mit Hydroxylapatit Nanokristalliten mineralisiert. Die Vernetzung des Hydrogels in der Paste wurde durch Wasser stimuliert, wobei in einem zunächst Isocyanatgruppen zu Aminen hydrolysiert wurden, die anschließend mit weiterem Isocyanat zu Urethanbindungen reagierten. Hier konnte der Vorteil von dualhärtenden Systemen im Vergleich zu Hydrogelen, denen nichtreaktive Partikel untergemischt werden, gezeigt werden. Durch den Aufbau der Zementmatrix im Hydrogel ergab sich eine um den Faktor 30 erhöhte Festigkeit. Zusätzlich ermöglicht diese Vorgehensweise den Einsatz von erhöhten Mineralgehalten. Die mechanischen Eigenschaften der Komposite mit 30 Gew.% NCO–sP(EO-*stat*-PO) wie Elastizität, Druckfestigkeit und E-Modul waren dabei vergleichbar mit den Eigenschaften von spongiösem Knochen.

Mit dem Ziel einen dualhärtenden, resorbierbaren Zement zu entwickeln, wurde ein Bruschit ($CaHPO_4 \cdot 2H_2O$) bildender Zement mit einer zweiten anorganischen Matrix aus einem silikatischen Precursor modifiziert. Letzterer wurde durch Hydrolyse von Tetraethylorthosilikat (TEOS) unter sauren Bedingungen hergestellt. Das so erhaltene Silicasol wurde anschließend mit dem Zementpulver aus β-Tricalciumphosphat und primärem Calcium-bis-dihydrogenphosphat gemischt, wodurch die Zementreaktion zu Bruschit durch einen Lösungs – Fällungsmechanismus gestartet wurde. Der zeitgleich einsetzende Anstieg des pH-Werts von initial ~1-2 auf Werte im Bereich von >4 führt dabei zur Kondensation des Silicasols. Resultat waren interpenetrierende Netzwerke, wobei die Mikroporen der Bruschitzementmatrix mit dem nanoporösem Silicagel gefüllt sind. Dadurch ergibt sich eine höhere Dichte der Zementmatrix und eine mit ~24 MPa um den Faktor 5-10 höhere Druckfestigkeit der Komposite gegenüber der Referenz bei gleich bleibendem Pulver-Flüssigkeits-Verhältnis. Der nanoporöse Charakter des Komposites beeinflusst die Freisetzung von Vancomycin als Modellwirkstoff, wobei im Gegensatz zur silicafreien Referenz ca. 25% des Wirkstoffs in der Matrix verblieben. Die Variation des TEOS Gehalts ermöglichte zeitgleich die gezielte Beeinflussung der Zusammensetzung der mineralischen Zementphase mit Bildung von Bruschit, dessen Anhydrid Monetit oder Mischungen aus beiden Verbindungen. Zytokompatibilitätstests an den Kompositen zeigten, dass die höchsten Silicagehalte zu einer verbesserten Proliferation von Zellen auf den Oberflächen gegenüber der silicafreien Referenz führten. Das Zellwachstum war vergleichbar mit einer Referenz aus Hydroxylapatit, wobei deutlich höhere Aktivitäten pro Zelle gemessen wurden. Mechanistisch konnte die verbesserte Zytokompatibilität nicht der Freisetzung von Silikationen zugeordnet werden, vielmehr war eine verminderte Freisetzung von Phosphat und eine geringere Tendenz zur Adsorption von Magnesiumionen aus dem Zellkulturmedium der Grund.

Ein abschließender Ansatz bestand aus der Kombination aus einem Bruschit-bildenden Zement und einer wässrigen Seidenfibroin-Lösung. Hier erfolgte der Aufbau der interpenetrierenden Bruschit – Fibroin Netzwerke über den sauren pH-Wert sowie den Anstieg der Ionenkonzentration im System durch die ablaufende Zementreaktion. Somit werden die Eigenschaften des elastischen Polymers und der festen Zementphase erfolgreich kombiniert. Mechanistisch führt dabei der initial saure pH Wert (~2) und die während der Reaktion vorhandenen freien Ca^{2+} Ionen zu

einer Konformationsänderung des gelösten Fibroins von eine Zufallsstruktur hin zur β-Faltblattstruktur. Dies führt zur schnellen Gelierung und Kontraktion der Fibroinphase, einhergehend mit einer Selbstverdichtung der gesamten Paste. Die abgebundenen Komposite zeigten typischerweise duktile Brucheigenschaften im trockenen Zustand und eine hohe Elastizität unter wässrigen Testbedingungen, wobei sich um eine Größenordnung höhere Festigkeiten gegenüber der fibroinfreien Referenz ergaben. Zellzahl und Aktivität von MG63 Zellen waren auf den Seidenfibroin-Zementkompositen bei späteren Messzeitpunkten deutlich erhöht, was ebenfalls auf eine geringere Ionenfreisetzung bzw. -adsorption aus dem Medium rückgeführt werden kann. Zeitgleich konnte hierdurch die in vitro Degradation der Zementphase in solchen Kompositen verringert werden.

Abbreviations

AM	additive manufacturing
BET	Brunauer, Emmett and Teller method
Bis-GMA	bisphenol-A-dimethacrylate
CaP	calcium phosphates
CDHA	calcium-deficient hydroxyapatite
CPC	calcium phosphate cements
DAHP	diammonium hydrogen phosphate
DCPA	dicalcium phosphate anhydride (Monetite)
DCPD	dicalcium phosphate dihydrate (brushite)
DMEM	Dulbecco's modified Eagle's medium
EWC	equilibrium water content
FRCPC	fiber reinforced calcium phosphate cements
FT-IR	Fourier Transform Infrared Spectroscopy
HA	hydroxyapatite
HEMA	hydroxyethylmethacrylate
HPMC	hydroxypropyl methyl cellulose
ICP-MS	inductively-coupled-plasma mass-spectrometry
IP6	inositol hexakiphosphate (phytic acid)
K_{sp}	solubility product constant
MCPA	monocalcium phosphate anhydrate
MCPM	monocalcium phosphate monohydrate
MPC	magnesium phosphate cement
OCP	octacalcium phosphate
PAA	polyacrylic acid
PBS	phosphate buffered saline
PCPP	poly[bis(carboxylatophenoxy)phosphazene

PCS	poly(carbamoyl sulfate)
PEO	poly(ethylene oxide)
PLGA	polylactic-co-glycolic acid
PLR	powder to liquid ratio
PMMA	polymethylmethacrylate
SBF	simulated body fluid
SEM	scanning electron microscopy
SF	silk fibroin
TEGDMA	triethyleneglycol-dimethacrylate
TEMED	N,N,N',N'-tetramethylethylenediamine
TEOS	tetraethyl orthosilicate
TTCP	tetracalcium phosphate
XRD	X-ray diffraction
α-TCP	α-Tricalcium phosphate
β-TCP	β-Tricalcium phosphate

Table of contents

Chapter 1

Introduction and aims

Inorganic cements and concretes can be considered as low-temperature forming ceramic matrices. Cement setting is usually based on a hydraulic reaction, which is characterized by a chemical reaction of the cement raw powder with water, which occurs even under aqueous conditions and forms a stable and practically insoluble ceramic matrix. This distinguishes hydraulic cements from other reactive compounds such as lime or calcium sulfate hydrates (gypsum), which either set only under atmospheric conditions by the reaction with carbon dioxide (lime) or which is unstable in water due to the high solubility of the setting product (gypsum). The setting reaction of cements is thermodynamically driven by the higher solubility of cement raw powder compared to the setting products. In a first step, the aqueous cement phase partially dissolves ions from the powder and forms an ionic solution, which is supersaturated with regard to the cement setting product. The latter precipitates from the liquid and leads to a hardening of the cement paste by a three dimensional entanglement of the precipitated crystals. Depending on the cement composition, one or more of such reactions can either simultaneously or subsequently take place.[1-2]

Table 1: Examples of cement types and applications known from literature. Excellent review articles regarding the different cement types can be found in literature: calcium phosphate cements.[3]

cement type	compounds	setting products	properties and applications
Portland	Ca_2SiO_4, Ca_3SiO_5, $Ca_3Al_2O_6$, $Ca_4Al_2Fe_2O_{10}$	$3CaO{\cdot}2SiO_2{\cdot}3H_2O$ (CSH) $4CaO{\cdot}Al_2O_3{\cdot}13H_2O$ $4CaO{\cdot}Al_2O_3{\cdot}Fe_2O_3{\cdot}13H_2O$	slow setting reaction over weeks; cheap; major compound for civil engineering application
Sorell	5 MgO, $MgCl_2$	$5Mg(OH)_2.MgCl_2.8H_2O$	High early strength and resistance against salts, but Cl^- leaching in aqueous environment
Hydroxy-apatite	$Ca_3(PO_4)_2$, $Ca_4(PO_4)_2$, CaO, $CaHPO_4$(·2H2O)	$Ca_9(PO_4)_5HPO_4OH$, $Ca_{10}(PO_4)_6(OH)_2$	Low solubility (0.2 mg/l) of HA in vivo, only slow resorption at cement surface by osteoclastic cells
Brushite (Monetite)	ß- $Ca_3(PO_4)_2$, $Ca_5(PO_4)_3OH$, $Ca_4(PO_4)_2O$, $Ca(H_2PO_4)(H_2O)$, H_3PO_4	$CaHPO_4{\cdot}2H_2O$, $CaHPO_4$	More soluble than hydroxyapatite under in vivo conditions with higher bone remodeling capacity; brushite cement may undergo phase compositional changes in vivo
Magnesium-phosphate	MgO, $Mg_3(PO_4)_2$, $NH_4H_2PO_4$, $(NH_4)_2HPO_4$, H_3PO_4	$MgNH_4PO_4{\cdot}6H_2O$ (struvite), $MgKPO_4{\cdot}6H_2O$ (k-struvite), $MgHPO_4{\cdot}3H_2O$ (newberyite)	Application as rapid repair cements in civil engineering due to high early strength development; high potential as degradable biocements anticipated
Puzzolane	$Ca(OH)_2$ + SiO_2 (amorphous)	$CaSiO_4{\cdot}nH_2O$	Used as additive for Portland cements

Table 1 gives an overview about the cement formulations known from literature including some basic properties of the set materials. Most cements are chemically based on silicate, phosphate, aluminate or sulfate salts of calcium and magnesium. Apart from applications as civil engineering construction materials with a worldwide use of several hundred tons, many cement types are also applied as biomaterials, e.g. for bone replacement or in dentistry.

Cements and concretes have a typical inherent brittleness, which applies for practical all known cement types from both civil and biomedical engineering applications. General strategies to reduce the brittleness of cements and concrete in civil engineering are based on the combination with ductile materials such as fiber reinforcement [4-5] or polymeric additives [6-8] as well as by a reduction of porosity and flaw sizes due to a calendaring processing technique [9-10]. This leads to macro defect free ultrahigh strength concretes with a compressive strength >150 MPa [11-12] and elastic properties even enabling the fabrication of a cementious spring (see Figure 1) [13].

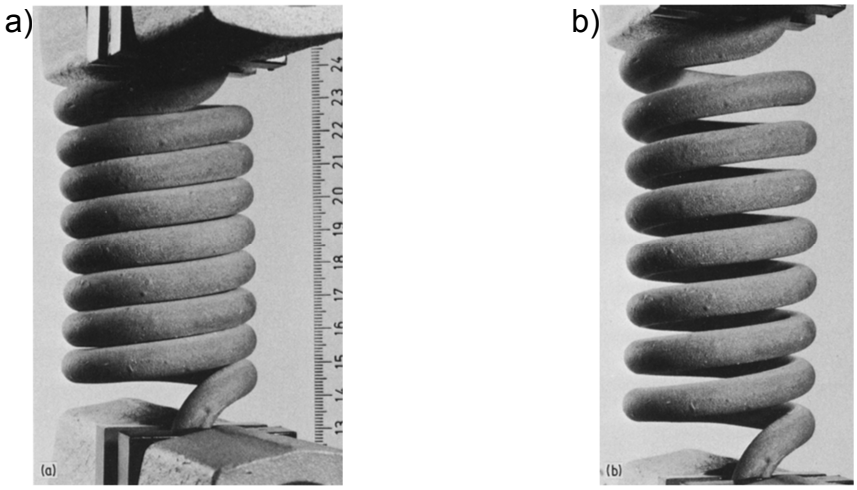

Figure 1: Spring made from macro defect free cement a) relaxed and b) expanded position (reproduced from [13] with the permission from Springer).

Many of the above mentioned cement matrices are also applied as mineral biocements in the human body. While calcium silicates have a long application history in dentistry (here named as “mineral trioxide aggregates”) [14-15], predominantly calcium phosphate cements (CPC) found an application as bone replacement material [3]. CPCs are similar to their silicate and aluminate counterparts brittle materials after setting with a comparatively high mechanical resistance against compressive forces, but with an order of magnitude lower tensile

or bending strength. For medical applications this fact is a big drawback, since the load behavior in and on the human bone skeleton is pretty complex and includes next to the usually analyzed compression strength also bending, torsion and tension in a 3-dimensional way. This implies the use of CPC only under non- or low-load bearing conditions, predominantly in cranio and maxillofacial applications. The above described reinforcement methods are also applicable to mineral bone cements based on calcium phosphate chemistry (CPC), e.g. porosity has been identified as the major critical strength determining parameter [16-17] and numerous articles have been published dealing with fiber reinforcement of CPC (summarized in [18-19]). Worth to note is that for biocement manipulation, further prerequisites such as cytocompatibility and degradability of additives as well as the specialized application techniques during surgery have to be taken into account.

An alternative way to reduce cement brittleness is based on the use of cement – polymer composites, which combine the flexibility of a polymeric phase with the hardness and compression strength of a cement matrix. Early approaches in the field of calcium phosphate cements were dealing with the addition of water soluble polymers containing Ca^{2+} ion binding groups (e.g. carboxylates, phosphates), such that cement setting occurred by both the formation of calcium chelates as well as the above mentioned dissolution - precipitation reaction.[20-27] A relatively new strategy is the use of “dual setting” cements, in which the polymeric phase is simultaneously build up from monomers or prepolymers during cement setting. This approach largely maintains basic properties of the fresh paste such as rheology or setting time. Previous works on such dual setting cements were dealing with a radical polymerization reaction to create the polymeric network.[28-31] This type of reaction requires the addition of a suitable initiator system (e.g. a tertiary amine in conjunction with ammonium peroxosulfate), which are often cytotoxic and may also not comply with the harsh pH conditions in for example brushite cements.

This thesis dealt with alternative strategies, in which the cross-linking and gelation of the second (polymeric or inorganic) cement phase is initiated by general chemical conditions of the setting reaction such that no additional initiator has to be added to the cement paste. Chapter 2 reflects the general aspects of calcium phosphate cement chemistry and in special the general underlying principles of reinforcement strategies (porosity reduction, fiber reinforcement, concept of dual-setting cements)

of CPC are presented as an already published literature review by the author of this thesis (Chapter 2.3). The following chapters are dealing with new dual-setting approaches: the use of an isocyanate modified star-PEG additive to an α-TCP cement paste (Chapter 3), in which cross-linking of the additive is an autocatalytic process induced by water; brushite – silca based cements obtained by using a prehydrolysed TEOS solution as cement liquid, whereby the increasing pH during cement setting initiates silica condensation (Chapter 4); finally, the use of a fibroin solution as cement liquid in brushite cements (Chapter 5), in which fibroin gelation is induced by the pH raise during setting as a result of a conformation change from random coil to ß-sheet structure. At the end of the thesis, the results of the novel approaches are discussed and concluded in terms of their clinical application potential and further development possibilities are presented (Chapter 6).

Chapter 2

Chemistry of mineral bone cements

Chapter 2.3 was published as original review article (Geffers M., Groll J., Gbureck U.; Reinforcement strategies for load-bearing calcium phosphate biocements. Materials 2015; 8 (5) 2700-2717 [16]). The article was mainly written by the author of this dissertation thesis Martha Schamel née Geffers, who also did the literature search as well as the conceptualization and implementation for the figures in this article.

Calcium phosphate cements are in the meantime essential materials for surgery applications in the field of bone substitution. In contrast to Portland cements or magnesium oxide (phosphate) cements (e.g. Sorell type, see table 1), which are known since centuries, CPC are a relatively new material class. A largely unknown first study by Kingery [32] in the early 1950s analyzed the mixture of different metal oxides with ortho-phosphoric acid and their possible setting into a crystalline phase. 30 years later, LeGeros reported their use in orthopedic and dental applications [33], whereby Brown and Chow [34-36] did further developments in this field and are mostly considered as the inventors of this material class[1]. Since the 1990ies, a large number of different CPC has been introduced into the medical market for the application in non-load-bearing, aseptic bone defects (Table 2).

Table 2: Composition of commercially available calcium phosphate cements for medical applications according to Dorozhkin 2011 [37]. The setting product consists of either hydroxyapatite (e.g. HA) or brushite (DCPD).

Manufacturer	Trade name	Composition	Setting product
Biomet (US) Interpore (US) Walter Lorenz Surgical (GER)	Calcibon®	powder: α-TCP (61%), DCPA (26%), $CaCO_3$ (10%), CDHA (3%); liquid: H_2O, Na_2HPO_4	apatite
	Mimix™	powder: TTCP, α-TCP, sodium citrate; liquid: aqueous citric acid	apatite
Calcitec (US)	Osteofix	powder: tricalcium phosphate and calcium oxide ; liquid: PBS	apatite
ETEX (US)	α-BSM®; Embarc; Biobon	powder: ACP (50%), DCPD (50%); liquid: aqueous NaCl-solution	apatite
	CarriGen	synthetic tricalcium phosphate, sodium carboxymethylcellulose, sodium hydrogencarbonate and sodium carbonate	apatite
Kasios (Fr)	Jectos Eurobone®	powder: ß-TCP (98%), $Na_2P_2O_7$ (2%); liquid: H_2O, H_3PO_4, (3,0M), H_2SO_4 (0,1M)	brushite
Kyphon (US)	KyphOs ™	powder: ß-TCP (77%), $Mg_3(PO_4)_2$ (14%), $MgHPO_4$ (4,8%), $SrCO_3$ (3,6%); liquid: H_2O, $(NH_4)_2HPO_4$ (3,5M)	apatite
Mitsubishi Materials (J)	Biopex®	powder: a-TCP (75%), TTCP (20-18%), DCPD (5%), HA (0-2%) liquid: H_2O, sodium succinate (12-13%), sodium chondroitinsulfate (5-5,4%)	apatite
Produits Dentaires SA (CH) CalciphOs (CH)	VitalOs4	liquid 1: ß-TCP (1,34g), $Na_2H_2P_2O_7$ (0,025g), H_2O, salts (0,05M PBS solution, pH 7,4); liquid 2: MCPM (0,78g), $CaSO_4 \cdot 2H_2O$ (0,39g), H_2O, H_3PO_4 (0,05M)	brushite

[1] According to a personal communication of Dr. L.C. Chow to U. Gbureck, the cement reaction was discovered by accident. Originally, Chow and co-workers were looking for dental remineralizing pastes and analyzed aqueous mixtures of different calcium phosphates. Some of these pastes (especially with the addition of tetracalcium phosphate) were found to be hardened after a couple of hours. This was further analyzed and denoted to a setting reaction to the new mineral phase hydroxyapatite.

Manufacturer	Trade name	Composition	Setting product
Skeletal Kinetics (US)	Callos ™	powder: α-TCP, $CaCO_3$, MCPM; liquid: sodium silicate	apatite
Stryker (US) Leibin-ger (GER)	BoneSource™	powder: TTCP (73%), DCPD (27%); liquid: H_2O, mixture of Na_2HPO4 and NaH2PO4	apatite
Stryker (US)	HydroSet™	powder: TTCP, DCPD, sodium citrate; liquid: H_2O, polyvinylpyrrolidone, sodium phosphate	apatite
Synthes (US)	Norian® SRS Norian® CRS	powder: α-TCP (85%), $CaCO_3$ (12%), MCPM (3%); liquid: H_2O, Na_2HPO_4	apatite
	chronOS™ Inject	powder: β-TCP (73%), MCPM (21%), $MgHPO_4 \cdot 3H_2O$ (5%), $MgSO_4$ (<1%), $Na_2H_2P_2O_7$ (<1%); liquid: H_2O, sodium hyaluronate (0.5%)	brushite
Teknimed (FR)	Cementek®	powder: α-TCP, TTCP, sodium glycerophosphate; liquid: H_2O, $Ca(OH)_2$, H_3PO_4	apatite

2.1 Solubility of cement components and setting mechanisms

The calcium salts of the tribasic orthophosphoric acid (H_3PO_4) can be classified into primary, secondary and tertiary phosphates and are the basis for the ternary system $Ca(OH)_2$-H_3PO_4-H_2O. The chemistry of CPCs is based on the different solubilities of the involved cement reactants and the final setting product and determines the reaction direction like dissolution, precipitation, phase transformation occurring in the aqueous system. For calcium phosphates, the solubility can change several orders of magnitude with other solution parameters, especially the pH (Figure 2). A fundamental parameter for describing solubility is the thermodynamic solubility product constant, K_{sp}, a quantity related to the Gibbs free energy of the solid. K_{sp} is expressed in a form related to the formula of the compound, e.g., for HA,

$$K_{sp}(HA) = [Ca^{2+}]^5[PO_4^{3-}]^3[OH^-] \quad (1)$$

where quantities in parentheses in the right hand side of the equation denote ionic concentrations [38] Table 3 lists the K_{sp} values for the various salts at 25 and 37 °C known from literature. The cement setting runs in two steps: (I) the dissolution of the reactants and the (II) reprecipitation of the setting product [39], whereby the different solubilities of the reactants and products at the prevailing cement pH is the driving force of reaction (Figure 2).

Table 3: Composition and solubility constant of calcium phosphates.

Compound	Formula	Ca/P ratio	-log (K_{sp}) at 25 °C	-log (K_{sp}) at 37 °C	solubility [mg·L^{-1}]
Monocalcium phosphate monohydrate (MCPM)	$Ca(H_2PO_4)_2·H_2O$	0.5	1.14 [40]	n. m.	66204.3
Monocalcium phosphate anhydrate (MCPA)	$Ca(H_2PO_4)_2$	0.5	1.14 [40]	n. m.	61477.3
Dicalcium phosphate dihydrate (DCPD, Brushite)	$CaHPO_4·2H_2O$	1.0	6.59 [41]	6.63 [41]	85.2
Dicalcium phosphate anhydride (DCPA, Monetite)	$CaHPO_4$	1.0	6.90 [42]	7.04 [42]	41.1
Octacalcium phosphate (OCP)	$Ca_8H_2(PO_4)_6·5H_2O$	1.33	96.6 [43]	95.9 [43]	0.5
α-Tricalcium phosphate (α-TCP)	α-$Ca_3(PO_4)_2$	1.50	25.5 [44]	n. m.	2.5
β-Tricalcium phosphate (β-TCP)	β-$Ca_3(PO_4)_2$	1.50	28.9 [45]	29.5 [45]	0.4
Hydroxyapatite (HA)	$Ca_5(PO_4)_3OH$	1.67	116.8 [46]	117.2 [46]	0.2

n. m.: not mentioned

Immediately after mixing cement powder and liquid, the cement raw materials start to dissolve and release calcium and phosphate ions. This process leads to a supersaturation of the cement liquid with regard to the reaction product resulting in first nucleations of the new phase, which generally occurs on the surfaces of the reactant particles [47].

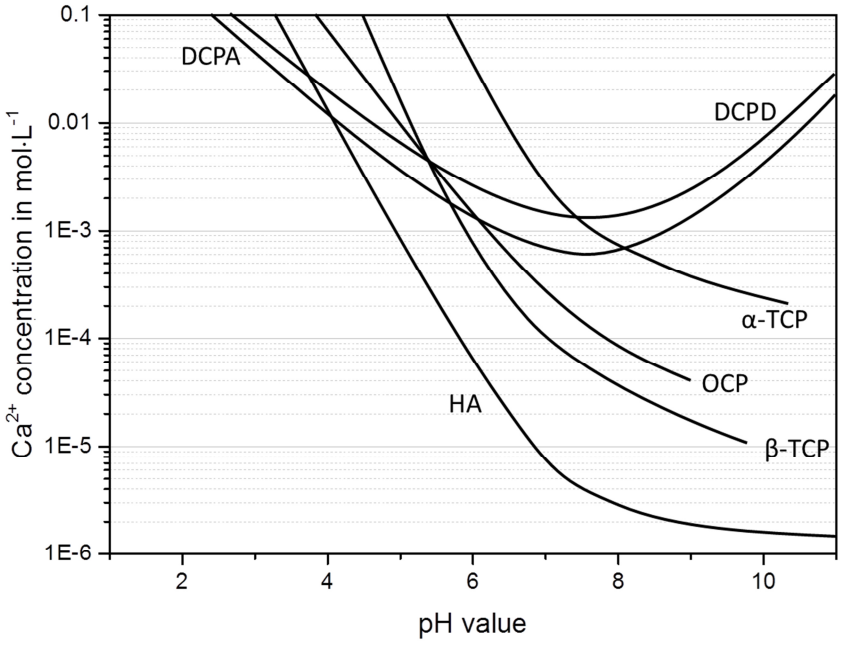

Figure 2: Solubility isotherms of several calcium phosphates in water (modified from [38;48-49]).

Further dissolution of the reactant particles results in the continuous supply of calcium and phosphate ions, whereby the product crystals grow and build up a solid matrix by crystal entanglement.

The kind of reaction product is highly determined by the pH value of the cement paste, but other parameters like temperature or the use of reaction modifiers also influence the reaction kinetics. Ginebra *et al.* [50] postulated a reduced setting time by a temperature increase from 22 to 37 °C for a HA forming α-TCP cement. The rate of reaction was about 5times higher at 37 °C than at 25 °C. This not negligible influence of the environmental temperature on the cement setting must be analyzed in detail for surgical applications, since the temperature slope can increase from about 20 °C in the conditioned operating theater to 37 °C in the patient body. Here, the reverse solubility behavior of calcium orthophosphates with temperature is a beneficial property, since the solubility decreases with a higher temperature resulting in a faster precipitation at a lower supersaturation level. The same effect could be seen by Driessens et al. [51] as well as by Grover et al. [52] for a brushite forming cement system.

The implementation of reaction modifiers is usually utilized to adapt the setting time of the CPC on the surgical requirements. Here the crystal growth rate could be de- or accelerated by the use of different reaction agents. The crystal growth of HA is relatively slow ($2.7 \cdot 10^{-7}$ mol $Ca_5(PO_4)_3OH$ $min^{-1} \cdot m^{-2}$ [53]) such that setting accelerators like sodium phosphates or phosphoric acid has to be used to obtain clinically required setting times [54-56] of cements within several minutes. In contrast, the rate of crystal growth of brushite is about two orders of magnitude higher ($3.32 \cdot 10^{-4}$ mol DCPD $min^{-1} \cdot m^{-2}$ [57]). This explains why brushite cements set very rapidly such that setting retarders, e.g. pyrophosphates, sulfates or citrates [58-59] has to be used in these systems to obtain clinically acceptable setting properties.

The specific surface area of the cement raw powder and therefore the particle size also influences the dissolution rate in a high degree and the properties of the set cement.[60] Especially for multicomponent reactant mixtures, the particle sizes of the used powders have to be adapted to their solubilities to run in the right order and velocity. For example, in an equimolar mixture of basic tetracalcium phosphate (TTCP) and acidic dicalcium phosphate anhydride (DCPA), the particle size aspect

ratio d_{50}(TTCP) : d_{50}(DCPA) must be approximately 10 : 1 to obtain a mostly similar rate of dissolution of both compounds and a setting cement system.[61] By grinding the powders in liquid or solid phase the suitable particle size distribution could be adjusted.[62-63] Ginebra *et al.* attributed the higher conversation from α-TCP into HA compared to the studies of Monma and Kanazawa [64] to the smaller particle size, since the hydration reaction is initially surface controlled.[65] However, after a certain time of grinding the milling energy is insufficient for a further particle size reduction, but leads to the formation of defects within the crystal lattice resulting in an additionally reactivity enhancement. Gbureck *et al.* was the first, who analyzed the influence of a high energy ball milling process on the solubility of calcium phosphate compounds and attributed the improved reactivity to the mechanically induced transformation from a crystalline into an X-ray amorphous phase.[66] The amorphisation increases both the absolute solubility and the rate of dissolution of the reactant, whereby a faster supersaturation level with regard to the product is reached.[67] Hurle *et al.* analyzed the dissolution of the crystalline and amorphous phase within such a mechanically activated α-TCP cement more in detail by X-ray diffraction (XRD) measurements and applying the so called G-factor method.[68] The G-factor facilitates the determination of the total amount of crystalline phases by the use of an external standard and hence enables the calculation of the amount of amorphous phases within a cement powder.[69] The amorphous phase dissolved instantly after mixing with the cement liquid confirming the assumptions of the studies by Gbureck and Ginebra, in contrast to results from Bohner *et al.*, who postulated the simultaneously dissolution of the amorphous and the crystalline phase [70].The use of amorphous TCP nanoparticles as additive or pure cement raw powder show further enhancement of the reactivity to improve the conversion into HA and the strength of the set cement.[71-72] Nevertheless, this method is limited, since the amorphous TCP nanoparticles production suffers from low batch to batch reproducibility.

2.2 Cement systems

By mixing a dry powder containing calcium and phosphate with an aqueous solution the initial calcium orthophosphates were dissolved rapidly and precipitate according to the solubility parameters of the product. Essentially, there are just two types of

cements classified according to their products – hydroxyapatite and brushite forming cements. Under certain conditions octacalcium phosphate may form instead of hydroxyapatite, which is known to be a possible intermediated precursor phase for hydroxyapatite crystallization. In few studies, also the anhydride monetite instead of brushite is formed. These two calcium phosphate phases persuade by their beneficial *in vivo* behavior.

2.2.1 Hydroxyapatite

Since the chemical composition of natural bone is comparable to an ion-substituted calcium-deficient hydroxyapatite, these kinds of cements have been investigated in a more detailed way. Apatite is formed in cement mixtures when the pH of the paste is neutral or basic. Most of the reported calcium phosphate cement formulations and medical products are hydroxyapatite forming systems (see Table 2). Practically all calcium phosphate salts from Table 3 as well as further compounds such as calcium carbonate or calcium oxide can serve as precursors for apatite forming cements, whereby the total stoichiometry (Ca:P ratio) of the cement paste has to be in the range of approx. 1.2 – 2 to ensure proper conditions for apatite nucleation. Commonly, the Ca/P ratio of HA is in the range between 1.50 and 1.67 [73], whereby 1.67 is the stoichiometric hydroxyapatite and the 1.5 one is often called calcium-deficient hydroxyapatite (CDHA). Although with a decreasing Ca/P ratio as well as crystallinity and crystal size the solubility increases.[48] Hydroxyapatite is (even when ionically substituted of calcium deficient) the most stable calcium phosphate (CaP) phase under physiological conditions (see Table 2) and can be resorbed only by acid producing osteoclasts.

The variety of HA forming formulations consists commonly of a one or two component powder system, which is mixed with an aqueous solution. Water is a reactant only in few cases and acts mainly as a medium for the reaction.[74-76] The introduced water amount has to be adapted on the needed paste viscosity for a good handling or other applications like injection with the background that the unconsumed water acts as a porogen and an increasing porosity declines the mechanical strength.[77]

Usually, the cement raw powder for the two compounds system consists of one phase with a higher calcium content and basic character such as tetracalcium phosphate (TTCP) [35-36;78-82] or calcite [83-84] and a second slightly acidic compound like brushite (DCPD) or monetite (DCPA), whereby the cement setting is given by Equation (1) and (2):

$$2\ Ca_4(PO_4)_2O + 2\ CaHPO_4 \rightarrow Ca_{10}(PO_4)_6(OH)_2 \quad (1)$$

$$4\ CaO + 6\ CaHPO_4 \rightarrow Ca_{10}(PO_4)_6(OH)_2 \quad (2)$$

The ratio of the two components is a critical parameter for the set cement`s properties. For TTCP/DCPA systems molar ratios between 0.25 and 2 were analyzed and the equimolar ratio turn out to be the best.[85-86] The theoretical Ca/P ratio for the equimolar TTCP/DCPA ratio is 1.67 similar to stoichiometric hydroxyapatite, nevertheless, further studies showed that CDHA is the main phase formed during setting. Although the first nuclei during setting form an almost stoichiometric hydroxyapatite [87], the latter interacts with the remaining DCPA to transform into CDHA.[88] Since DCPD has a higher solubility under physiological condition, the combination of TTCP and DCPD enforced this effect due to a faster setting.

Single component cements are often based on the use of α-tricalcium phosphate, but are also known for other compounds such as TTCP, β-TCP or alkali substituted CaPs following mechanical activation of the materials.[67;89-90] The latter was extensively analyzed by the working group around Berger, who postulated a cement system of $Ca_2KNa(PO_4)_2$ without a phase transformation during setting and thus a higher degradation rate compared to HA.[91-92] Even after the storage in simulated body fluid (SBF) for four weeks the phase composition remained unchanged without any obviously HA deposition.[93] The cement setting was attributed to the reaction of a small amorphous phase within the material with citric acid from the cement liquid by a chelating reaction.[94] Driessens *et al.* [95] combined the potassium and sodium doped powder with MCPM as a feasible hydroxyapatite forming cement system. Thereby a lower Ca/P ratio was possible in comparison to the commonly used hydroxyapatite forming cements resulting in a faster degradation by the loss of phosphate, K^+ and Na^+ under physiological conditions.

Nevertheless, the most commonly used single component system refers to the hydration of α-TCP to calcium deficient hydroxyapatite in the presence of an aqueous phase [50;64;68;96-101]:

$$3\ Ca_3(PO_4)_2 + H_2O \rightarrow Ca_9(PO_4)_5(HPO_4)OH \quad (3)$$

Although Monma and Kanazawa first described the setting reaction of α-TCP [64], cement formulations substantially containing α-TCP with clinically acceptable setting properties were described by Driesens *et al.* and Ginebra *et al.*[98;102] They investigated the setting reaction of a mixture of 81 % α-TCP, 17 % β-TCP and 2 % precipitated HA with a 2.5 % Na_2HPO_4 solution as liquid phase at 22° and 37°C.[50;100] X-ray diffraction analysis showed that the hydrolysis reaction of the α-TCP component was responsible for cement hardening, while the β-TCP fraction remained unreacted. About 80 % of the α-TCP reacted after 24h setting time. The 2.5 % Na_2HPO_4 solution acts as a reaction accelerator by providing an additional phosphate source in the system, which reacts much faster with the rapidly dissolved calcium ions of the α-TCP particles. In the case of a two component TTCP/DCPA cement system Na_2HPO_4 solution works as a buffer during the setting reaction prohibiting the pH increase in a high alkali range, so that after the fast dissolution of TTCP the DCPA particles were still dissolved.[55]

Beside the use of reaction accelerators, the setting time can be fastened by the particle size reduction of the raw powder to increase the surface area as mentioned above (see chapter 0). Since the dissolution of the metastable calcium phosphate raw powder is diffusion controlled, the dissolution rate and thereby the degree of supersaturation increases with an increasing surface area.[62] As the degree of supersaturation is the driving force of nucleation, a higher amount of crystals nuclei is formed resulting in smaller needle-like structures. This high amount of nuclei can be further more favored by the addition of apatite particles to the cement raw powder.[103-105] Contrary, a bigger initial particle size will reduce the supersaturation level and hence less nuclei precipitates are formed, however their crystal growth is favored resulting in larger plate-like particles.[106] Furthermore, the hydration rate is favored by a higher surface area (smaller particles) as analyzed by Liu *et al.* in a systematic way.[107] Thereby the combination of a better packaging density of the finer initial powder, higher conversion rates and finer crystals with enlarged contact areas for a better crystal entanglement improve the mechanical strength of the set cement.[60;62;107] Thus, it becomes obvious, that the microstructure of the cement is the key point between setting reaction and the mechanical performance of the cement. Cement microstructure and porosity as the most crucial property for the mechanical performance are influenced by a number of

different parameters such as the setting temperature and pH, the powder to liquid ratio (PLR), the initial calcium orthophosphates system and additives for the adaption of the setting reaction as well as reinforcing phases. This results in a high variety for mechanical strength values in literature, which range for the commonly measured compressive strength from below 1 MPa [108-110] to values two orders of magnitudes higher (~180 MPa) [111-113] for hydroxyapatite forming cements. These values are in the requested dimension for cancellous (2 – 12 MPa) as well as cortical bone (100 – 230 MPa) [114-115], however the current available cements can just be used for low or non-load bearing defects, due to their lack of flexibility and load absorption for tensile and torsion stress.

Calcium orthophosphates are generally resorbed by two possible mechanisms *in vivo*: by the cellular activity of macrophages, osteoclasts and other types of living cells [116-118], which is called the active resorption, and by the passive resorption due to dissolution or hydrolysis (for brushite) [119-120], whereby the solubility under physiological conditions is the most prominent fact. Since the surrounding body fluids are supersaturated with regard to HA, the cell mediated degradation is the prevailing resorption mechanism. As the micro porosity of cement does not enable cells to penetrate the implant, the degradation is limited to the surface [107] yielding in a slow resorption *in vivo*, but excellent osteoinductive and osteoconductive properties [121].

2.2.2 Dicalcium phosphate (brushite and monetite)

Brushite (dicalcium phosphate dihydrate, DCPD) and its anhydride monetite (DCPD) are the least soluble calcium phosphate minerals at pH < 4.2. Brushite forming cements have been firstly described by Mirtchi et al. [122-123] by the reaction of β-tricalcium phosphate with primary calcium phosphate. Although brushite precipitation in solution can occur up to pH of 5 - 6 [38;124], brushite forming cements require (at least initially) much lower pH of 2-3 for an adequate setting reaction. This is commonly adjusted by either using phosphoric acid solution as cement liquid (equation (4)) or by adding the primary calcium phosphates MCPA or MCPM (equation (5)) as the most acidic and water soluble calcium orthophosphate compound of the ternary system $Ca(OH)_2$-H_3PO_4-H_2O [125]:

$$Ca_3(PO_4)_2 + H_3PO_4^+ + 6\,H_2O \rightarrow 3\,CaHPO_4 \cdot 2H_2O \qquad (4)$$

$$Ca_3(PO_4)_2 + Ca(H_2PO_4)_2 + 8\,H_2O \rightarrow 3\,CaHPO_4 \cdot 2H_2O \quad (5)$$

The latter reaction has the advantage that the degree of cement conversion can be adjusted in a broad range (up to a quantitative conversion when equimolar amounts are used). Here, the MCPM or MCPA is dissolved very rapidly in contact with the aqueous cement liquid, whereby a pH drop is effected providing the right environment for the following TCP dissolution.[126-127] β-TCP is the favored crystallographic form of TCP for brushite cement formulations due to the lower solubility compared to α-TCP. By using the latter, the cement paste would react vigorously within seconds, which is prolonged by β-TCP to approximately 30 – 60 sec.[122;128] Another way for prolonging the setting of brushite cements is similar to hydroxyapatite cements the increase of the specific surface area of cement reactants by granulation prior to setting.[129-130] A big drawback of this system is however its storage stability. Gbureck et al. [131] have shown that powder mixtures of β-TCP with primary calcium phosphates undergo a phase conversion into monetite, even when stored in sealed bottles. The authors identified this conversion to be catalyzed by atmospheric or surface adsorbed moisture, which could be suppressed for at least 21 days by either adding solid citric acid to the powder or by storage under dry conditions in a desiccator. In contrast, the components of the TCP/H_3PO_4 system offer an unlimited shelf-life, since both the powder (predominantly β-TCP) as well as the acid solution can be stored for years without changes of reactivity. Due to the omitted step of powder mixing it is easier and faster to prepare, the chemical composition is more controllable and it has improved physio-chemical properties, e. g. mechanical properties, since the paste could be produced in a more homogenous way.[127]

Contrary to HA forming cements, brushite crystallization is fast with a crystal growth rate of $3.32 \cdot 10^{-4}$ mol DCPD $min^{-1} \cdot m^{-2}$ [57], which leads in seconds to an initial hardened cement (the full conversion lasts about 24 h [132-133]). Hence, the setting reaction has to be retarded by different additives to prolong the mixing period. Namely, pyrophosphates, sulfates and citrates are commonly applied to enable the preparation of cements with setting times in the range of 3 to 8 min.[58-59] Pyrophosphoric acid [52] as well as calcium [134] and sodium pyrophosphates [135] are used to inhibit the mineralization and regulate the setting time. Sulfates can be added to the cement in the powder (calcium sulfate dehydrate or hemihydrate) and in the liquid (sulfuric acid) phase. Thereby sulfate substitutes the phosphate ions and

modifies the setting reaction.[58] The mostly used citric ions interact with the β-TCP particles by building a surface layer [136] reducing their dissolution. Additionally, all the mentioned reaction retardants prohibit brushite precipitation, whereby the setting pH is constant on a lower level and the setting time is prolonged, which can be verified by the measurable delay in the exothermic heat flow release of the setting cement.[126]

In contrast to apatitic cements, brushite cements are resorbable under physiological conditions, because brushite has a much higher solubility at pH 7.4 compared to HA (Table 3). Following immersion in aqueous media, the DCPD component in a brushite cement may, depending on conditions, be stable, dissolve, hydrolyse to hydroxyapatite (HA) [137] or even disintegrate. In order for dissolution of DCPD to occur, the aqueous medium must be under saturated with calcium and HPO_4^{2-} ions. Subsequently, if saturation occurs with respect to HA, e.g. in the absence of rapid fluid turnover, hydrolysis of DCPD to HA observes. [138] The *in vitro* degradation of brushite cements in bovine serum has been investigated by Grover *et al.* [139] showing that under dynamic conditions with a daily change of the immersion liquid a medium mass loss of about 60-70 % was achieved after 28 d immersion. *In vivo*, brushite is in addition resorbed by cellular activity. [135;140-141] Since the brushite degradation is slightly faster *in vivo* than the bone regeneration, this results in an increased porosity, mass loss and decreased mechanical properties of the cement implant at the implantation side [142] and bone material gabs are build [143]. By an excess of β-TCP as reactant in the cement formulation, the degradation can be regulated due to its lower solubility.[144] Furthermore, the remaining β-TCP particles may serve as anchor points to encourage natural bone formation.[145-146]

Although brushite cement porosity as most crucial factor for strength is lower than in hydroxyapatite cements due to the participation of water in the cement setting reaction (see Equations (4) and (5)), the compressive strength of brushite cements is on average lower than for apatitic ones in a range between 8 and 26 MPa.[147-149] Due to the water consuming cement reaction, it should theoretical be possible to produce near-zero porous brushite ceramics as examined by Hofmann *et al.*[150]. By carefully adapting cement additives as well as initial particle size and distribution, the porosity could be reduced by 60 % improving the compressive strength to the highest value (52 MPa) in literature for hand mixed brushite cement without any exterior

compaction step.[150-151] The adjustment of the utilized cement retardants is important for the later mechanical performance of the set cement. They could be positively affect the strength by a delayed cement setting [152] and a higher degree of conversion [153]. On the other hand, Hofmann et al. [154] analyzed the correlation between the citric acid concentration and different parameters like the compressive strength. The citric acid seems to have a negative influence at concentrations higher than 800 mM, which was attributed to the formation of citric-β-TCP complexes prohibiting cement setting. At higher citric acid concentration the strength decline was explained by the increasing formation of monetite and the accompanied porosity rising. Since monetite does not consume water during reaction, this results in a higher porosity.

Actually, monetite is the thermodynamically more favored (less soluble) dicalcium phosphate phase than brushite. Nevertheless, brushite is the commonly formed phase during the dissolution/precipitation reaction due to a faster rate of crystal growth and a higher degree of supersaturation. Thereby only a few publications deal with a monetite forming cement and the setting reaction has to be carefully adjusted to monetite favoring conditions. Monetite formation is known to occur if precipitation during setting is slowed down, which is either the fact at low pH [127;155-156] or by reducing the supersaturation level in the cement liquid due to a high ionic strength of the liquid. A prolonged setting time also decreases the maximum temperature of the exothermic setting reaction [126], which is an important factor for *in vivo* applications. Desai *et al.* developed a single component monetite forming cement by using calcium hydroxide powder and mixing it with phosphoric acid.[157] Since at low pH (< 2.5) MCPM occurred as the stable form [40], they elevated the pH in the monetite favoring pH range between 2.5 and 4.2 by the addition of $NaHCO_3$.[157] Monetite can be also achieved by the dissolution of tricalcium phosphate in phosphoric acid, whereby the α crystallinity form reacts faster.[158]

Cama *et al.* attained the formation of a monetite cement by enhancing the ionic strenght in the system.[159] The authors added NaCl in the liquid (6.2 M solution) or to the solid (60 % granules) cement phase to produce micro and macroporous monetite cement. To analyze the influence of the ionic strength in a more detailed way Şahin and Çiftiçioğlu had a closer look at the monetite precipitation in a NaCl solution.[160] According to the Pitzer equation, the authors calculated the

supersaturation level of brushite and monetite in the presence of sodium chloride (NaCl; 0 – 6 M) (Figure 3).

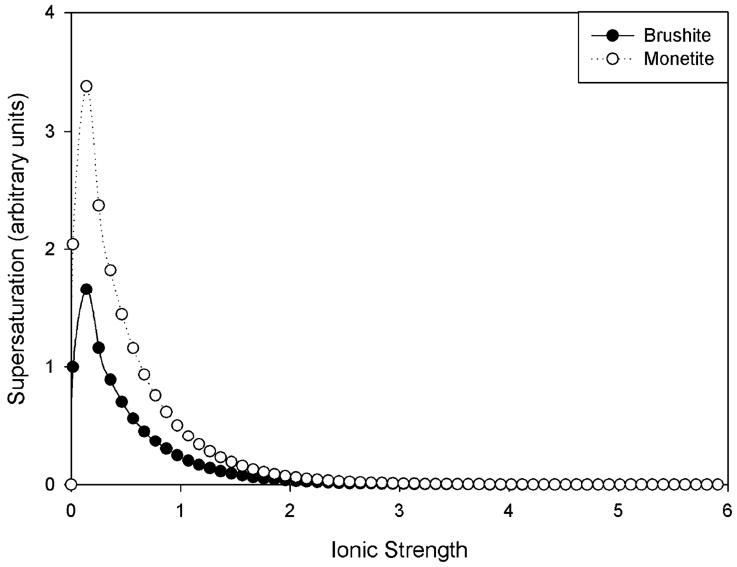

Figure 3: Supersatutration of brushite and monetite in the presence of NaCl as predicted by Pitzer equation (reproduced from [160] with permission from Royal Society of Chemistry).

At NaCl concentrations over 3 M, the supersaturation gap becomes almost equal, whereby the faster precipitation of brushite is prohibited and the reaction is thermodynamically controlled. Monetite is formed instead of brushite. Due to the higher porosity of pure monetite forming cements their mechanical properties are reported to be lower than for corresponding brushite cements in a range between 4 MPa (PLR=1,5 g/ml; 0.65g/ml) [52;157] and 12 MPa (PLR=3 g/ml) [159] for compressive loading.

Beside the direct preparation of monetite by a cement reaction, it is also possible to produce monetite implants by hydrothermal treatment of a brushite monolith.[161-163] Of course, a disadvantage is here the loss of beneficial cement properties such as free moldability and injectivity. Brushite loses its crystal water at a temperature above 60 °C [38;156] and transforms into the thermal stable monetite. This thermally induced phase transformation of the cement bulk may cause cracks due to shrinkage by the water loss. Therefore, Alshaaer *et al.* developed a hydrothermal post curing technique, where the bulk shrinkage is compensated by a decreasing bulk density caused by increasing pore sizes.[164] This can be realized in an autoclave, where the required temperature is given, the prevailing water pressure supports the bulk skeleton structure and forces the released bound water to remain inside the pores.

Tamini *et al.* reported a higher amount of infiltrated bone in the highly interconnective porous monetite scaffolds *in vivo* in comparison to brushite samples.[165] Additionally, monetite shows a higher resorption capacity, since it does not transform into HA *in vivo* in contrast to brushite resulting in a continuous higher degradation rate, although brushite is theoretically more soluble (see Table 3).[166-167] Montazerolghaem *et al.* postulated the active resorption of monetite by osteoclasts *in vitro* in addition to the chemical resorption under physiological conditions.[168]

2.2.3 Octacalcium phosphate

Octacalcium phosphate (OCP; $Ca_8H_2(PO_4)_6 \cdot 5H_2O$) is a highly hydrated calcium phosphate with a layer-like structure consisting of hydrated and apatitic layers resulting in plate-like crystals [169] and it is discussed as precursor of hydroxyapatite mineralization *in vivo* [170]. The spontaneously and rapid transformation of OCP into the thermodynamically favored HA [171-172] is therefore both the incentive and challenge to develop a OCP forming cement.

OCP appears as pathological calcification [173] and it is often found as a recrystallization product of brushite cements, likely because the Ca:P ratio of OCP (1.33) is lower than that for HA (1.5 – 1.67), such that a smaller amount of Ca^{2+} ions have to be present for forming crystalline reprecipitates [174-176]. Temizel *et al.* [177] pointed out that an additional driving force for brushite conversion into OCP *in vitro* are bicarbonate ions as buffer system.

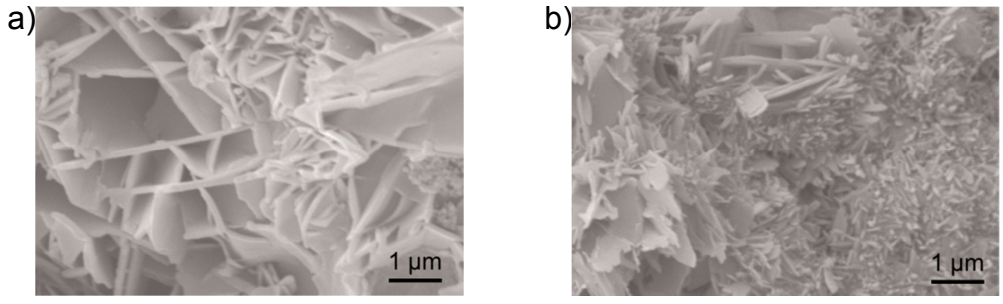

Figure 4: SEM images of a) HA produced by α-TCP/DCPA with water and b) OCP produced by α-TCP/DCPA with phosphate solution. (modified from [178]; Articles published in these journals are in the public domain and may be used and reproduced without special permission).

OCP is commonly formed by brushite [179] or α-TCP hydrolysis [180] at neutral pH in the presence of strontium ions [181], acetate ions or dicarboxylic acids. There are only few studies in literature describing the formation of OCP as setting product in

cements. OCP crystallization is pretty slowly, since it is metastable and rapidly precipitates in the thermodynamically more stable HA lattice.

Monma *et al.* described in the late 80ies an OCP forming cement by the combination of TCP and DCPD as raw powder and observed OCP formation according to equation (6) in a Ca/P ratio range between 1.2 and 1.47 [182]:

$$2\ Ca_3(PO_4)_2 + 2\ CaHPO_4 \cdot 2H_2O + H_2O \rightarrow Ca_8H_2(PO_4)_6 \cdot 5H_2O \quad (6)$$

For mechanical improvement and adjustment of the setting time, Bermudez *et al.* analyzed this cement system in detail with the replacement of DCPD by DCPA.[183] The optimum Ca/P ratio turn out to be 1.36 ± 0.03 in correspondence with the OCP Ca/P ratio. This yielded in compressive strength and setting time comparable to HA cements. In contrast, Markovic *et al.* [178] observed no OCP formation with the system of Bermudez. Only with the use of phosphate solution (pH 6.1), the authors achieved an OCP forming cement, however with reduced mechanical strength (4.3 MPa) due to a higher porosity (42 %) in comparison to the HA samples (σ = 9 MPa; ε = 37 %). The authors attributed the differences to Bermudez to a smaller particle size of the initial α-TCP particles and the resulting higher pH (8-9) due to the faster dissolution [183].

Although the cement formulation development involves some difficulties caused by a narrow parameter adaption range to form OCP instead of HA, OCP persuade by its biological behavior and is worth for further research. A diversity of literature evidences synthetic OCP as an osteoconductive material [184-187] as coatings on metallic implants [188-189], granules [190-191] or self-assembled macrocrystals [192-193]. *In vitro* studies showed a stimulation of osteoblastic cell differentiation [191-193] and the conversion of OCP into HA is discussed to be the reason for the stimuli [191;194] resulting in the formation of newly formed bone by the resorption of the original OCP [184-185;187].

2.2.4 Chelate setting cements

Chelation is the bonding between a single center ion and a ligand with multiple bonding sides as so called chelation agent. For mineral cements, this setting mechanism occurs when Ca^{2+} or Mg^{2+} binding motifs are present in one of the cement components, e.g. carboxyl or phosphate groups. Additional to the chelation

the common cement reaction by dissolution and precipitation may occur resulting in a two-step setting reaction with improved initial and final strength of the hardened matrix.[195]

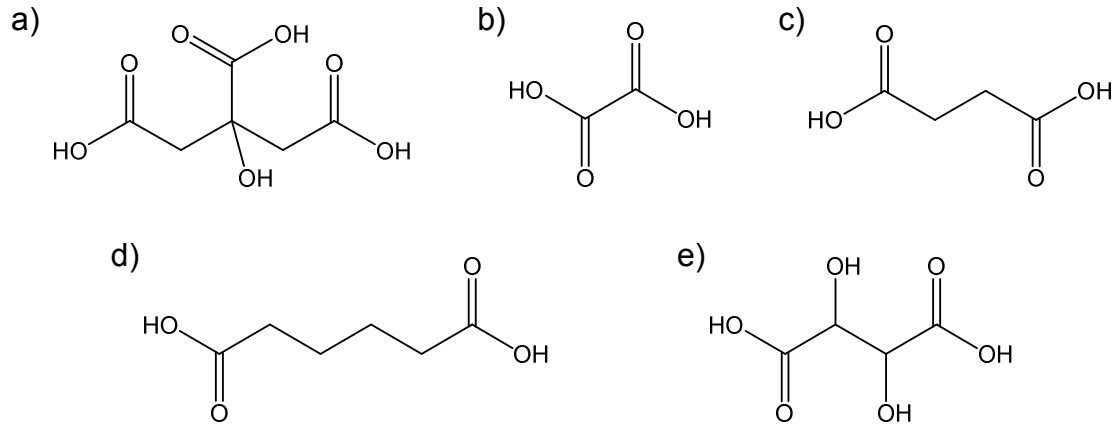

Figure 5: Chemical structure of a) citric acid, b) oxalic, c) succinic, d) adipic and e) tartic acid.

Citric acid has three carboxy groups (Figure 5 a), which can interact with the calcium phosphate powder to form chelates. The addition of 10 and 45 % citric acid to the cement system accelerates the initial hardening and shows improved initial mechanical strength due to the chelation reaction [196-197]. However, Yokoyama *et al.* reported a higher inflammatory response to such cements *in vivo* due to the low pH.[197] Besides citric acid, a diversity of other carboxylic acids like oxalic, tartaric, succinic and adipic acid were previously used as chelation agents for cement setting, resulting in different cement properties due to their chain length (see Figure 5).[198-200]

Carboxylic acid binding motifs are used as functional groups on the backbone of a polymer chain as polyacrylic acid (PAA) (Figure 6). PAA interacts with the calcium phosphate particles by chelation and hydrogen bonds, whereby the chains are aligned parallel to the calcium phosphate crystals.[201] The chelating reaction is able to work as a cross-linker between several polymer chains leading to a rapid hardening of the cements.[202] Chen *et al.* observed a changing fracture behavior during mechanical loading from the typically brittle character of pure CPC over ductile-tough to ductile-soft by an increasing PAA concentration in the composite.[203] However, the polymer phase often prohibits the calcium phosphate cement reaction since the diffusion is suppressed resulting in a pure chelation hardening, whereby the original calcium phosphate phase remains stable. This can be beneficial for the degradation behavior *in vivo* due to the absence of HA

formation.[25;204] An additional advantage *in vivo* is that the calcium polycarboxylated network does not only interact with calcium ions from the cement, but also with ions of the surrounding tissue for a better implant/tooth or bone interface adhesion.[205] Furthermore, the cement composites show a better washout resistance, which is an important prerequisite for medical applications like for the use as root-end filling material in endodonic surgery [206].

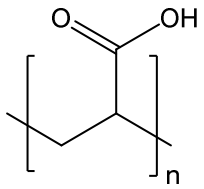

Figure 6: Chemical structure of structure of polyacrylic acid.

Another chelation motif for calcium phosphates are phosphonate groups. Phosphonates are well known pharmaceutical agents for osteoporosis treatment, which build up polymeric agglomerates on the mineral bone surface due to their chelating affinity with calcium ions and hence prohibit osteclastic cell activity.[207] The interaction is not only a result of calcium complexation, moreover the phosphonate groups can be exchanged by the phosphate ions on the calcium phosphate surface.[208]

The group around Greish extensively investigated composites of polyphosphonates and CPCs in the past two decades. Here, the composites were not prepared by a normal cement reaction, where the cement powder is mixed with a cement liquid, but by hot pressing, where the raw powder mixture is heated above the glass temperature of the polymer under pressure. The softened polymer flows around the calcium phosphate grains increasing the interface between the two phases, whereby the reaction is facilitated.[21] Figure 7 shows the possible interactions between the dissolved Ca^{2+} from the CPC raw powder and the phosphonate side group of Poly(vinyl phosphonic acid). Greish *et al.* found an improvement in the mechanical properties by increasing the preparation parameters (pressure, temperature and compacting time) and attributed this to a higher composite density/compacting and better CPC conversion.[209]

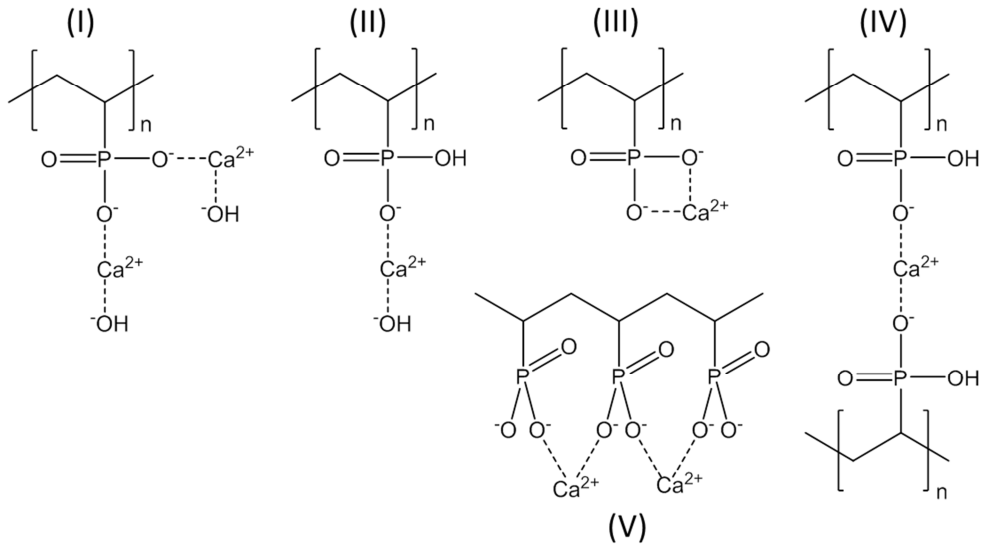

Figure 7: possible interactions between Ca^{2+} and poly(vinyl phosphonic acid) (modified from [21]).

On the basis of the knowledge to coat HA nanoparticles with phosphonate acid [210-211] Paramanik *et al.* introduced 2-carboxyethylphosphonic as a linker between the polymer chain and the mineral particles to improve the mechanical properties by enhancing the adhesion and interaction of the polymer matrix with a precipitated HA filler.[212] The HA fillers were coated with 2-carboxyethylphosphonic, whereby the phosphonic acid group interact with the HA particles, the free carboxylic group can than chemically bond to the poly(ethylene co vinyl alcohol) to form a stable composite (Figure 8).

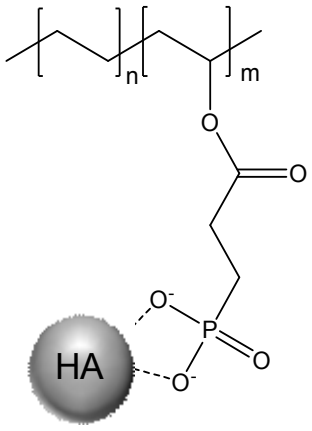

Figure 8: Scheme of the interfacial bonding between the polymer and the phosphonic acid coated HA nanoparticles (modified from [212]).

As a further development, Greish *et al.* used polyphosphazenes as chelation agent for CPC. Polyphosphazenes have two organic side groups at every phosphorous atom in the backbone, which alternates with a nitrogen atom. [213] Advantageous of

this polymer is the high diversity of possible substituents, the flexibility of the backbone to form noncovalent bindings and the possibility to degrade by hydrolysis due to the inorganic backbone.[214] Additionally, they were found to be biocompatible and osteoconductive.[215-216]

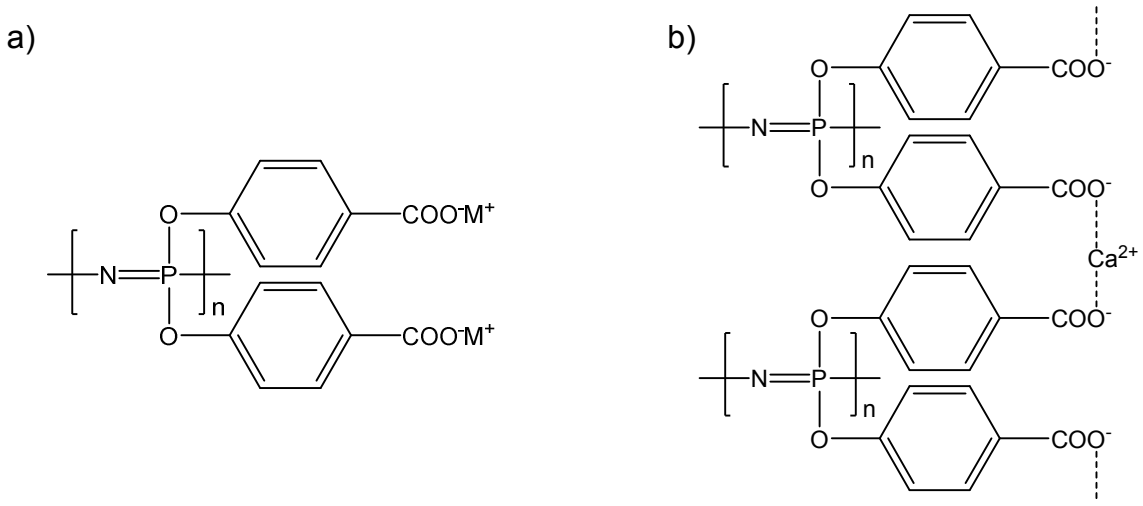

Figure 9: a) Structure of poly[bis(carboxylatophenoxy)phosphazene] with M^+ stands for monovalent ions like Na^+ or K^+ and its b) chelation by Ca^{2+} (modified from [217] and [218]).

Greish *et al.* synthesized poly[bis(carboxylatophenoxy)phosphazene] (PCPP) as sodium or potassium salt and mixed them with a TTCP/MCPM cement system to form HA-PCPP composite (Figure 7).[217-219] By the dissolution of the cement raw powder the divalent Ca^{2+} ion replace the monovalent Na^+ or K^+ ion to form a bridge between two PCPP chains and interact with the calcium phosphate.[220]

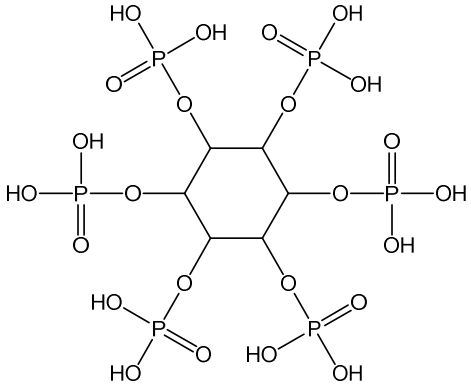

Figure 10: Chemical structure of phytic acid.

Apart from the above mentioned polymeric chelating compounds, also low molecular weight inositol hexakiphosphate (IP6, common name: phytic acid) has been investigated as cement raw material with phosphate groups. This strong chelation agent for polyvalent cations is a natural plant antioxidant and plays an important role

for the storage of phosphate and calcium in grains and nuts [221] and is thereby an optimal candidate for the chelation of calcium or magnesium phosphates (Figure 10).

Hirabayashi *et al.* found an improved metallic ion bonding on tooth by the combination with phytic acid.[222] Due to this discovery a new mineral cement was developed, where the setting mechanism and hardening of the cement is solely effected by the chelate formation between phytic acid and calcium phosphate powder. Precipitated HA particles are mixed with phytic acid solution and a chelatin reaction forms a stable cement with compressive strength of about 23 MPa.[223-224] Since HA is slowly resorbable *in vivo,* the group around Konishi developed a chelate-setting system with α- or β-TCP and phytic acid with improved anti-washout and degradation properties.[225-226] Sheikh *et al.* transferred this chelation mechanism to an alkali substituted calcium phosphate to adapt the degradation behavior *in vitro* by the phytic acid concentration.[227] Christel *et al.* expanded the chelation reaction by an additional cement setting, where a magnesium phosphate raw powder is dissolved in an aqueous environment and set by the precipitation of a more thermodynamically favored magnesium phosphate phase.[228] Here the cohesion is not only attributed to the chelation complex formation, but also to the entanglement of the newly formed mineral crystals. It is also possible to transfer the simultaneously occurring chelation and cement setting mechanism to a brushite forming cement matrix. An additional convincing factor for using phytic acid solution instead of citric acid as cement liquid and retarder is the improved cytocompatibility.[229] Citric acid is known to inhibit cell attachment by the formation of dicalcium phosphate-citrate acid complexes.[230]

2.3 Reinforcement strategies for load-bearing calcium phosphate biocements

Self-setting cements based on calcium phosphate chemistry combine the advantages of the high biocompatibility of calcium phosphates with the free moldability of cements and the mechanical stability of ceramic implants.[3;231] Such calcium phosphate cements (CPC) are usually based on freshly prepared mixtures of crystalline or amorphous calcium orthophosphate, calcium hydroxide or calcium carbonate powders with an aqueous solution, which undergo setting in a continuous dissolution–precipitation reaction. Although various mixtures of calcium and phosphate sources can serve as raw materials, there are in principle only two cement types as products of the setting reaction: At neutral or basic pH the calcium phosphate cement sets to nanocrystalline hydroxyapatite (HA, with a variable stoichiometric composition between $Ca_9(PO_4)_5HPO_4OH$–$Ca_{10}(PO_4)_6(OH)_2$), while at low pH < 4.2, orthophosphate ions are protonated and the secondary phosphates brushite ($CaHPO_4 \cdot 2H_2O$, DCPD) and monetite ($CaHPO_4$, DCPA) are the least soluble calcium phosphates [232-233] and hence precipitated during setting of acidic cement pastes until an end pH of close to 5 [3;127;151;160;231]. Detailed reviews about CPCs reflecting their synthesis, setting reaction, rheological properties or biological performance can be found in literature [3;234-235]. CPC are resorbed *in vivo* and replaced by new bone tissue [137;236], whereas the speed of degradation depends on the final composition of the cement matrix. Hydroxyapatite forming cements degrade only slowly within years since the surrounding extracellular fluid ($[Ca^{2+}]$ ~ 2.5 mmol·L^{-1}, $[HPO_4^{2-}]$ ~ 1 mmol·L^{-1} [237]) is supersaturated regarding HA (solubility of hydroxyapatite ~ 0.2–0.3 mg·L^{-1}) [3]. HA forming cements degrade solely by osteoclastic bone remodeling, which is limited to surface degradation since cells cannot penetrate the microporous cement structure. Osteoclastic cells resorb the cement by providing a local acidic environment increasing the solubility of the mineral.[118;142;238-239] In contrast, cements forming brushite or monetite have a higher solubility (calculated solubility in water for monetite: 41–48 mg·L^{-1}, brushite: 85–88 mg·L^{-1} [240]) and many studies have demonstrated the bone remodelling capacity of such cements in various animal models within a time period of 8–52 weeks.[140-141;241-242] A passive resorption of such cements by simple chemical dissolution is a topic of contention in the literature, whereas some authors postulate that the extracellular liquid is in equilibrium with brushite [243], while others have calculated a thermodynamic instability of brushite in simulated body fluid [244]. The

latter is supported by the fact that brushite forming cements are indeed dissolved *in vivo* even in the absence of osteoclastic cells (e.g., after intramuscular implantation).[176] Worth noting is that for brushite forming cements a phase transformation into lower soluble minerals like octacalcium phosphate, hydroxyapatite or whitlockite can occur *in vivo* by a dissolution–reprecipitation reaction, which slows down biodegradation.[144;245]

Calcium phosphate bone cements have been shown to provide compressive strength of up to 80 MPa measured under application near conditions without a precompaction of the cement paste leading to lower porosity/higher strength, since this is not applicable under *in vivo* conditions.[246] Set CPC can be considered as porous ceramic materials with an inherent brittleness and comparatively low flexural strength compared to natural hard tissues such as bone or teeth. A comprehensive characterization of the elastic and failure properties for both hydroxyapatite and brushite forming CPC by Charrière *et al.* [147] indicated brushite cements to be suitable as bone fillers, while hydroxyapatite cements were attributed to having the potential to be a structural biomaterial. The low fracture toughness restricts the use of CPC to non-load-bearing defects [247]. Typical applications are the treatment of maxillofacial defects or deformities [231] or the repair of craniofacial defects [248]. An extension of the application of calcium phosphate cements to load-bearing defects, e.g., in vertebroplasty or kyphoplasty [249-251], would require less brittle cements with an increased fracture toughness. This is of high interest since the application of commonly used polymeric cements have strong drawbacks near the spinal cord due to their strong exothermic setting reaction and cytotoxic monomer release [252-254]. Common approaches to reduce brittleness of CPC and to improve their mechanical performance for load-bearing applications cover the modification of the cement liquid with polymeric additives such as collagen [255-258], the addition of fibers to the cement matrix [18;259] or the use of dual-setting cements in which a dissolved monomer is simultaneously cross-linked during cement setting [29-31] (Figure 11). This article aims to feature the most significant reinforcement strategies for calcium phosphate cements based on either intrinsic (porosity) or extrinsic (fiber addition, dual setting cement) material modifications.

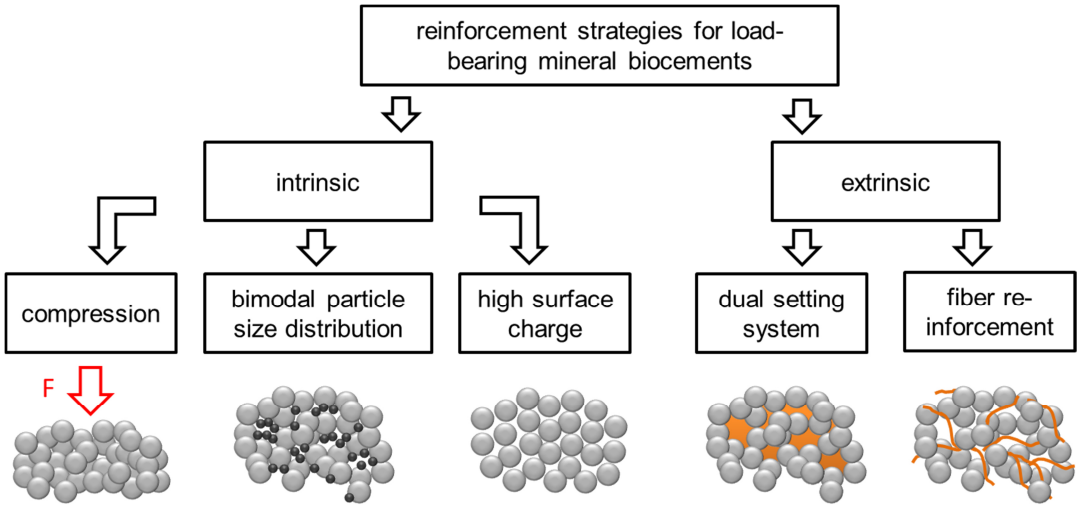

Figure 11: Strategies to reinforce mineral biocement for load-bearing applications.

2.3.1 Porosity reduction for strength improvement of CPC

Calcium phosphate biocements set by a dissolution–precipitation reaction, during which the cement raw material continuously dissolves to form a supersaturated solution with regard to the setting product. The latter is precipitated from the aqueous cement phase and forms an entangled cementitious crystal matrix. The mechanical strength of a cement matrix is a direct result of this crystal entanglement and several factors determine the final strength of the matrix, such as degree of conversion, setting product or porosity. The latter is likely the most important factor and it is known from literature that porosity reduction in cements from 50 % to 31 % by compression can increase compressive strength by nearly an order of magnitude.[17] Porosity in biocements predominately originates from the presence of unreacted cement liquid after setting located in the voids between the entangled crystal matrix. Since any excess of water used for paste mixing, which is not consumed during the setting reaction creates porosity, the main influencing parameter on the total cement porosity is the powder to liquid ratio (PLR) used for cement processing. Pore sizes in CPC typically have a diameter range spanning from a few nanometers to several micrometers [260-261] and are occupying about 22–55 vol.-% of cements without further paste manipulation (e.g., compaction, porogen addition) [150;262].

Generally, pores in hydroxyapatite cements are smaller than in brushite cements (due to smaller crystal size of HA), whereas the total porosity is mostly smaller for

brushite cement. The latter is a result of an increased water consumption during brushite cement setting.

Porosity considerably lowers the strength and stiffness (Young's modulus) of the cements matrix with an inverse exponential relationship between cement porosity and compressive strength:

$$\sigma_c = \sigma_{c,0} \cdot e^{\sim 2KP} \quad (7)$$

where σ_c is the compressive strength at a given porosity; $\sigma_{c,0}$ is the maximum theoretical strength of the material; K is a constant; and *P* is porosity [17]. Porosity is usually measured by helium pycnometry [139], mercury intrusion porosimetry [263] or it is calculated based on the phase composition of the set cements and their densities [264]. Due to the disadvantages of these methods (destructive, long analysis times, toxicity of mercury, misleading results due to amorphous phases), Unosson *et al.* [265] have investigated a method which is based on the assumption that the evaporated water from a dried cement sample equals to the volume of pores within the cement. Since the accuracy of this method depends on a quantitative drying of samples without affecting the phase composition, the authors evaluated several drying conditions (vacuum, elevated temperature) for cement samples and compared the results with porosity determined by the above mentioned methods. Since the measured porosity was found to vary between the different methods, the authors recommended using more than one method to determine cement porosity, whereas the water evaporation method (24 h in vacuum) proved to be fast, easy and precise in estimating the porosity of CPCs.

Porosity reduction by decreasing the amount of cement liquid used for mixing is a key parameter to increase the intrinsic strength of any biocement matrix. This, however, is limited, since every cement powder requires a formulation specific minimum amount of water ("plastic limit") for surface wetting of all cement particles and for filling the space between the particles.[266] A correlation between the powder to liquid ratio used for forming a cement paste and the resulting porosity/compressive strength is displayed in Figure 12 for both HA and brushite forming cements. An effective method to reduce cement porosity is based on both creating a bimodal size distribution of cement raw materials and the creation of a high surface charge (zeta-potential) of the particles. A bimodal size distribution is thought to fill space in cement pastes normally occupied by water. The possibility to reduce porosity has been

demonstrated for both hydroxyapatite [246] and brushite [139;150] forming biocements. In addition, a high surface charge (zeta-potential) will help to disperse agglomerates of fine sized particles by reducing attractive interparticulate forces. The zeta-potential can be influenced by using multiple charged ions as additives to the cement liquid, e.g., tatrates or citrates [267], which adsorb at the particle surface and increase the zeta-potential to values of ~−40 to −50 mV. Applying these two principles to a matrix of α-tricalcium phosphate (monomodal size distribution with d_{50} ~9.8 µm) by using 13 – 33 wt.-% fine sized $CaHPO_4$ filler (d_{50} ~ 1.16 µm) and 0.5 M trisodium citrate solution increase the plastic limit of the cements from 3.5 to 5.0 $g \cdot mL^{-1}$. At the same time, porosity was decreased from 37 % to 25 % and a strength improvement from 50 to 79 MPa could be found [246] Another study by Engstrand *et al.* [262] investigated the effect of β-TCP filler particles on the mechanical properties of a brushite forming cement (β-TCP-MCPM system). The results showed that the addition of low amounts of a filler (up to 10%) in combination with 0.8 M citric acid solution can effectively increase the powder to liquid ratio and hence decrease porosity from ~ 30 % to ~ 23 %. This strongly affects compressive strength of the cements with an increase from ~ 23 MPa (no filler and citric acid) to ~ 42 MPa. Space in cement pastes may also be filled by using hard agglomerates similar to civil engineering Portland cements as shown by *Gu et al.*.[268] In this study, the dispersion of 20 % high-strength β-tricalcium phosphate granules with a size of 200–450 µm in the cement showed an increase of the compressive strength by 70 %, while maintaining the rheological properties (injectability through 2.2 mm needle by applying a 5 kg weight on the syringe plunger) of the cement paste.

Caution must be exercised when comparing the obtained strength values from different studies, since many parameters during cement sample preparation and testing can affect the results. Unlike polymeric polymethylmethacrylate (PMMA) based bone cements [269], testing of calcium phosphate bone cement is not regulated, and our own experiences show that strength of set cement can vary by several times depending on the sample preparation and testing conditions. Generally, strength of dried samples is superior to that of (application near) wet specimen, mainly because water acts as a lubricant between the entangled crystals of the precipitated matrix. In addition, sample preparation may cause changes of cement porosity, e.g., by precompacting the paste in a mold. This ejects liquid from the paste (through the narrow gap between mold and plunger) leading to a lower

porosity and hence a higher strength compared to uncompacted samples.[113;270-271]

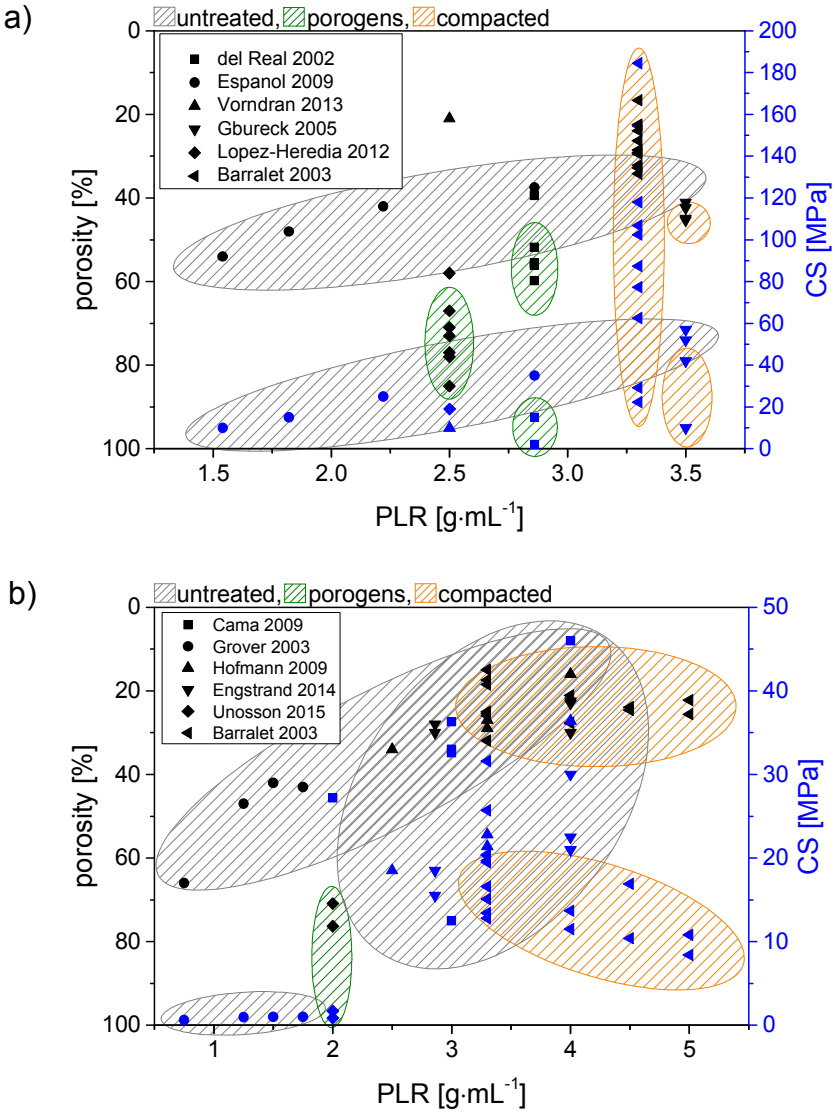

Figure 12: Correlation between powder to liquid ratio and porosity/compressive strength for a) hydroxyapatite and b) brushite cement from different studies. Cements were either set without compacting manipulation (untreated), processed by pre-compaction or porogens were added to create artificial macroporosity. Data were obtained from: (a) del Real 2002 [272], Espanol 2009 [260], Vorndran 2013 [273], Gbureck 2005 [246], Lopez-Heredia 2012 [274], Barralet 2003 [113], b) Cama 2009 [275], Grover 2003 [139], Hofmann 2009 [150], Engstrand 2014 [262], Unosson 2015 [276], Barralet 2004 [149].

2.3.2 Fiber reinforment of CPC

Similar to reinforcement approaches of sintered hydroxyapatite ceramics [277], the addition of fibers to CPC is one of the most successful reinforcement technique [18-19]. The mechanical behavior of such fiber reinforced calcium phosphate cements (FRCPC) is a result of the complex interaction between all of the composite

constituents. Contributions to the macroscopic behavior come from strength and stiffness of both fiber and cementitious matrix, matrix toughness, mechanical interaction between fibers and matrix as well as supplementary effects of polymeric additives or aggregates.[19]

Fiber reinforcement studies have been performed with many different types of fibers (degradable *vs.* non-degradable, see Table 4 showing a strong increase of the mechanical strength depending on several parameters such as (1) matrix composition and strength, (2) fiber volume fraction, orientation, aspect ratio and tensile modulus as well as (3) the interface properties between matrix and fibers.[19]

In addition to an increase of the bending strength from approx. 10–15 MPa for pure CPC to a maximum strength of 45 MPa (polyglactin fibers) – 60 MPa (carbon fibers), especially the work of fracture for fiber reinforced cement composites usually increases by at least one order of magnitude (Table 4).

As illustrated in Figure 13, there is not only a complex interaction of factors, but in clinical application the properties of the fiber–cement composites are also time dependent since both the cement matrix and the fibers may degrade during tissue regeneration.

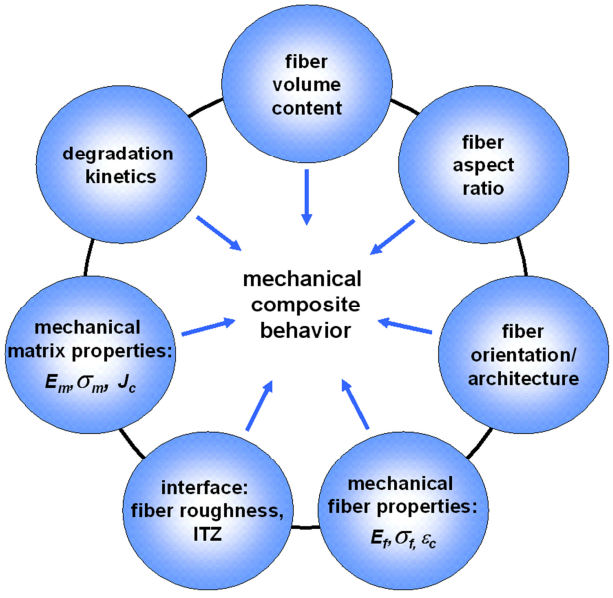

Figure 13: Interaction of material parameters which influence the time dependent mechanical behavior of the FRCP**C** composite (reproduced from [19] with permission from Elsevier).

Generally, the load-bearing capacity of fibers increases with their Young's modulus, whereas the maximum tensile stress within the fiber is determined by the fiber's modulus and the matrix strain [278]:

$$\sigma_f^{max} = E_f \cdot \varepsilon_m \quad (8)$$

When the composite is loaded, differences between Young's moduli of fiber and matrix lead to additional strain near the interface, mainly in the softer material.[279] The diameter of the fibers directly influences the total interface area between fibers and matrix for a given fiber volume fraction and affects both homogeneity and processability of the fiber–cement mixtures. Most biomedical composites are reinforced by discontinuous fibers. Their length and diameter are of great relevance, since substantial load has to be transferred from the matrix to the fiber via the interface for a reinforcing effect. Load is predominantly transferred by shear stresses at the lateral surface of the fibers rather than via the end faces of the fibers. Reinforcement effects are only observed, if the fiber length exceeds a critical value l_c, which can be calculated based on the assumption that the fiber is loaded up to the fracture strength.

$$l_c = \frac{d\sigma_{f,b}}{2\tau_i} \quad (9)$$

where σ_{fB} and τ_i denote fracture strength of the fiber and shear stress at the interface and d is the diameter of the fiber. Optimum fiber volume content has been addressed by many researchers. Civil engineering concretes typically are reinforced with < 5 vol.-% of steel, glass, natural or synthetic polymer fibers.[280] In many studies on medical FRCPC, the fiber content is one order of magnitude higher than in fiber reinforced cements for civil engineering. This is attributed to a frequently observed trend in FRCPC research [281-283] that strength and ductility of the composites increased with fiber content. Moderate load transfer due to non-optimized interface strength and low modulus of the fibers require such high fiber volume fraction. Furthermore, fiber costs are not such a limiting factor, at least in the research stage.

Biodegradable polylactic-co-glycolic acid (PLGA) is one of the most frequently used reinforcement fiber materials for CPC. For a high fiber volume, considerable increase in bending strength has been reported, e.g., from 2.7 MPa (unreinforced CPC) to 17.7 MPa for CPC with 45 vol.-% polyglactin fibers.[282] This strengthening effect can be further enhanced to 40.5 MPa by incorporation of chitosan lactate into the

matrix. The synergistic strengthening of the CPC by chitosan and fibers together is stronger than from either suture fibers or chitosan alone [282], which was explained by both a much stronger cement matrix after chitosan incorporation supporting the suture fibers to better resist cracking as well as an improved suture-matrix bonding [282].

Table 4: Examples for the reinforcement of calcium phosphate cements with either degradable or non-degradable fibres. (3 p.b.: Three point bending, 4 p. b.: Four point bending. # UD: Unidirectional fibers. TTCP: Tetracalcium phosphate. HA_w: Hydroxyapatite whiskers) (reproduced from [19] with permission from Elsevier).

Composition Fiber/Additive/Matrix	Fiber Volume Fraction	Strength [MPa]	Work of Fracture [kJ·m^{-2}]	Test Method	Ref.
DEGRADABLE FIBRES					
HA matrix (TTCP + DCPA (+ Na_2HPO_4 − solution))	-	10–15	0.032–0.05	3 p. b.	[284-285]
Polyglactin 910/-/HA (TTCP + DCPA)	25 vol.-%	17.5–25	2.6–3.6	3 p. b.	[284]
Polyglactin 910/-/HA (TTCP + DCPA)	Mesh multilayer	8.5–24.5	0.75–3.1	3 p. b.	[286]
Polyglactin 910/chitosan lactate/HA (TTCP + DCPA)	45 vol.-%	41	11	3 p. b.	[282]
Polyglactin 910/chitosan lactate/HA (TTCP + DCPA)	Mesh multilayer	43	9.8	3 p. b.	[287]
Polyglactin 910/(poly(caprolactone))/ brushite (β-TCP + H_3PO_4)	24 vol.-% random short 6–25 long fibers UD #	7.5–20	n.a.	4 p. b.	[288]
NON-DEGRADABLE FIBRES					
Carbon/-/HA (TTCP + DCPA)	2–10 vol.-%	32–60	3.5–6.5	3 p. b.	[280]
CNT/-/HA (α-TCP + HA)	0.2–1.0 wt.-%	8.2–10.5	n.a.	3 p. b.	[289-290]
Aramid/-/macroporous HA (TTCP + DCPA + Na_2HPO_4)	6 vol.-%	7.5–13.5	0.8–6.5	3 p. b.	[283]
HA_w/-/HA (TTCP + DCPA)	10–40 vol.-%	5.4–7.4	57–102	4 p. b.	[290]

Generally, strength increases with length to diameter aspect ratio of fibers, whereas occurrence of fiber aggregation leading to inhomogenities in fiber distribution represents the practical upper limit for the aspect ratio. Xu and co-workers [281;291] systematically varied the length of carbon fibers in HA cement and found a continuous increase of

strength between 3 and 75 mm fiber length (aspect ratio of 1000 and 9000), which was followed by a strength decrease for 200 mm long fibers (aspect ratio 25,000). While the use of such long fibers strongly alters the workability of cement pastes and impedes a minimal invasive application by injection, cement pastes filled with short fibers have been demonstrated to maintain their injection properties up to a fiber length of 1 mm and a fiber volume of 7.5%.[292]

Cements may also be modified by using fiber meshes instead of single fibers, especially in cases where biomechanical stresses will primarily be oriented linearly or biaxially to the cement implant. Meshes provide a strength enhancement (in linear or biaxial direction) beyond that of randomly directed fibers and have the advantage that even thin bony structures (e.g., malar, orbital bones) or extensive cranial deficiencies can be reconstructed.[248;286;293] Von Gonten [248] could demonstrate that such a polyglactin mesh–CPC composites have a similar work of fracture to PMMA cements up to seven days' immersion in a buffered electrolyte, which was considered to have potential for structural repair of bone defects.

Most of the studies about FRCPC deal with both non-degradable fibers and with a poorly soluble hydroxyapatite cement matrix (see Table 4 and references [18-19]). This will initially result in long term stable cement composites with only minor changes of mechanical properties. However, even the slow matrix degradation by osteoclastic cells will dissect fibers in a longer time frame, which will be encapsulated in newly formed tissue with the possibility of foreign body reactions. Especially, approaches using technical fiber types (e.g., carbon fibers) or even carbon nanotubes are questionable regarding this point due to their low biocompatibility. The use of degradable fibers in FRCPC may solve this problem and the *in vivo* behavior of such FRCPC has been proven in various studies and is part of a recent review article by Krüger *et al.* [19]. However, at the same time, the use of degradable fibers will result in a time dependent loss of the reinforcement effect due to dissolution of the fibers in an aqueous environment. This effect of fiber degradation on the composite strength was simulated for polyglactin/PLGA fiber material by immersion of reinforced hydroxyapatite cement in a simulated physiological solution.[281-282] These studies confirmed a strength decrease of the reinforced composite after 4–6 weeks' immersion [281], which could be compensated by a simultaneous chitosan infiltration of the cement matrix [287]. As a solution to the above mentioned problems of either a

loss of mechanical properties during fiber degradation or the release of non-degraded fibers, the different degradation kinetics of fibers and cement matrix need to be adjusted. An approach is the use of more degradable cements based on the formation of dicalcium phosphate dehydrate (brushite) in conjunction with PLGA fibers.[292] Other promising works are dealing with degradable magnesium phosphate cements, which are reinforced with magnesium metal wires [294]. Especially, the latter provides strong reinforcement effects with a maximum bending strength of the composites of 139 MPa.

2.3.3 Dual setting cements

While the addition of non-reactive polymers (e.g., collagen, chitosan, hyaluronic acid, cellulose derivates) [255-257;295-296] is commonly used for improving cement cohesion or biological performance, it is only of small benefit for the mechanical cement performance. A reduction of the brittleness of CPC and an increase of strength can be achieved by using polymeric compounds which can be cross-linked by binding calcium ions due to a high density of either carboxylic acid or organic phosphate moieties in the polymer chain, e.g., polyacrylic acid [22;24;27;203;297] polymethyl vinyl ether maleic acid [24;27], poly[bis(carboxylatophenoxy)phosphazene] [219] or poly(vinyl phosphonate) [21]. Such polymer modified cements set both by the aforementioned dissolution–precipitation mechanism as well as by deprotonating the organic acid following the formation of intra- or inter-chained bonding Ca^{2+}–acid chelates [219] with a highly reactive cement component (mostly tetracalcium phosphate) from the cement powder. Processing of such polymer–cement composites is either possible by reacting an aqueous solution at ambient conditions with the cement powder or by reacting dry cement/polymer mixtures at elevated temperature/pressure in a solid state reaction.

An alternative approach is the use of reactive monomer systems, which are dissolved in the cement liquid and simultaneously react during cement setting by a gelation–polymerisation process. This forms within several minutes a hydrogel matrix with embedded cement particles, which are subsequently converted into the setting product by a continuous dissolution–precipitation reaction. The result is finally an interconnecting hydrogel matrix within the porous cement structure as shown in

Figure 14. The advantages of this strategy are the possibility of a high polymer loading of the cement (and hence a large strength and toughness increase) as well as practically unchanged rheological properties of the fresh cement paste. Both are related to the fact that the dissolved monomers are commonly small, water miscible liquids with low viscosity such that even high monomer concentrations are not strongly altering the initial cement viscosity.

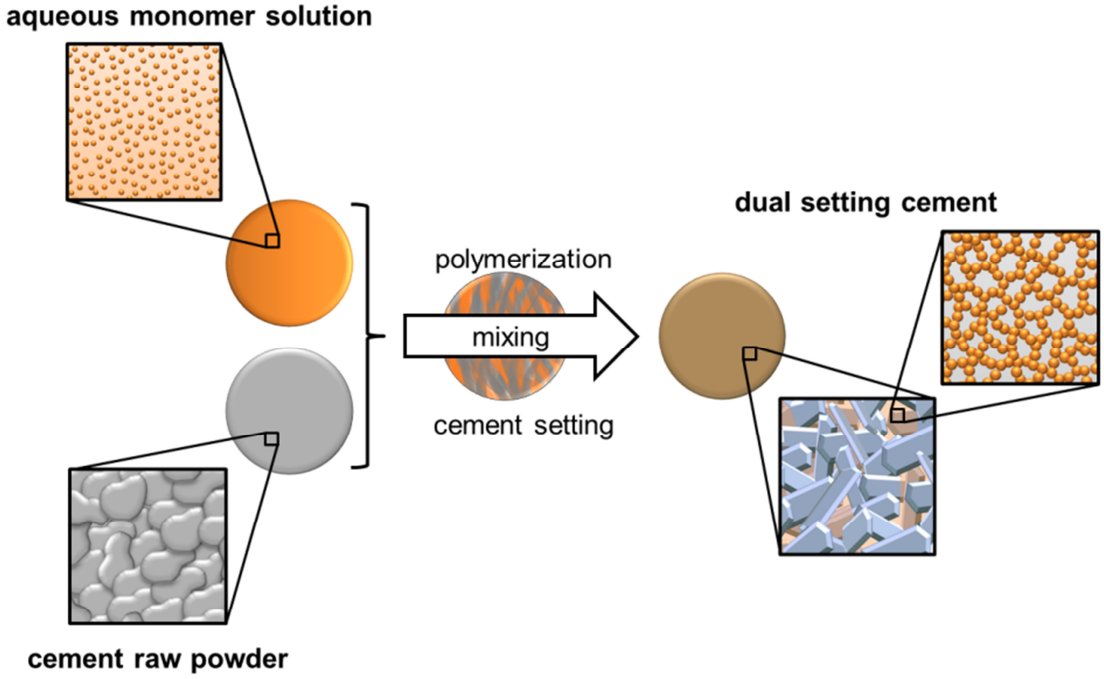

Figure 14: Hardening mechanism of dual-setting cements with the formation of interconnected matrices of hydrogel and precipitated cement crystals.

An early study regarding this concept was using mixtures of triethyleneglycol-dimethacrylate (TEGDMA), Bisphenol-A-dimethacrylate (Bis-GMA), hydroxyl-ethylmethacrylate (HEMA) and 10% water as cement liquid. After adding this liquid to an equimolar mixture of TTCP and DCPA, polymerization was initiated by benzoylperoxide (coating on cement particles) and di-(N,N)-2-hydroxyethyl-p-toluidine (added to the cement liquid) [26]. Although this study revealed high diametral tensile strengths of up to 26 MPa for such composites, no hydroxyapatite formation of the cement was observed even after 30 d storage in water. This was attributed to the low water content of the cement liquid as well as to an adsorption of the hydrogel on TTCP/DCPA cement particles. This problem was overcome by Dos Santos *et al.* [29-30;298] who modified the cement liquid of an α-tricalcium phosphate cement by the addition of 5 % – 20 % acrylamide and 1 % ammonium polyacrylate. While the latter was used to increase initial cement viscosity and to reduce cement

wash out in an aqueous environment, the acrylamide was chemically polymerised during cement setting by the use of 0.25 % of N,N,N',N'-tetramethylethylenediamide (TEMED) and 0.01 % ammonium persulfate. This modification doubled the compressive strength of the set cement from 25 – 50 MPa while the tensile strength was increased from 9 MPa to < 21 MPa. At the same time, the high water content of the cement liquid enabled setting of α-TCP cement particles to calcium deficient hydroxyapatite within seven days. A follow up study by the same authors extended the approach to a fiber reinforced–double setting cement matrix [30] by using 1 – 4 wt.-% of 4 – 10 mm long carbon, nylon and polypropylene fibers. The addition of the fibers was found to reduce the compressive strength of the cement, which was attributed to an increase of porosity. However, this was compensated by strong increase of the cement toughness and tensile strength, which increased from 17 – 28 MPa.

A major concern about this matrix is the toxicity of non-reacted acrylamide monomer. To overcome this problem, Christel *el al.* [28] investigated the modification of alpha-tricalcium phosphate cement (α-TCP) with 30 % – 70 % of less-toxic 2-hydroxyethylmethacrylate (HEMA), which also resulted in mechanically stable polymer-ceramic composites with interpenetrating organic and inorganic networks. Four-point bending strength was found to increase from 9 MPa to more than 14 MPa when using 50 % HEMA, and the bending modulus decreased from 18 GPa to approx. 4 GPa. In addition, cement composites with ≥ 50 % HEMA showed strongly reduced brittle fracture behavior with an increase of the work of fracture by more than an order of magnitude. While bending of pure ceramic samples was possible only to a maximum of 0.07 mm, samples with 50% or more HEMA monomer had a higher flexibility and bending was possible for 0.4 – 1.5 mm until fracture. At the same time, the authors could prove that important cement characteristics such as compressive strength or injectability were not significantly altered by using HEMA modification. Another study by Wang et al. [31] used methacrylate modified dextran as monomer in a cement matrix of tetracalcium phosphate/dicalcium phosphate anhydrous in a weight ratio of 10:1 - 1:3 (CPC: Meth.-dextran). The results showed an increase of the compressive strength from 24 – 83 MPa for a polymer content of 16.7 %, as well as improvement of the fracture energy by nearly two orders of magnitude from 0.084 – 8.35 $kJ \cdot m^{-2}$.

Apart from using organic monomers to form a second network in cements, it is also possible to apply the concept of dual setting cements to pure inorganic materials. Silica addition to CPC is a common approach to modify bioactivity, cement paste cohesion and mechanical cement properties.[299-300] However, most studies either used non-reactive silica fillers in cements [301-303] or they added non-reactive calcium phosphate particles to an in situ forming silica matrix prepared by sol-gel processing.[304-306] In contrast, Geffers *et al*. [261] modified a brushite forming cement paste with a second inorganic silica based precursor, which was obtained by pre-hydrolysing tetraethyl orthosilicate (TEOS) under acidic conditions. The addition of the cement powder (mixture of β-tricalcium phosphate and monocalcium phosphate) provoked an increase of the pH of the silica precursor such that cement setting by a dissolution–precipitation process, and the condensation reaction of the hydrolysed TEOS occurred simultaneously. This resulted in an interpenetrating phase composite material in which the macro pores of the cement (pore sizes in µm range) were infiltrated by the micro porous silica gel (pore sizes in nm range), leading to a higher density and a compressive strength approximately 5 – 10 times higher than the CPC reference.

2.3.4 Conclusion and outlook

This article features reinforcement strategies of biocements to improve their strength and toughness for an application at load-bearing defect sides. While porosity reduction is based on the optimization of an intrinsic cement property leading to higher strength, the addition of fibers or the creation of dual setting cement matrixes are extrinsic approaches not only improving strength but also toughness of the matrix. Surprisingly, most studies devoted to the mechanical properties of calcium phosphate biocements only deal with one of the presented strategies. Here, the simultaneous application of the different methods will definitely bring further improvements such that those optimized cements can likely be applied for load bearing defects. Desired mechanical properties would be likely similar to those of polymeric PMMA cements (bending strength ≥ 50 MPa, bending modulus ≥ 1800 MPa) compressive strength ≥ 70 MPa according to ISO 5833:2002 [307]), whereas few studies have already reached or even exceeded one of these parameters [246;294]. However, practically all strength values for CPC in literature

were obtained by test methods under static conditions and there are only few reports dealing with the fatigue properties of calcium phosphate cements in load-bearing defect models.[308-309] Hence, testing of cement strength under cyclic loading is one of the most important parameters which needs to be addressed in future research. In addition, since most of the studies on mechanically reinforced biocements were performed with only slowly degradable hydroxyapatite cement matrices and poorly or even non-degradable additives (fibers, polymers), the major challenge for the future is a transfer of the presented concepts to fully degradable materials. This is demanding since degradable cements based on the formation of brushite have harsh setting conditions (low pH, heat release, fast crystallization) and consume a considerable amount of water during setting. Especially, the latter may interfere with the formation of a second hydrogel phase, since the formation of hydrogel and hydrated cement setting product will compete for the available water in the cement liquid.

Chapter 3

Simultaneous formation and mineralization of star-PEO hydrogels

Chapter 3 is written in form of a publication manuscript, which is however not submitted or published by the time of the submission of this thesis.

Hydrogels are commonly used to mimic the extracellular matrix of soft tissues in tissue engineering applications. Due to their highly porous network structure and hydrophilicity, hydrogels provide a high water uptake capacity, whereby adequate diffusion rates of nutrients and biological agents can be realized resulting in the possibility to encapsulate bioactive drugs or even living cells.[310] Entrapped cells in such hydrogels are protected by the surrounding water against mechanical forces due to its incompressibility. Poly(ethylene oxide) (PEO) is a common basis polymer to build up three dimensional hydrogel matrices due to its cytocompatibility and the availability in a wide range of molecular weights.[311-312] PEO is a linear or branched molecule, which can be functionalized by hydroxy, amine, carboxylic acid, thiol and others end groups, whereby its chemical as well as physical properties can be modified and adapted to the specific application.[313] In comparison to the commonly used linear PEO molecules, branched PEOs (e.g. star shaped PEOs) give the opportunity of a higher end-group-density with more functionalization points.[314] Star shaped PEOs consist of a core molecule branched with three or more polymer chains, which can be equal or different in size and structure. This kind of polymers distinguishes by their unique properties caused by the defined structure of the arm`s number and length.[315-316] Based on the stereoscopic arrangement of the arms, the higher functional group density results in crosslinked gels with a comparable higher strength compared to gels from linear PEO molecules.[317]

Here a six armed star molecule functionalized with isocyanate groups as reactive termini (NCO–sP(EO-*stat*-PO)) was used.[318] The arms consist of a statistical copolymer of 80 % ethylene oxide and 20 % propylene oxide resulting in star molecules with a molecular weight of 12 kDa. In previous studies this system was used to produce ultrathin coatings on polymeric substrates to avoid unspecific protein adsorption due to the hydrophilic character, whereas a specific protein and ligand adsorption was possible by further functionalization of the isocyanate groups.[319-326] The hydrolysis of NCO–groups in aqueous solutions forms amines, which lead to an autocatalytic crosslinking of the star molecules to dense and well defined hydrogel structures by forming biocompatible urea groups with unreacted isocyanates.[319] A controlled freezing of the water in the hydrogel enabled the fabrication of oriented channels within the structure.[327] Furthermore, NCO–sP(EO-*stat*-PO) hydrogels were proved to be promising drug delivery systems.[328]

This chapter aimed to transfer the NCO–sP(EO-*stat*-PO) hydrogel system from soft tissue applications into hard tissue bone regeneration by applying an in situ mineralization step occurring simultaneously to hydrogel formation. Natural bone is an organic-inorganic composite of highly ordered collagen I fibrils (~95 % of the organic phase) and ~60-70 % nanocrystalline hydroxyapatite (HA) crystals resulting in a high fracture resistance for various mechanical loading situations.[329-330] It is hence obvious that mimicking the mechanical properties of bone tissue requires the defined mineralization of a polymeric template matrix.[331] Since many hydrogels commonly show only a low intrinsic mineralization capacity [332], nucleation sites for the mineralization have to be introduced. Gkioni *et al.* summarized the strategies for hydrogel mineralization in three groups: I) a biomimetic mineralization approach, II) chemical modification of the hydrogel with ion binding motifs and III) mineralization by adding inorganic particles.[333] The latter strategy includes a high diversity of nanocomposite hydrogels based on the addition of carbon [334], metal [335-336] silica [337-339], HA [340-341] or bioglass [342-343] particles to the hydrogel prior to gelation. The mineralization commonly leads to a mechanical reinforcement of the hydrogels by the embedded particles caused by their higher strength. However, the preparation of such nanocomposite is challenging due to insufficient mixing properties of two dissimilar phases with potential inhomogeneity caused by agglomeration and sedimentation of the nanoparticles within the gel.[344] Thereby the nanoparticle concentration is usually limited and a concentration between 60 and 70 wt.-% mineral phase similar to natural bone [345-346] cannot be realized. An approach to fabricate organic/inorganic composites with adequate mineral concentrations is to work with a dual setting system by adding relatively large (~10 µm) and reactive particles to the gel, which simultaneously convert into nanoparticles during gelation by a dissolution/precipitation reaction. This creates a composite with high mineral loads of up to 75 wt.-% and two entangled polymer and ceramic matrices. As a suitable ceramic particle systems, α-tricalcium phosphate (α-TCP) was applied in this study, which is known to form calcium deficient hydroxyapatite in a cementious reaction within a couple of hours [3;231]. Here, it is hypothesized that the combination of an autocatalytically cross-linking NCO–sP(EO-*stat*-PO) hydrogel with α-TCP particles results in a hydrogel mineralization equal to natural bone and a mutual reinforcing effect of the elastic hydrogel by the brittle inorganic mineral phase.

3.1 Materials and methods

Hydrogel preparation and mineralization

Hydrogels were produced by mixing NCO–sP(EO-*stat*-PO) (DWI Leibniz-Institute for Interactive Materials, Aachen, Germany) in 2.5 wt.-% $(NH_4)_2HPO_4$ solution at a concentration of 10, 30 and 50 wt.-% casted in cylindrical molds (Ø = 5 mm; h = 7 mm) and sealed for 24 h. For the mineralization 50, 67 or 75 wt.-% α-TCP powder was mixed with the NCO–sP(EO-*stat*-PO) hydrogel precursor and treated the same way. α-TCP was prepared by sintering $CaHPO_4$ (Mallinckrodt-Baker, Germany) and $CaCO_3$ (Merck, Germany) in a molar ratio of 2:1 for 5 h at 1400 °C following quenching to room temperature. The sintered cakes were crushed and passed through a 125 µm pore size-sieve followed by ball milling at 200 rpm for 4 h.

Characterization of non-mineralized hydrogel

Gelation kinetics were analyzed by Fourier Transform Infrared Spectroscopy (FT-IR; Nicolet is10, Thermo Scientific, Waltham, MA) in a range from 400 to 4000 cm^{-1} with spectral a resolution of 4 cm^{-1}. Compression test was performed using a dynamical mechanical testing machine (BOSE 5500 system, ElectroForce, Eden Prairie, MN, USA) and a 200 N load cell. The samples were loaded parallel to their long axis and tested at a constant cross head displacement rate of 0.01 $mm \cdot sec^{-1}$. For the swelling stress measurement the samples were fixed in the mechanical testing machine, phosphate buffered saline (PBS) was added and the emerging force due to swelling was recorded over time. To analyse the swelling behaviour the hydrogels were stored in 1 ml PBS, which was changed every 24 h whereby the hydrogel`s mass and dimension were measured. The equilibrium water content EWC (10) was determined by

$$EWC = \frac{w_s - w_d}{w_d} \cdot 100\ wt.-\% \tag{10}$$

and the swelling ratio based on the weight Q_w (11) by

$$Q_w = \frac{w_s}{w_d} \tag{11}$$

where w_s is the weight of the swelled hydrogel and w_d the weight of the dried hydrogel.

Mineralized hydrogel characterization

Mechanical testing of mineralized NCO–sP(EO-*stat*-PO) hydrogels was performed using a static mechanical testing machine (440, Zwick, Ulm, Germany) and a 2.5 kN load cell. For compression tests the samples were loaded parallel to their long axis and tested at a constant cross head displacement rate of 1 mm·min^{-1} under water. X-ray diffraction (XRD) patterns of samples were recorded using monochromatic CuK$_\alpha$ radiation (D5005, Siemens, Karlsruhe, Germany) in a 2Theta range from 2θ = 10 - 40° with a step size of 0.02° and a normalized count time of 3 sec·step^{-1}. The phase composition was checked by means of JCPDS reference patterns for α-TCP (PDF Ref. 29-0359) and HA (PDF Ref. 09-0432). A crossbeam scanning electron microscope CB 340 (Zeiss, Oberkochen, Germany) was used to analyse the surfaces of the composite monoliths. Samples were imaged using an accelerating voltage of 1 kV.

3.2 Results

Within five hours the isocyanate peak at 2263 cm^{-1} in the 30 wt.-% NCO-sP(EO-*stat*-PO) solution disappears completely, whereby the peak for the urea bridge (2715 cm^{-1}) increases indicating the successful polycondensation according to the reaction schema (Figure 15). As described above it was hypothesized that it is possible to reach a higher mineral content in the hydrogel by using a dual setting system, where the mineral particles were dissolved and precipitate as an additional network within the hydrogel, in comparison to the commonly used addition of unreactive mineral filler particles.

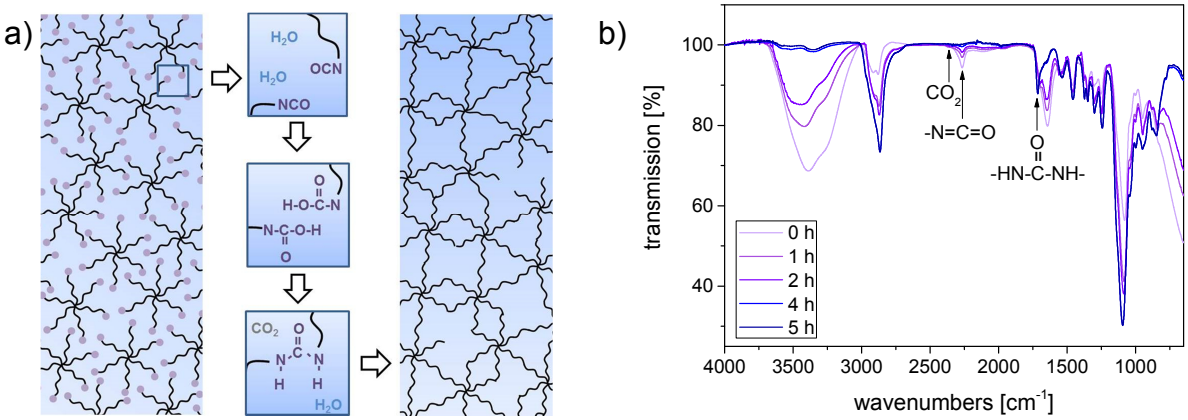

Figure 15: a) reaction schema and b) FT-IR spectra of 30 wt.-% NCO-sP(EO-*stat*-PO) solution during gelation.

To prove our hypothesis we compared the reactive mineral particles with unreactive ones. Tricalium phosphate (TCP) exists in two crystal forms: α-TCP reacts according to equation (12) to calcium-deficient hydroxyapatite (HA) due to its high solubility under physiological pH [96-97], whereas β-TCP do not hydrolyze readily and can be seen as unreactive counterpart. Indeed, up to 75 wt.-% α-TCP particles can be mixed with the aqueous monomer solution to get processible pastes, which can be molded and yield in a compressive strength of 15.7 ± 1.4 MPa after 24 h setting. Although β-TCP can be added in the same amount, the resulting strength is 30 times lower than for the α-TCP mineralized hydrogels (Table 5).

Additionally, we used precipitated HA nanoparticles as unreactive mineral phase, since this is the product of the α-TCP reaction.

$$3\ Ca_3(PO_4)_2 + H_2O \rightarrow Ca_9(PO_4)_5(HPO_4)OH \qquad (12)$$

For the HA nanoparticles an amount of only 50 wt.-% can be mixed with the aqueous NCO-sP(EO-*stat*-PO) solution, since higher contents result in a dry and friable bulk due to insufficient wetting of the particles. The HA nanoparticles are much smaller and have a plate like structure (Figure 16 c), which results in a higher surface area in comparison to the boulder like TCP particles. Furthermore the strength is only half of the comparable α-TCP mineralized hydrogel. This shows the positive effect by using a reactive mineralization system for the hydrogel`s properties, which is furthermore analyzed in detail below for the system with α-TCP as mineral source.

Table 5: Overview of the workability and strength of 30 wt.-% NCO-sP(EO-*stat*-PO) hydrogels mineralized with α-TCP, β-TCP or HA nanoparticles.

	mineral material					
	α-TCP powder		**β-TCP powder**		**HA nanoparticles**	
reactivity	yes		no		no	
mineral content	workability	strength in MPa	workability	strength in MPa	workability	strength in MPa
50 wt.-%	yes	2.1 ± 0.1	yes	n.a.	yes	1.0 ± 0.1
67 wt.-%	yes	6.9 ± 0.4	yes	n.a.	no	-
75 wt.-%	yes	15.7 ± 1.4	yes	0.5 ± 0.1	no	-

n.a. = not analyzed

All mineral particles show a good adhesion to the hydrogel phase and a homogeneous distribution within the hydrogel (Figure 16) at a mineral content of 50 wt.-%.

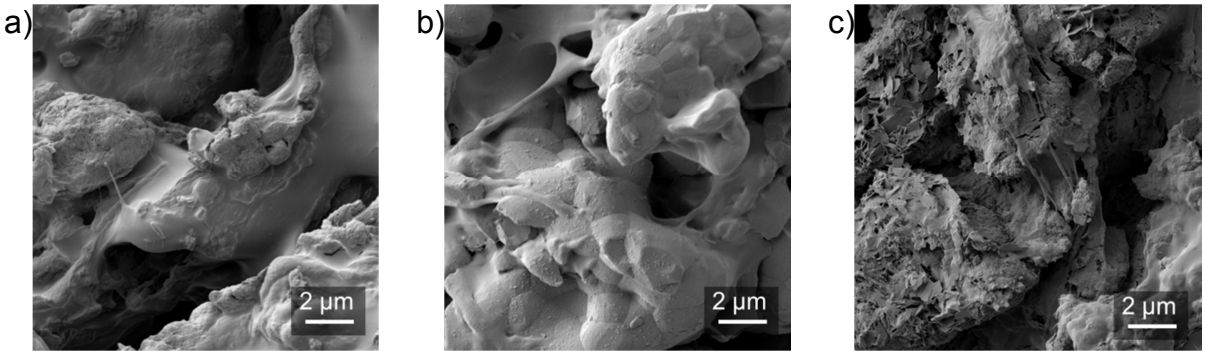

Figure 16: SEM images of of 30 wt.-% NCO-sP(EO-*stat*-PO) hydrogels mineralized with 50 wt.-% a) α-TCP, b) β-TCP or c) HA nanoparticles.

Figure 17 shows the mechanical properties of the 10 – 50 wt.-% NCO-sP(EO-*stat*-PO) hydrogels with a mineral content between 0 and 75 wt.-%. The elasticity and compressive modulus of the non-mineralized hydrogels decreased with an increasing amount of NCO-sP(EO-*stat*-PO) in the hydrogel, whereas the compressive strength increased. Generally, the mineralized hydrogels showed a reduced elasticity, but improved strength, Young`s modulus and toughness values.

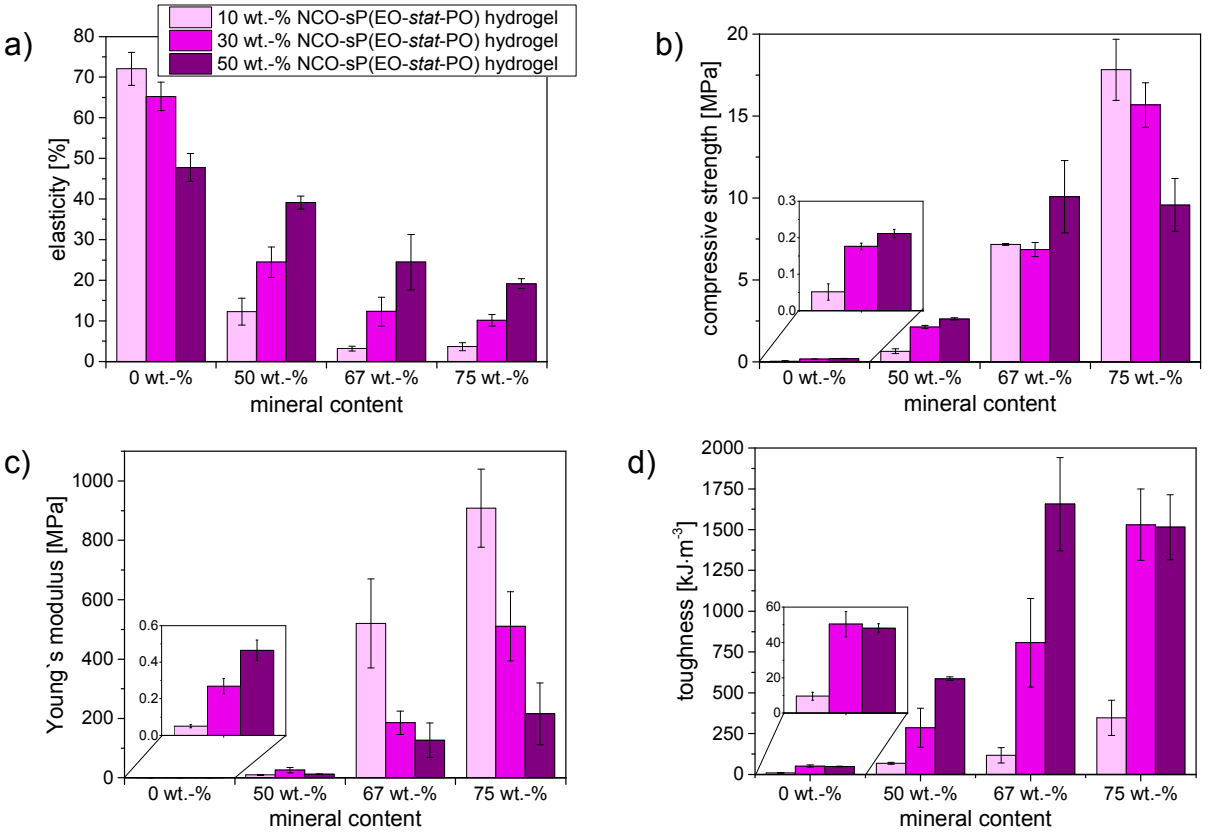

Figure 17: Mechanical properties of the compression test: a) elasticity, b) strength, c) E-modulus and d) toughness of 10, 30 or 50 wt.-% NCO-sP(EO-*stat*-PO) hydrogels with a mineral content between 0 and 75 wt.-%.

The properties of the pure hydrogels are clearly affected by the additional mineral phase. The relationship between elasticity or Young`s modulus and polymer content is reversed by mineralization. With a lower polymer content of the hydrogel the mineral phase properties becomes more dominant. Here, the mineral framework prohibits the elastic hydrogel phase from deformation, which results in improved strength and Young`s modulus. With a mineral content of 75 wt.-%, the strength values decreased with an increasing polymer content. This can be attributed to the reduced conversion rate of the mineral phase to calcium deficient hydroxyapatite, whereby the mineral matrix is not completely set due to the denser polymer network working as a diffusion barrier for calcium and phosphate ions and hence prohibiting HA precipitation. The crystal growth is reduced with a simultaneous decrease of crystal entanglement and mechanical performance.

The as prepared mineralized hydrogels includes the water amount, which was used for the preparation. After placing the gels in an aqueous environment, the as prepared hydrogels are able to absorb additional water by swelling until the osmotic force and the elastic force are in equilibrium.[347-348] This results in a volumetric change of the hydrogel. Since the hydrogel and the mineral phase inwrought each other, the swelling stress from the water uptake is a crucial factor for the composites properties. Such pre-stressed hydrogels could be beneficial for the mechanical composite properties, if it is tensed in the opposite direction than the exterior applied load. On the other hand, a higher swelling pressure than the matrices strength may cause damages of the hydrogel as well as the mineral network within the composite bulk. Table 6 shows a summary of the swelling properties. After 24 h the swelling equilibrium is reached and did not change further over the following 14 days. Here especially the water uptake from the as prepared (ap) to the swollen (s) state and in detail the volumetric change $\Delta V_{s,ap}$ is important for the characterization phenomena within the mineralized hydrogel.

Obviously a concentration of 90 wt.-% water in the 10 wt.-% NCO-sP(EO-*stat*-PO) hydrogel represents the maximum water uptake ability of the polymeric network since nearly no mass and volumetric change from the as prepared to the swollen state was observed.

Table 6: A summary of the swelling properties of 10 – 50 wt.-% NCO-sP(EO-*stat*-PO) hydrogels like equilibrium weight content (EWC), swelling ratio (Q) and its change from as prepared to swollen ($\Delta Q_{s,ap}$), and volumetric change (ΔV) of the hydrogels.

hydrogel	EWC in wt.-%	Q_{ap}	Q_s	$\Delta Q_{s,ap}$	$\Delta V_{s,ap}$ in %
10 wt.-%	90.5 ± 0.1	10.2 ± 0.1	10.1 ± 0.4	0.1 ± 0.4	105.1 ± 1.8
30 wt.-%	84.4 ± 1.8	3.0 ± 0.2	6.6 ± 0.7	3.6 ± 0.7	195.3 ± 35.9
50 wt.-%	84.9 ± 1.6	1.8 ± 0.1	6.8 ± 0.7	5.0 ± 0.7	277.6 ± 22.5

The 30 and 50 wt.-% NCO-sP(EO-*stat*-PO) hydrogels show almost the same EWC value of ~ 84. This in comparison to 10 wt.-% hydrogel lower value can be explained by the smaller mesh size of the network, since the higher polymer content results in an increased crosslinking with the availability of less “dead” end groups. The denser network has a lower ability to extend and hence a reduced total water absorption capacity. Nevertheless, the water uptake from the as prepared hydrogels is increasing with the polymer content, as it is obviously by the comparison of the swelling ratio ($\Delta Q_{s,ap}$) and the volumetric ($\Delta V_{s,ap}$) change.

While the volume of the 10 wt.-% hydrogel remains constant, the 50 wt.-% is almost tripled. In composite, the mineral matrix acts as a frame and prohibits the expansion caused by the water uptake of the hydrogel. Thus inner stress appears, which may lead to a breakdown of the mineralized hydrogel. Therefore we analyzed the arising swelling pressure within the non-mineralized hydrogels over the first 24 h of swelling (Figure 18 a).

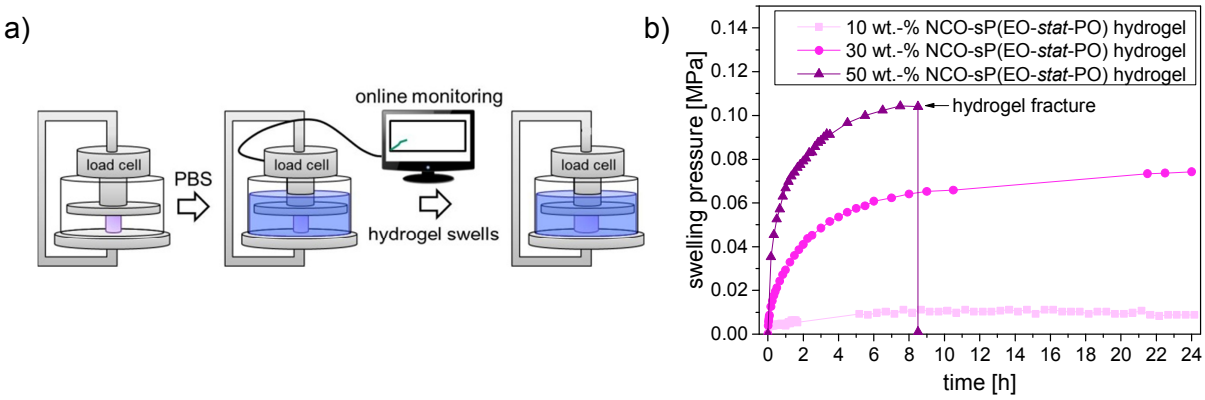

Figure 18: a) model of the swelling pressure measurement set up and b) exemplary swelling pressure vs. time curves of as prepared 10 – 50 wt.-% NCO-sP(EO-*stat*-PO) hydrogel.

While the fixed 10 and 30 wt.-% NCO-sP(EO-*stat*-PO) hydrogels survived this swelling regime, 50 wt.-% NCO-sP(EO-*stat*-PO) hydrogels failed within the first 10 h

(Figure 18 b). The swelling pressure exceeds the tensile strength of the hydrogel, which agrees with the compressive test results for the 50 wt.-% hydrogels (Figure 17 b).

On the basis of these previous results, 30 wt.-% NCO-sP(EO-*stat*-PO) hydrogel with 75 wt.-% mineral content and a balanced combination of elasticity and strength resulting in a high toughness, was chosen for further long-term studies over 28 days. Additionally, the corresponding pure mineral phase in form of a calcium phosphate cement (CPC) was used as a second reference to rank the received values.

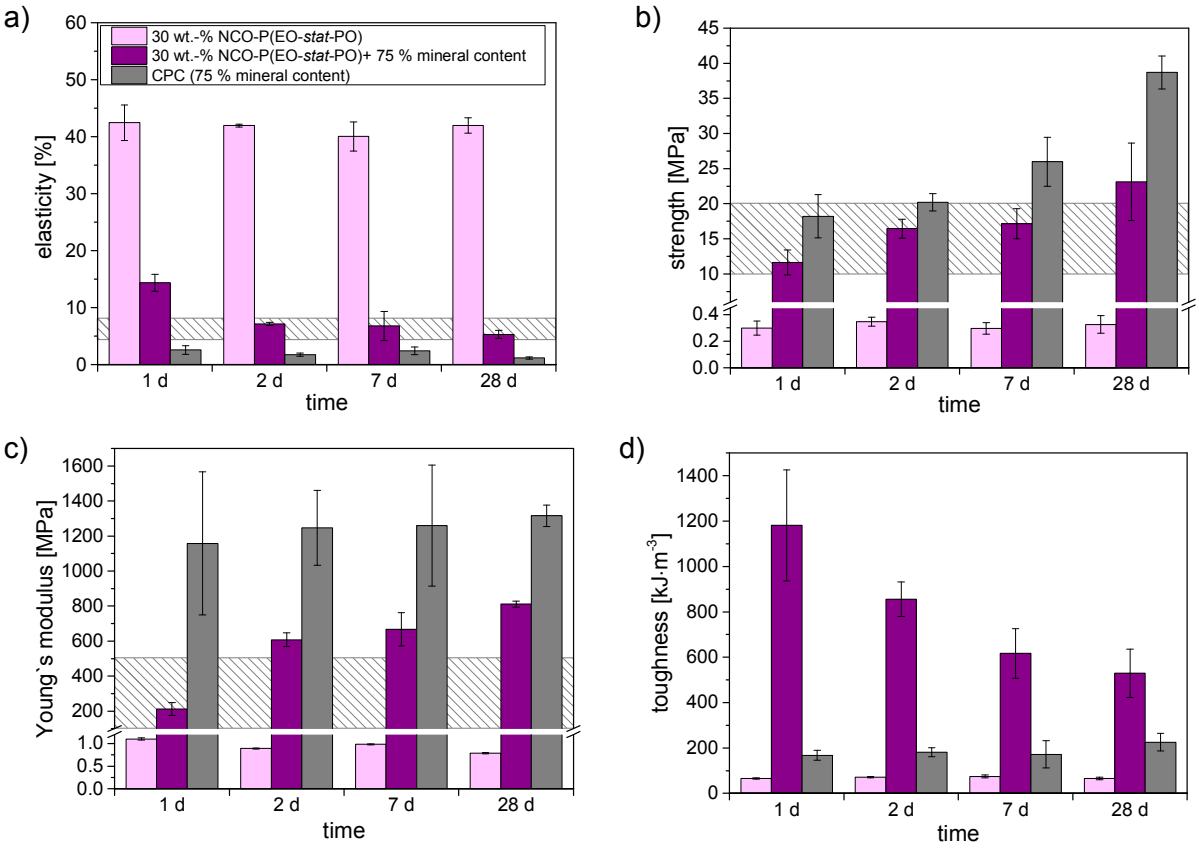

Figure 19: Mechanical properties of the compression test: a) elasticity, b) strength, c) E-modulus and d) toughness of 30 wt.-% NCO-sP(EO-*stat*-PO) hydrogels with a mineral content of 0 or 75 wt.-% and the corresponding CPC with a mineral content of 75 wt.-%; the shaded area indicates the mechanical properties of cancellous bone range [114].

As expected, the mechanical properties of the non-mineralized hydrogel remained constant over the 28 days, since NCO-sP(EO-*stat*-PO) crosslinking is complete after 24 h. In contrast, the mineralized hydrogel showed a time dependent change of the mechanical properties. While the elasticity as well as the toughness decreased, both strength and compressive modulus increase with time (Figure 19).This is probably caused by the proceeding setting reaction of the mineral phase over several days, whereby the cement matrix properties are subsequently dominating the hydrogel

component. Nevertheless, the mechanical properties of the mineralized hydrogels remain within the range of cancellous bone during the whole time period. Although the compressive strength and modulus of pure CPC are higher than those of the mineralized hydrogel, pure CPC suffers from a low elasticity and thereby an insufficient toughness. The elasticity was always below the value needed for cancellous bone. As shown in Figure 20, the reactant α-TCP is still present after one day and only a slight conversion into HA was observed. The mineral phase continuously set into HA over the following 28 days, whereby the mineral matrix is built up by the entanglement of the new formed HA crystals.

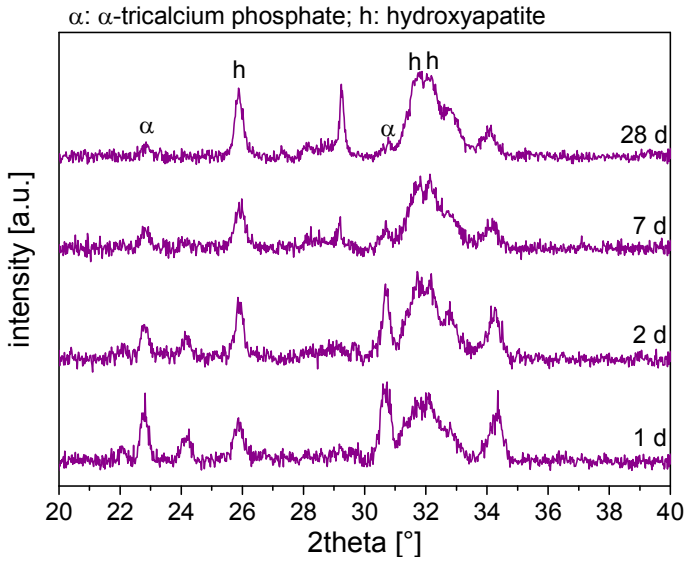

Figure 20: XRD patterns of the mineral phase in 30 wt.-% NCO-sP(EO-*stat*-PO) hydrogel on day 1, 2, 7 and 28 after fabrication. α indicates α-tricalcium phosphate and h indicates hydroxyapatite.

As the hydrogel works as a diffusion barrier, the crystal dimension of HA is smaller than by a precipitation in a low viscous fluid like water. This was further analysed by applying the Scherrer equation (13) to the XRD patterns from Figure 20:

$$d = \frac{k \cdot \lambda}{\beta \cdot \cos(\Theta)} \tag{13}$$

where K is the dimensionless shape factor, λ the X-ray wavelength, β is the full width at half maximum of the characteristic peak and θ the diffraction angle. This results in crystal dimensions of 28.9 ± 2.0 nm for the minerals grown in NCO-sP(EO-*stat*-PO) hydrogel and 40.4 ± 5.3 nm for the mineralization in water.

3.3 Discussion

Hydrogels are of high interest for the use as biomaterial scaffold and are widely used in soft tissue engineering applications. With regard to hard tissue, they suffer from low mechanical strength and insufficient mineralization properties. Therefore mineralization nuclei have to be provided, which can be realized by a variety of strategies.[333] Since HA is the natural inorganic phase in hard tissue, most approaches to mimic bone matrix composition deal with the incorporation of precipitated HA nanoparticles into a suitable hydrogel. The preparation of such mineralized hydrogels is typically a two-step process: (I) The gelation of the hydrogel and (II) the precipitation of the HA nanoparticles. After hydrogel formation, it is usually soaked in calcium and phosphate containing solutions such as simulated body fluid [349] or a combination of $CaCl_2$ and Na_2HPO_4 [350] at a neutral pH, whereby crystalline hydroxyapatite is deposited in the pores of the hydrogel over a time course of several days [351]. Alternatively, HA nanoparticles are precipitated separately in highly diluted calcium/phosphate solutions to prohibit their agglomeration and added afterwards as dry powder by mixing with the monomer solution previous gelation.

The grading of a newly developed mineralized hydrogel system within the literature is challenging, since a high diversity of application fields and hydrogels with different gelling/polymerization mechanisms and properties are available (Table 7). Nevertheless, our system distinguishes from a one-step preparation regime by the possibility of a high mineral content comparable to natural bone even at high polymer concentrations (up to 50 wt.-%) and a remarkable mechanical improvement due to the additional entangled mineral matrix (~100 times).

The percentages of dried natural bone with 30 wt.-% organic and 70 wt.-% inorganic material are well known numbers in biomaterial science and are often adducted for the comparison with mineralized hydrogels with negligence of the water amount. Indeed, hydrogels are commonly prepared by polymer concentrations between 3 and 20 wt.-% (Table 7). Especially, for the mineralization by soaking calcium and phosphate ions low concentrated hydrogels are used to guarantee fast ion diffusion and mineral precipitation, however resulting in low density composites. In contrast, the water content in bone is low with values between 5 and 25 wt.-% [352-353] yielding in a highly concentrated “collagen hydrogel” (54 – 85 wt.-%) with a mineral

content of 60 – 70 wt.-%. Here, we were able to realize a composite with a similar highly concentrated hydrogel (up to 50 wt.-% NCO-sP(EO-*stat*-PO)) as well as a mineral content in the range of natural bone (50 – 75 wt.-%). In contrast to the maximum of 50 wt.% non-reactive HA nanoparticles, which were simply mixed into the monomer solution prior to gelation, up to 75 wt.-% of more reactive α-TCP could be added to the solution still resulting in a processible paste. Additionally, the compressive strength was doubled (compared to HA nanoparticles) or even 30 times higher (compared to non-reactive β-TCP) for this system. This can be attributed to the simultaneously occurring setting reaction of the mineral phase. Here, the mineral particles are not only fillers, but react to an entangled matrix with a skeleton like function for the hydrogel. This property of α-TCP (and mixtures of other calcium phosphates) is commonly used for the hydraulic setting reaction of calcium phosphate cements (CPC). The latter are of high interest for clinical applications since their phase composition is similar to natural bone, but suffer from their brittle fracture behavior with a low elasticity in comparison to bone. While crystalline α-TCP reacts to HA within 48 h at a setting temperature of 37 °C [354-355], prolonged ball milling leads to a partial amorphisation with a strong increase in solubility and hence reactivity.[66] Thereby the particles are immediately dissolved in contact with aqueous monomer solution and a higher content of mineral can be homogeneous mixed in consequence of the lower viscosity. Furthermore, 2.5 wt.-% Na_2HPO_4 solution was used to prepare the monomer solution instead of pure water, which works as a reaction accelerator for cement setting [356]. Thus it was possible to simultaneously trigger NCO-sP(EO-*stat*-PO) gelation and cement conversion into HA according to equation (12). Thereby a one-step preparation regime without any further stimuli could be realized without the use of crosslinking agents or UV irradiation for the polymerization as well as post treatment for the mineralization step. Moreover the strength of the hydrogel was increased by two orders of magnitude by the mineralization step (Figure 17), since a second matrix was built within the hydrogel network by the entanglement of the precipitated HA nanocrystals [16]. Thereby we matched the mechanical properties of cancellous bone (Figure 19).[114;357] While the mineral matrix works as a skeleton within the composites, the hydrogel is prohibited from extreme deformations, e.g. by swelling. Thus the mineralized hydrogel remained both shape and volume (100.4 ± 2.4 vol.-% related to the as prepared mineralized hydrogel) and a low swelling ratio of 1.32 ± 0.02.

Table 7: Literature overview of mineralized hydrogels and their properties concerning composition, preparation duration and mechanical strength.

polymer	hydrogel concentration	mineral content		mineralization method	mineralization duration	strength	
		hydrogel	dried composite			pure hydrogel	mineralized hydrogel
collagen [358]	-	-	60 – 70 wt.-%	Soaking in $CaCl_2$ and Na_2HPO_4	5 min – 5 h	-	6 – 11 MPa [TS; d]
gelatin [359]	3 wt.-%	50 wt.-%	-	wet precipitation method & mixing	-	70 ± 30 kPa [TS; HG]	230 ± 40 kPa [TS; HG]
gelatin [360]	4 wt.-%	-	79 wt.-%	wet precipitation method & mixing	-	-	-
chitosan/gelatin [361]	-	-	50 wt.-%	wet precipitation method & mixing	48 h	10.5 ± 1.5 MPa [CS; d] 29 MPa [TS; d]	6.53 MPa [CS; d] 4.2 ± 2.9 MPa [TS; d]
pectin [362]	10 wt.-%	-	-	Soaking in $CaCl_2$ and SBF	7 d	-	37.7 ± 5.9 MPa [TS; d]
cellulose [363]	-	-	50 – 90 wt.-%	Soaking in $CaCl_2$ and Na_2HPO_4	2 – 10 d	-	-
cellulose/poly (acrylic acid) [364]	40 - 57 wt.-%	-	6 – 25 wt.-%	Soaking in $CaCl_2$ and $(Na_4)_2HPO_4$	5 d	-	-
alginate [365]	1 – 3 wt.-%	0.1 – 1.2 wt.-%[c]	-	commercial particle were mixed	-	-	-
poly(acryl amide) [366]	10 – 25 wt.-%	-	29 – 39 wt.-%	electrophoretic mineralization	-	12 - 25.3 MPa [CS; HG]	16.5 - 35.5 MPa [CS; HG]
poly(vinyl alcohol)/ collagen [367]	15 wt.-%	33 – 41 wt.-%	-	spray coated particles were mixed	24 h	-	19 – 28 kPa [CS]
poly(ethylene glycol) [340]	20 wt.-%	5 – 15 wt.-%	-	commercial particle were mixed	1 h	100 ± 16 kPa [TS; HG]	372 ± 68 – 796 ± 223 kPa [TS; HG]
poly(ethylene imine) [368]	50 mg	-	10 wt.-%	Soaking in Na_2HPO_4 and SBF	24 d	-	-

- not mentioned; TS = tensile strength; CS = compression strength; d = dried state; HG = hydrogel state; c = calculated

The hindered water uptake and swelling due to the mineral matrix creates internal loads such that the hydrogel is pre-stressed resulting in further improvements of strength. Pre-stressing of structural elements is an established method in construction industry to adapt the crack behavior and capacity to absorb energy. Here, a pre-determined stress is applied to a system to enhance the resistance against external loads.[369-370]

3.4 Conclusion

It was possible to mineralize even highly concentrated NCO-sP(EO-*stat*-PO) hydrogels with a mineral content comparable to natural bone by using a mineralization method, where an additional inorganic matrix was built up within the hydrogel network by a calcium phosphate cement. Key requirements to combine such dissimilar materials are (I) an aqueous monomer solution, in which the CPC raw powder can be dissolved and (II) that the cement setting as well as the polymerization are not prohibited by the reaction properties of the other component. Since HA is the main mineral component in hard tissue, it was used here as a model inorganic phase, but other calcium or magnesium phosphate phases should also be processible by this manufacturing approach.

Chapter 4

Dual setting brushite - silica gel cement

Chapter 4 was published as original research article (Geffers M., Barralet J. E., Groll J., Gbureck U.; Dual-setting brushite-silica gel cement. Acta Biomaterialia 2015; 11 467-476; reproduced from [261] with permission from Elsevier). The article is based on the work of the author of this dissertation thesis Martha Schamel née Geffers, who developed and characterized the composite material, designed and performed all experiments, interpreted and graded the data and wrote the manuscript.

Mineral biocements based on calcium phosphate chemistry (CPC) set by a continuous dissolution – precipitation reaction, in which the cement reactants dissolve after contact with an aqueous phase leading to a supersaturated liquid with regard to the setting product. The latter simultaneously precipitates from the liquid cement phase leading to a hardening of the cement pastes after sufficient crystal entanglement. [3] The type of setting product formed by the reaction is affected by the pH conditions in the cement paste. While at neutral or basic pH nanocrystalline hydroxyapatite ($Ca_{10}(PO_4)_6(OH)_2$, HA) is precipitated, a strong acidic pH<4.2 has been shown to lead to a matrix predominantly composed of secondary, protonated calcium phosphates such as brushite (CaHPO4•2H2O) [151] or monetite (CaHPO4) [159-160]. The final mechanical strength of set CPC matrices were found to depend on several factors, such as the degree of cement conversion [67], cement porosity [17], kind of setting product [48], crystal size [371] or the use of filler particles [372]. Due to their brittle behavior and their compared to polymeric cements low mechanical performance, CPC are indicated only to non- or low-load bearing applications such as defects in craniomaxillofacial surgery.[231] Most approaches for a reinforcement of CPC are based on an optimization of the above mentioned parameters as well as on the addition of fibers [18] to increase bending strength and work of fracture due to fiber pull-out and energy dissipating mechanisms. However, fiber reinforcement has a detrimental effect on the rheological and injection properties of CPC and the fibers used in many studies are of a non-degradable nature. [18-19] A relatively new approach are dual setting CPC, in which the cement liquid is modified by a water soluble monomer, which is simultaneously polymerized during cement setting such that an interconnecting hydrogel matrix within the porous cement structure is formed.[28-30]

In the current study, we extended this dual setting concept by combining the brushite forming cement paste with a second inorganic silica based precursor. The latter is formed via the sol gel process by the hydrolysis and condensation of tetraethyl orthosilicate (TEOS) forming a nanoporous silica network under acidic conditions. The reaction conditions of the cement pastes were altered in such a way, that following combination of the cement powder with the liquid silica precursor both the cement setting reaction and silica gelation occurred simultaneously such that interpenetrating silica – brushite networks with a bimodal pore size distribution are formed in the set matrix.

4.1 Materials and methods

β-TCP was prepared by sintering $CaHPO_4$ (Baker, Renningen, Germany) and $CaCO_3$ (Merck, Darmstadt, Germany) in a molar ratio of 2:1 for 5 h at 1050 °C. The sintered cakes were crushed and sieved with 100 µm pore size-mesh followed by ball milling in a planetary ball mill (Retsch, Haan, Germany) for 60 min at 200 rpm. Brushite cements were produced by mixing the β-TCP powder in an equimolar ratio with dicalcium phosphate anhydrous ($Ca(H_2PO_4)_2$, MCPA, Aldrich, Steinheim, Germany) in a coffee grinder for 30 sec. Silica gel was produced by the sol gel process under acidic conditions. Briefly, the precursor tetraethyl orthosilicate (TEOS, Sigma-Aldrich GmbH, Steinheim), 0.1 M HCl and deionized water were mixed and stirred to form an acid catalyzed sol. Different H_2O to TEOS ratios (X) with $3 \leq X \leq 15$ were used to analyze the influence of this parameter on the composite properties. Finally, cement pastes were formed by manually mixing CPC powder and the liquid sol. The pastes were then transferred into silicon moulds and sealed. After three days of setting at 37 °C the cement blocks were transferred into a water bath with 100 % relative humidity and 37 °C for further 24 h. As reference, the CPC powder was mixed with either water or a 0.5 M citric acid solution and treated just as the composite material. Modification with vancomycin hydrochloride as a model drug was performed by adding 5 wt.-% vancomycin to the cement liquid phase. After setting, these cement samples (10 x 5 x 5 mm^3) were immersed in 1 ml PBS-buffer at 37 °C, which was changed every second day. The vancomycin content of the eluate was determined by UV/VIS spectroscopy at 280 nm.

Cement characterization

Initial setting time was measured by the Gilmore needle test in a humidity chamber at 37 °C and >90 % rel. humidity. Setting pH and temperature were measured at room temperature (22 ± 1 °C). For compressive strength measurements the CPC/silica gel composites were produced with different silica and CPC contents. The sol gel component was produced with water to TEOS ratios (X) between 3 and 15 and the powder to liquid ratio (PLR) was varied between 0.5 and 2.5 g/ml. For each parameter five samples (10 x 5 x 5 mm^3) were measured after setting for 24 h at 37°C under wet conditions. Mechanical testing was performed using a static mechanical testing machine (440, Zwick, Ulm, Germany) and a 2.5 kN load cell,

samples were loaded parallel to their long axis and tested at a constant cross head displacement rate of 1 $mm \cdot min^{-1}$. Porosity characteristics such as pore size distribution, median pore size and pore volume were measured by nitrogen adsorption (BET-method, Autosorb-iQ-AG, Quantachrome, Odelzhausen, Germany) and mercury (Hg) porosimetry (PASCAL 140/440, Porotec GmbH, Hofheim, Germany). Set cement samples were dried at 37 °C for 24 h prior to measurement. For BET, the samples were additional dried in vacuum for 48 h at 50 °C and outgassed for 72 h. Scanning electron microscopy (SEM; Zeiss DSM930) was used to analyse the gold coated fracture surfaces of the ceramic monoliths. Samples were imaged using an accelerating voltage of 10 kV. X-ray diffraction (XRD) patterns of samples were recorded using monochromatic CuK_α radiation (D5005, Siemens, Karlsruhe, Germany). Data were collected from $2\theta = 20 - 40$ ° with a step size of 0.02 ° and a normalized count time of 1 $step \cdot sec^{-1}$. The phase composition was checked by means of JCPDS reference patterns for brushite (PDF Ref. 09-0077), monetite (PDF Ref. 09-0080) and β-TCP (PDF Ref. 09-0169).

In vitro cytocompatibility testing

The osteoblastic cell line MG 63 (ATCC no. CRL-1427, Rockville, MD) was cultured at 37 °C and 5 % CO_2 in Dulbecco's Modified Eagle's Medium (DMEM, Invitrogen Life Technologies, Karlsruhe, Germany). The culture medium was supplemented with 10 % foetal calf serum, 100 $U \cdot mL^{-1}$ penicillin, and 100 $mg \cdot mL^{-1}$ streptomycin (all from Invitrogen Life Technologies). The medium was changed in fixed intervals of 2 days. During the experiments cells were cultivated on polystyrene (PS), hydroxyapatite (PLR: 3 $g \cdot mL^{-1}$), brushite (fabricated with H_2O or 0.5 M citrate acid; PLR: 1 or 2 $g \cdot mL^{-1}$) or CPC/silica gel composite (X: 15, 9 or 3; PLR: 1 or 2 $g \cdot mL^{-1}$). Previously every cement disk was washed for 24 h in 3 mL PBS at 37 °C. For biocompatibility tests samples were placed in quadruplicate into the wells of a 24-well plate and covered with cell suspension. The cytocompatibility tests of the cement surfaces were performed by means of cell counting and determination of cell activity after 2, 6, 10, and 14 days in culture on all surfaces as described in detail elsewhere.[373] Briefly, cell proliferation was analyzed by electronic cell counting using a CASY 1 TTC cell analyzer (Schärfe System, Reutlingen, Germany), while cell viability was analyzed using the cell proliferation reagent WST 1 (Roche Diagnostics, Mannheim, Germany).

After incubating the cells for 30 min with the WST reagent diluted 1:10 in DMEM at 37 °C, the absorption of the supernatant was quantified in a Tecan spectra fluor plus photometer (Tecan, Crailsheim, Germany). For each method and sample four readings were recorded and the mean values and standard deviations were calculated. Statistical analysis was performed using the ANOVA t-test in Microsoft Excel, in which CPC/silica gel composites were compared with the CPC reference (1 g·mL^{-1} brushite). Ion concentrations (Ca, P, Si and Mg) in the used cell culture medium were determined using inductively-coupled-plasma mass-spectrometry (ICP-MS, Varian, Darmstadt, Germany). The quantitative measurement was carried out against standard solutions (Merck, Darmstadt, Germany) containing defined concentrations of all ions of interest.

4.2 Results

With a decreasing X the setting time increased from few minutes (2.2 ± 0.3 min) of the pure CPC to 43.0 ± 2.6 min of the composite with X of 3 (Table 8). The composite shows a thixotropic behavior during the setting reaction such that the paste could be refluidized by mechanical load until the cement was completely hardened. Both the CPC reference and the CPC/silica gel composites set at an acidic pH between 1.5 and 5 (Figure 21 a), whereas lower pH values were obtained with decreasing X due to the higher absolute HCl content in these cements. After 60 min the pH of the different composites rised by approximately 0.3 (X=3) up to 1.5 (X=15).

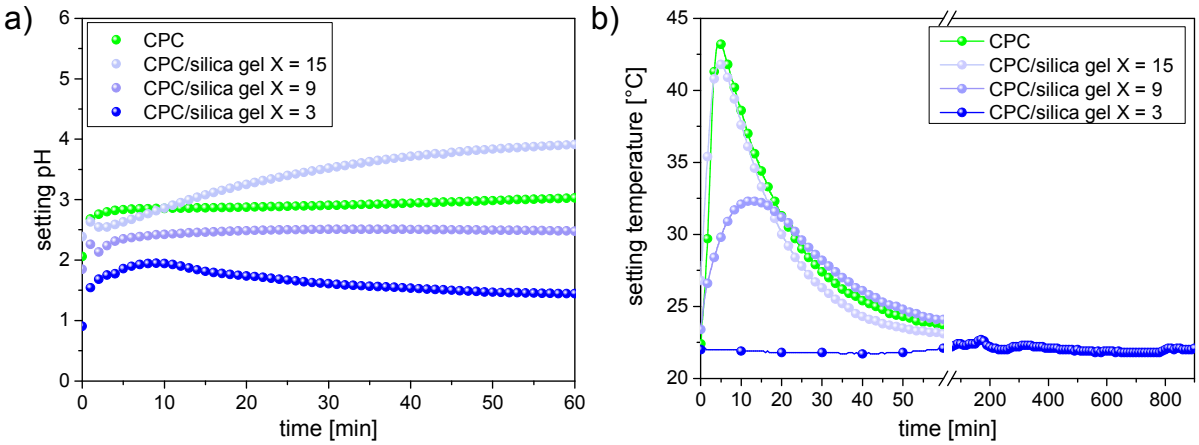

Figure 21: Setting pH (a) and temperature (b) of CPC reference (with water, PLR = 1 g/ml) and CPC/silica gel composite (PLR = 1 g/ml), where the acidic sol of the composite was produced with H_2O/TEOS of 15, 9 and 3 (n=3).

The pure CPC shows a fast and exothermic reaction with a maximum temperature difference during setting ($\Delta_{max}T_{set}$) of 19.2 ± 0.8 °C (Table 8), which results in a maximum setting temperature of 41.2 ± 0.8 °C. For silica – cement composites with a high water content (X=15) $\Delta_{max}T_{set}$ was found to be nearly the same (17.8 ± 1.0 °C), while a decrease of the water content in the liquid sol (X=9) decreased $\Delta_{max}T_{set}$ to 8.5 ± 1.2 °C. The setting temperature of the CPC/silica gel composite X=3 showed no exothermic behavior at all (Figure 21 b).

Table 8: pH and gelation time of the pure silica gels and setting time, pH and temperature of CPC reference (H_2O) and the CPC/silica gel composite with X of 15, 9 and 3 (n=3).

material	pH of liquid phase	gelation time pure silica gel [h]	setting time [min]	setting pH after 60 min	Δ_{max} setting temp. [°C]	max. setting temp. [°C]
CPC reference	ca. 5	-	2.2 ± 0.3	4.7 ± 0.1	19.2 ± 0.8	41.2 ± 0.8
CPC/silica gel X=15	2.2 ± 0.2	230	2.8 ± 0.3	3.7 ± 0.2	17.8 ± 1.0	39.8 ± 1.0
CPC/silica gel X=9	1.9 ± 0.1	192	5.2 ± 0.6	2.5 ± 0.1	8.5 ± 1.2	30.5 ± 1.2
CPC/silica gel X=3	1.2 ± 0.2	138	43.0 ± 2.6	1.5 ± 0.1	-	22

BET analyses of the pure CPC reference indicated only a marginal fraction of pores below 100 nm (Figure 22 a). As expected the pure silica gel showed a clear pore size distribution between 1 and 10 nm (Figure 22 b). BET measurements on combined materials confirmed the presence of these pores in the CPC/silica gel composite (Figure 22 c).

Larger pores >100 nm were analysed in the CPC reference and the CPC/silica gel composite with X = 3, 9 and 15 by Hg porosimetry. All pore size distributions of the CPC reference as well as the different composites show nearly the same trend with most pores being in the range between 0.1 and 10 µm and an absence of pores >10 µm (Figure 23). The pore size distribution shifted to smaller values with decreasing X (increasing silica gel content) indicating that the bigger pores are subsequently filled with silica gel. At the same time, the total cement porosity decreased from approximately 63.5 ± 0.2 % (pure CPC) to a value of 42.1 ± 2.5 % for the composite produced with a sol with a X=3.

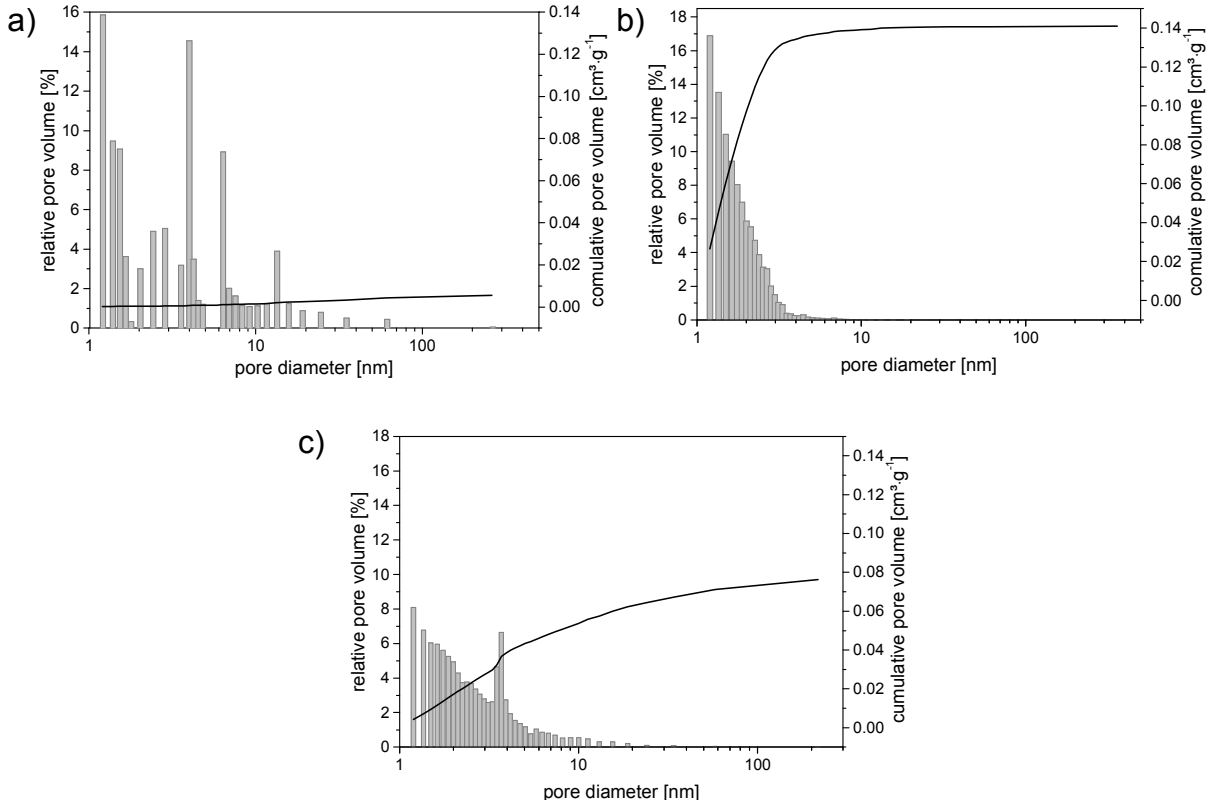

Figure 22: Pore size distribution analyzed by BET porosimetry in a range of 1-500 nm of a) CPC reference (PLR=1 g·mL^{-1}), b) silica gel (X=9) and c) CPC/silica gel composite (X=9, PLR=1 g·mL^{-1}).

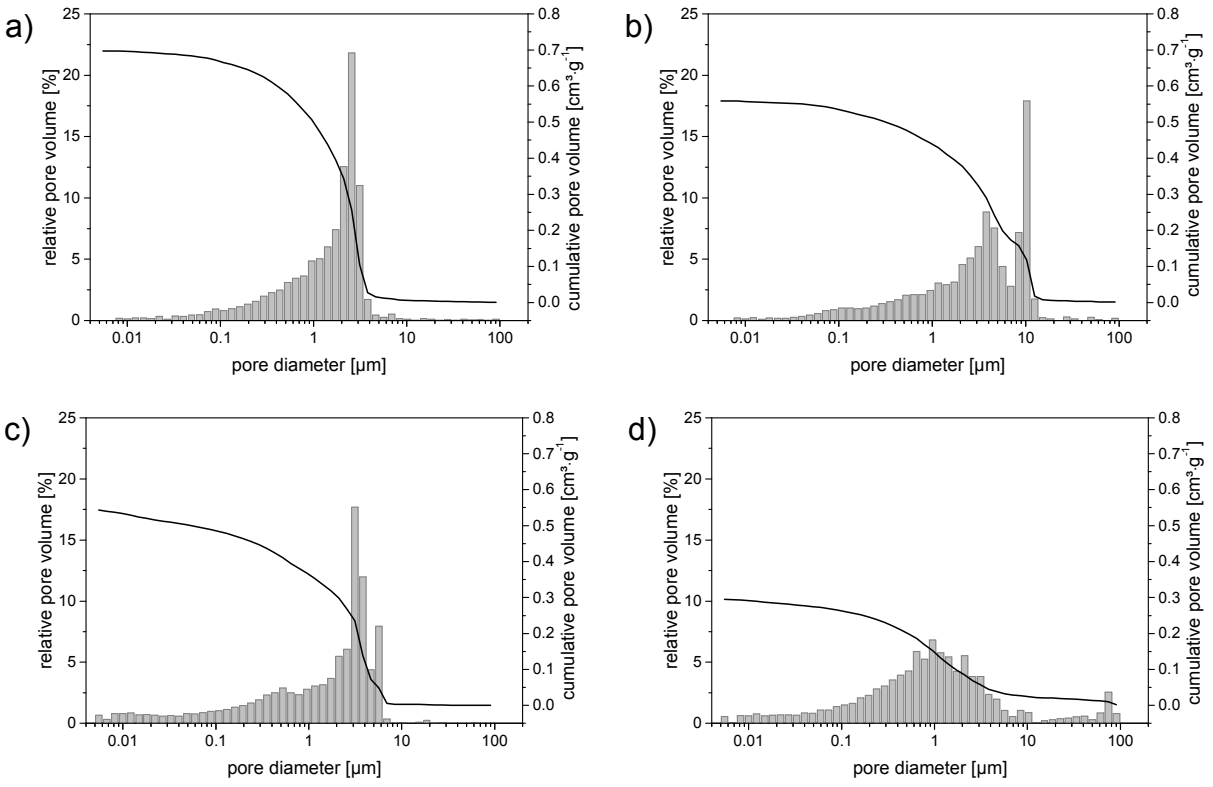

Figure 23: Pore size distribution analyzed by Hg porosimetry in a range of 0.05 -100 µm of a) CPC reference (PLR=1 g·mL^{-1}) and silica gel composite (PLR=1 g·mL^{-1}) with X of b)15, c) 9 and d) 3 (n=3).

Due to these additional micro pores in the composite, the release kinetic of biological agents such as vancomycin could be slowed down (Figure 24).

Table 9: Residual vancomycin content of cement monoliths after 2 weeks in PBS (n=3).

material	**CPC**		**CPC/silica gel**	
insert component	liquid	powder	liquid	powder
residual vancomycin content	8.0 ± 2.5 %	12.4 ± 3.0 %	16.9 ± 1.9 %	24.5 ± 1.6 %

After 14 days immersion in PBS one quarter of the inserted vancomycin still remained in the composite, whereby almost the whole vancomycin was released from the silica-free reference cement (Table 9).

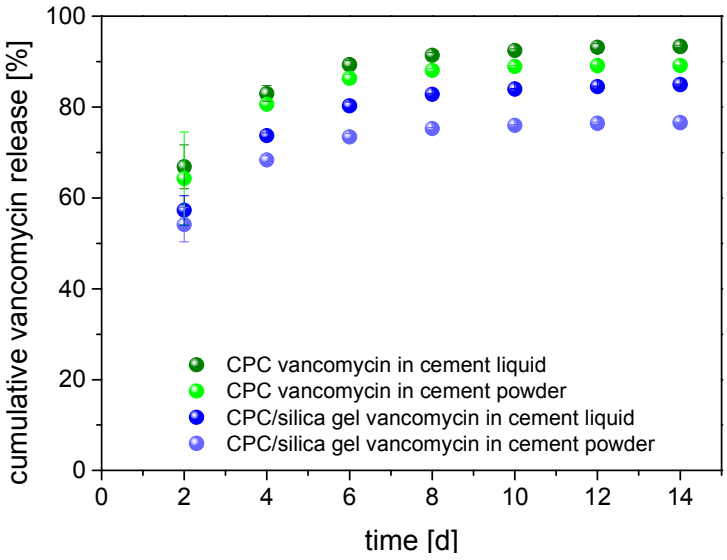

Figure 24: Release of vancomycin from CPC/silica gel composite (X=9, PLR=1 g·mL^{-1}) and CPC reference (PLR=1 g·mL^{-1}). Vancomycin was added either to the cement liquid or powder phase before cement mixture (n=3).

Figure 25 shows the SEM images of the set reference (0.5 M citric acid (a) or H2O (b)) and composite cements (X=15 (c), 9 (d) or 3 (e)). The brushite reference made with water has a small structured phase (Figure 25 a) with irregular crystal morphologies in a size < 2µm. In contrast the brushite reference fabricated with 0.5 M citric acid shows the typical needle like brushite structures [149] with a needle length of about 10 – 20 µm. In comparison to that the CPC/silica gel composites showed a brick-like morphology (X = 15) in a size range of 5 – 10 µm as well as spherical like structures in a range between 20 and 50 µm (X=3 - 9).

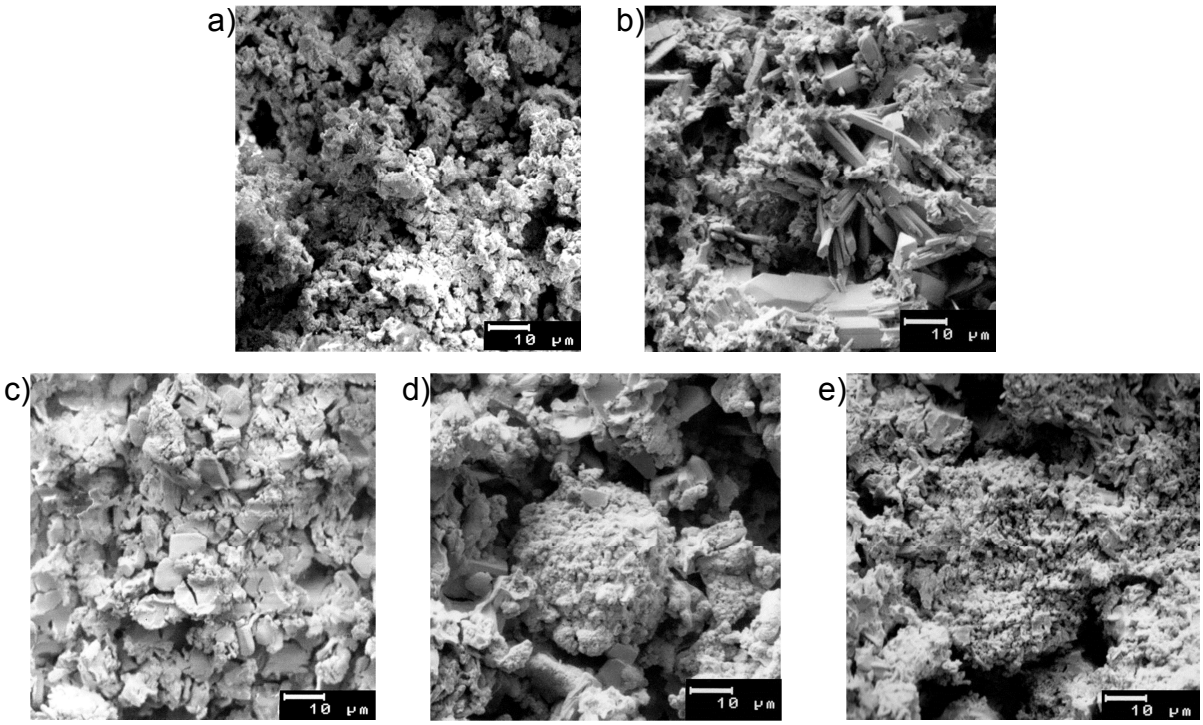

Figure 25: SEM images of CPC-reference, which was mixed with a) water or b) 0.5 M citric acid and CPC/silica gel composite with a H_2O/TEOS ratio of c) 15, d) 9 and e) 3. All cements were mixed with a PLR of 1 g·mL^{-1}.

Compressive strength of the set composite cements showed a high dependency on the H_2O/TEOS ratio (X) of the used sol gel (Figure 26 a). The reference CPC had a compressive strength of 0.89 ± 0.07 MPa and with a high H_2O/TEOS ratio (X = 15) the CPC/silica gel showed a compressive strength in the same range (0.96 ± 0.21 MPa) as the reference.

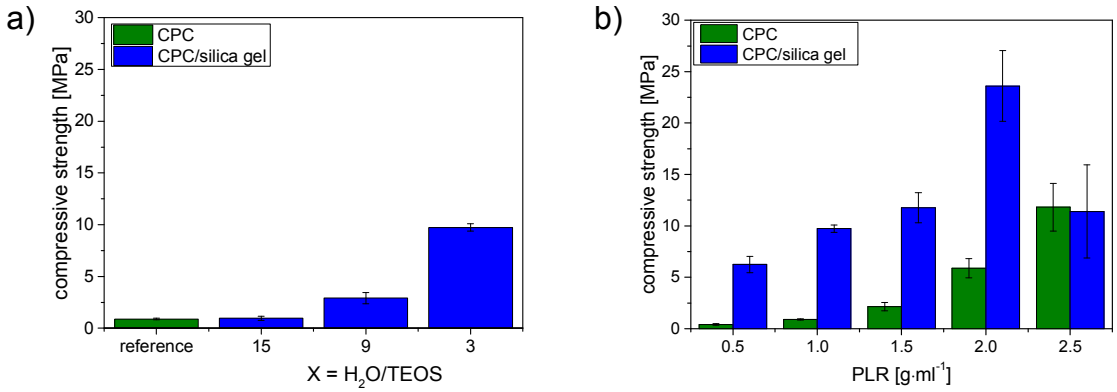

Figure 26: Compressive strength of CPC reference (green) and CPC/silica gel composite (blue): a) a PLR of 1 g·mL^{-1} was used and the acidic silica sol of the composite was produced with H_2O/TEOS ratios between 3 and 15; b) a PLR between 0.5 and 2.5 g·mL^{-1} was used and X of the sol was constant 3; (n = 5).

However, at a higher percentage of TEOS in the sol gel, the composite became more stable (CS at X = 3: 9.74 ± 0.36 MPa), most likely because the silica gel fills the gaps between the brushite crystals resulting in a denser matrix with lower porosity.An

additional mechanical reinforcement was achieved by mixing the CPC/silica gel at a higher PLR (Figure 26 b) such that the compressive strength was increased up to 23.60 ± 3.44 MPa at a PLR of 2 $g \cdot mL^{-1}$ and X = 3. A further increase of the PLR the CPC/silica gel paste led to dry and inhomogenously mixed cements with a CS of 11.41 ± 4.54 MPa. At PLRs > 3 $g \cdot mL^{-1}$ the paste could not be mixed at all.

Figure 27 shows the XRD patterns of the CPC/silica gel composite and the CPC reference. The main component of the CPC reference was found to be brushite with a well-defined peak at 21° with minor amounts of the anhydrous form monetite (peak at 26.5°). The absence of ß-TCP peaks indicated a full conversion of the precursor components. With a decreasing X in the composite (decreasing water content), the amount of monetite increased continuously, until at X = 3 the cement matrix was quantitatively formed by this compound.

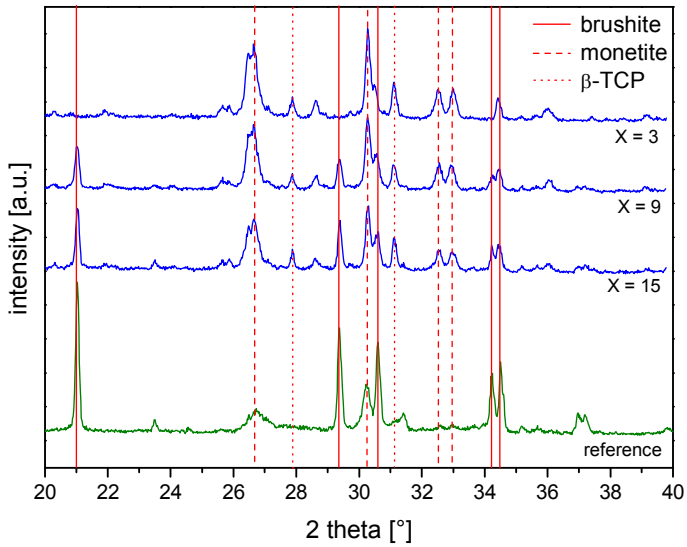

Figure 27: XRD patterns of the CPC-Reference (green, PLR=1 $g \cdot mL^{-1}$) and the CPC/silica gel composite (blue, PLR=1 $g \cdot mL^{-1}$), where the acidic silica sol of the composite was produced with H_2O/TEOS ratios between 3 and 15; full lines indicates typical brushite peaks, broken lines indicates typical monetite peaks and dotted lines indicate typical ß-TCP peaks.

Figure 28 shows the cell number and cell activity of MG-63 cells grown on hydroxyapatite (HA, reference), brushite (H2O; citric acid) and the CPC/silica gel composite surfaces with different X. All samples were one-time washed before the testing in PBS buffer at 37 °C leading to pH of the washing solution of approximately 4.2 – 6.5 (Table 10).

Table 10: pH values of the washing solution after washing each sample disk in 3 ml PBS (pH 7.4) for 24 h at 37 °C.

material	HA	brushite	CPC/silica gel composite			
PLR and composition	3 g·mL^{-1}	1 g·mL^{-1} H_2O	1 g·mL^{-1} X = 15	1 g·mL^{-1} X = 9	1 g·mL^{-1} X = 3	2 g·mL^{-1} X = 3
pH	6.7	6.5	5.9	6.0	5.9	5.8

The brushite reference either mixed with H_2O as cement liquid as well as the CPC/silica gel composites with high X of 9 or 15 showed poor cell proliferation and activity compared to the HA reference surface.

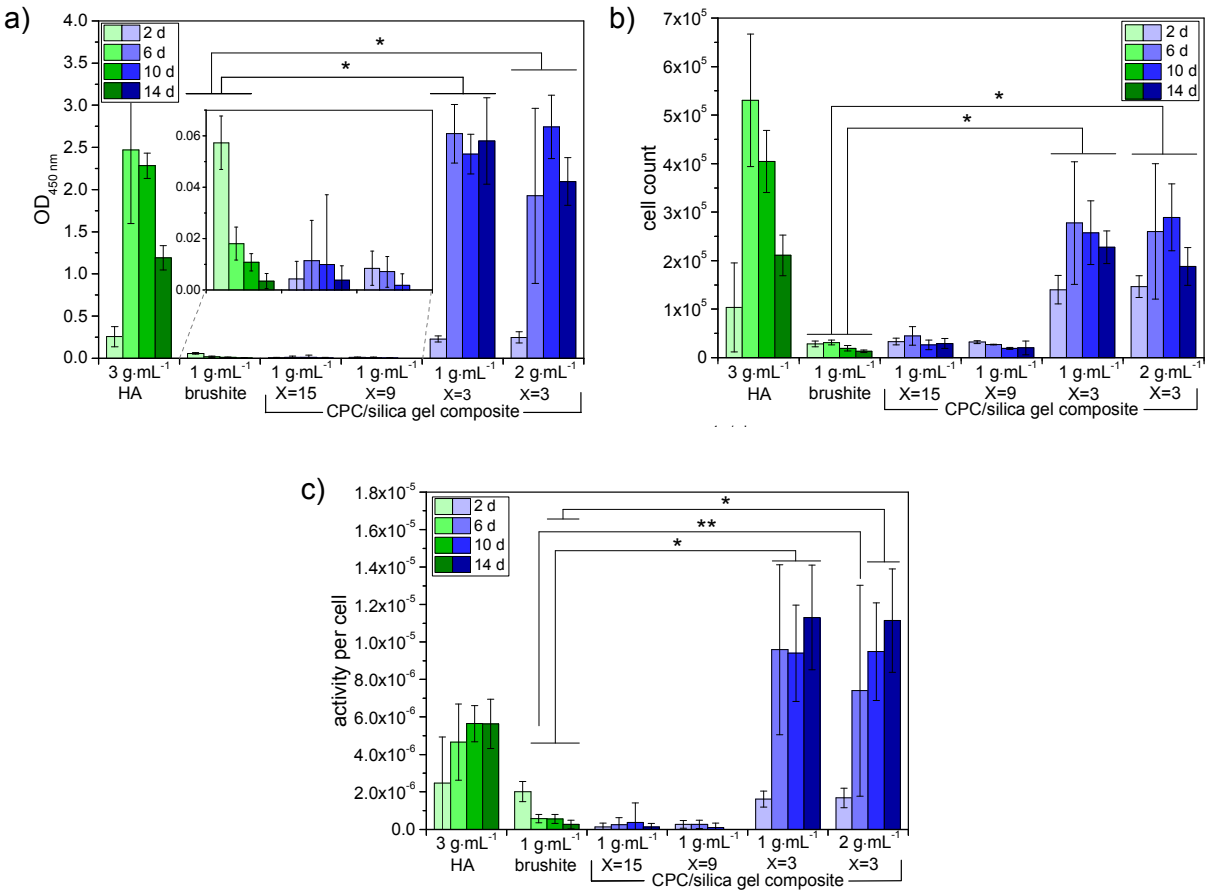

Figure 28: a) Cell activity, b) proliferation and c) activity per cell of osteoblast-like MG 63 cells cultivated on HA, brushite and CPC/silica gel composites with X between 3 and 15 over 14 days after washing each sample disk in 3 mL PBS for 24 h at 37 °C (n = 4). CPC/silica gel composites with X = 3 significantly affect cell activity, proliferation and activity per cell in comparison to the CPC reference (1 g·mL^{-1} brushite): * = p ≤ 0.01; ** = p ≤ 0.05.

The values decrease over time, which indicated cell apoptosis on these cement surfaces. In contrast the cell activity and proliferation on the CPC/silica gel composites with an X of 3 increased significantly from day 2 to 6 and remained on a constant high level over testing period.

The used cell medium was collected during the culture time to analyze changes of the calcium, phosphor, silicon and magnesium ion concentration by ICP-MS (Figure 29). Calcium was adsorbed by most cements in relation to fresh cell medium and only composites with X = 3 released calcium after day 10. All cements released phosphate, whereby the content for brushite (H_2O) and the composites with high X (15 and 9) was approximately 15 - 25 times the concentration of pure medium. The silicon release of the composites was as expected to be much higher than that of the reference cements, whereas no influence of X on the release profile was observed. Magnesium was adsorbed by all cements, practically no magnesium was available in the cell medium of brushite (mixed with H_2O) and the composites with a high X (15 and 9).

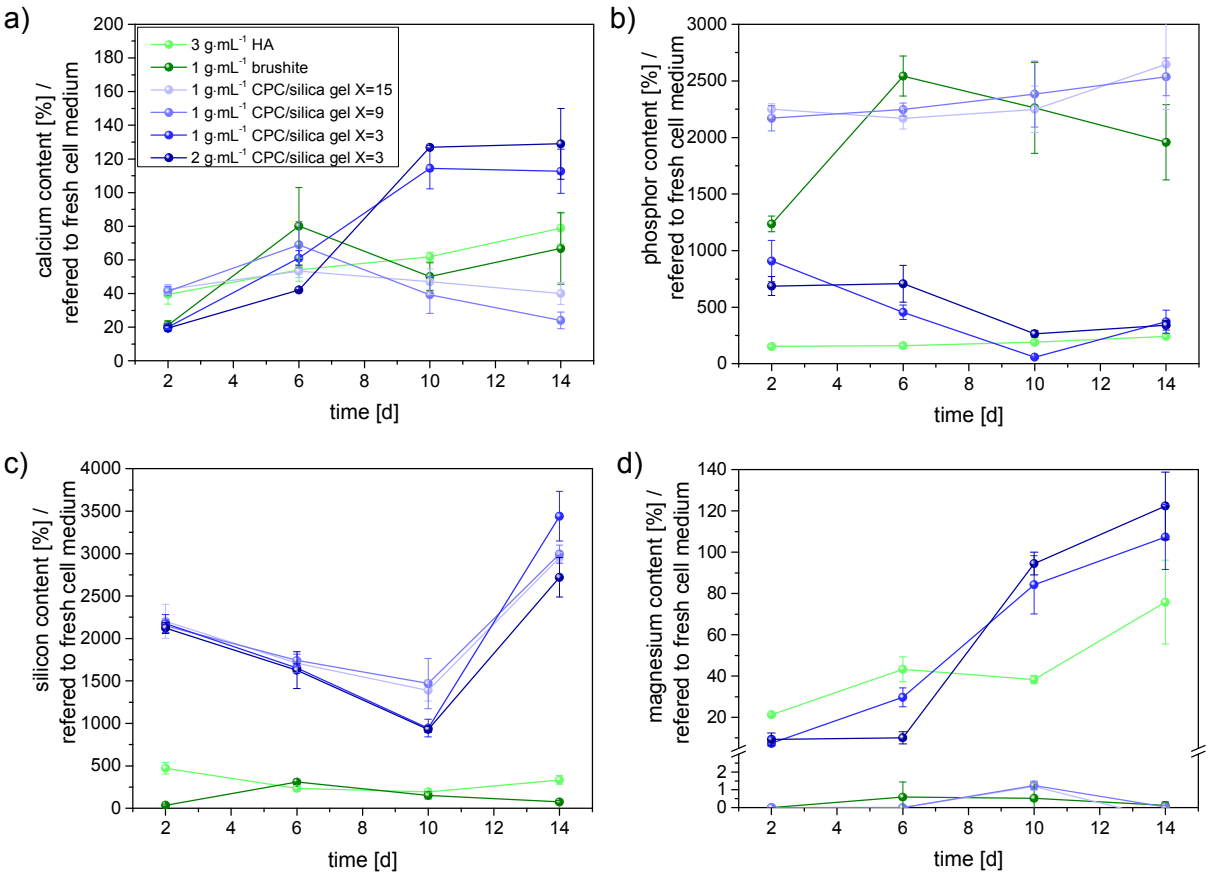

Figure 29: a) calcium, b) phosphor, c) silicon and d) magnesium ion concentration in cell medium during cell tests in relation to fresh cell medium: 100 % calcium ≙ 75 mg·L^{-1}; 100 % phosphate ≙ 36 mg·L^{-1}; 100 % silicon ≙ 5 mg·L^{-1}; 100 % magnesium ≙ 27 mg·L^{-1} (n=3).

4.3 Discussion

This study aimed to develop a dual setting biocement system based on a brushite forming CPC and a TEOS based silica gel, whereas both inorganic components set simultaneously resulting in two interpenetrating matrices. This coexistence of two setting reactions distinguishes our material approach from previous works dealing with either silica modified CPC [303;374] or calcium phosphate modified silica gels [305;375], in which one component was only an unreactive filler in the other matrix forming component. For example, Alkhraisat *et al.* used also a CPC/silica gel system. The difference to our system is that the silica sol was gelled prior to mixing it with the CPC powder and hence acts as a non-reactive additive without any influence on the CPC reaction [303]. For a simultaneous setting of both components, the hydraulic cement setting reaction has to be harmonized with the silica condensation reaction such that both reactions lead to a solidification within the same time frame. This was achieved by using changes of the chemical environment, which rapidly appear during cement setting and which are inducing gelation of the silica sol. The calcium phosphate cement component sets by a continuous dissolution and precipitation reaction in which the cement powder dissolves and following a certain supersaturation level, nucleation and crystal growth of the setting product occurs.[151] For the here used ß-TCP/MCPA system firstly MCPA is dissolved, which results in a pH drop, allowing ß-TCP dissolution and brushite precipitation.[127;376] In contrast, silica gel formation is based on the sol gel process, whereas in a first step the precursor TEOS is hydrolyzed at low pH, followed by the condensation of the generated monomers at higher pH to form a Si-O-Si network.[377] Since at the isoelectrical point of TEOS (pH 2) the hydrolysis of –Si-OEt is favored and the condensation rate of -Si-OH has a minimum [378-379] it is possible to prepare pre-hydrolysed and long term stable (> 5 d) silica-containing cement liquids (Table 8).

Gelation is initiated after mixing with the cement powder by both the pH increase during the cement reaction (Figure 21) and the water consuming formation of brushite. The latter leads to a shorter medium distance between the silanol groups and hence condensation and gelation reaction run faster. Cement solidification was found to be fast (2 – 5 min) at higher water:TEOS ratio ($X \geq 9$) with a clear increase of the pH during the first hour of setting. In contrast, at the lowest $X = 3$, the setting time of the composites was extremely prolonged to more than 40 min, which is likely an effect of the slowly increasing pH for this cement composition. This is due to the

doubled amount of hydrochloric acid (from TEOS hydrolysis) present at low X = 3 in the cement liquid. By reducing the HCl concentration by an order of magnitude, the setting pH rose to a range (pH 2.6-2.8) comparable with the setting pH of the CPC reference. In vivo studies showed that this cement system does not affect any necrosis.[245] Reducing the amount of HCl for TEOS hydrolysis would also have the positive side effect of a reduced setting time since the higher pH accelerates the condensation of the pre-hydrolysed TEOS, whereby the needed water for the cement reaction is available earlier and the setting reaction runs faster.

The decrease of pH during cement setting also affected the final composition of the set cements. While the reference cement without silica addition predominantly formed brushite, dual setting cements were either biphasic mixtures of brushite and the water free form monetite (X = 15 and 9) or solely composed of anhydride (X = 3) (Figure 27). Although monetite is thermodynamically more stable (less soluble) than brushite, the latter is usually formed in cements due to a faster rate of crystal growth and a higher degree of supersaturation. Monetite formation is known to occur if precipitation during setting is slowed down, which is either the fact at low pH [127;155-156] or by reducing the supersaturation level in the cement liquid due to a high ionic strength of the liquid. The latter can be achieved by dissolving sodium chloride in the cement liquid as demonstrated by Cama *et al.* [159], whereby the supersaturation of the cement liquid is controlled by the amount of dissolved NaCl. Şahin and Çiftiçioğlu demonstrated that at low ionic strength brushite achieves supersaturation faster and precipitated first, while an increase of the ionic strength (e.g. by adding 3 M NaCl) the supersaturation levels of brushite and monetite became more equal such that the thermodynamically more stable monetite is formed.[160] All these monetite forming parameters were supported by the use of the silica sol gel as the liquid cement phase in our study. An additional determining factor is the low water content of the silica sol at X = 3 as the only source of cement setting. The quantitative hydrolysis of TEOS requires a theoretical water:TEOS molar ratio of X = 4 and the full conversion to silica after silanol condensation at least X = 2:

$$Si(OEt)_4 + 4H_2O \longrightarrow Si(OH)_4 + 4\,EtOH \longrightarrow SiO_2 + 2H_2O$$

At the lowest X = 3 used in our study, most water is likely consumed during TEOS hydrolysis prior to cement mixing. After adding the cement powder, the water necessary for cement setting stems from the condensation reaction of silanol groups.

Although there is only a small amount of water present in the mixture, this is enough to achieve a full cement conversion to monetite after 72 h setting (Figure 27). This is not surprising since it is known, that even (dry) powder mixtures of β-TCP and MCPM are converted to monetite after 48 h due to surface adsorbed water.[131] A positive side effect of monetite formation is a decreased exothermic setting reaction (Figure 21) [126], which is an important factor for in vivo applications since it may prevent thermal tissue necrosis.

The compressive strength values of the dual-setting cements from our study are up to 23.6 ± 3.4 MPa (PLR = 2.5 g·mL^{-1}; X = 3), which are 5 - 10 fold higher than the CPC references and are at least doubled in comparison to literature values for monetite cements or non- double setting silica – CPC composites. For pure monetite forming cements compressive strength are reported to be in the range between 4 MPa (PLR = 1.5 g·mL^{-1}; 0.65 g·mL^{-1}) [52;157] and 12 MPa (PLR = 3 g·mL^{-1}) [159]. Even Alkhraisat *et al.*, who worked with a system based on dissolved and pre-geled aerosil 200 as liquid cement phase, described compressive strength values below 4 MPa (PLR = 2.5 g·mL^{-1}).[303] Interestingly, a linear relationship was found between strength and porosity instead of the well-known exponential relation reported in many previous studies (Figure 30).[17;150;271]

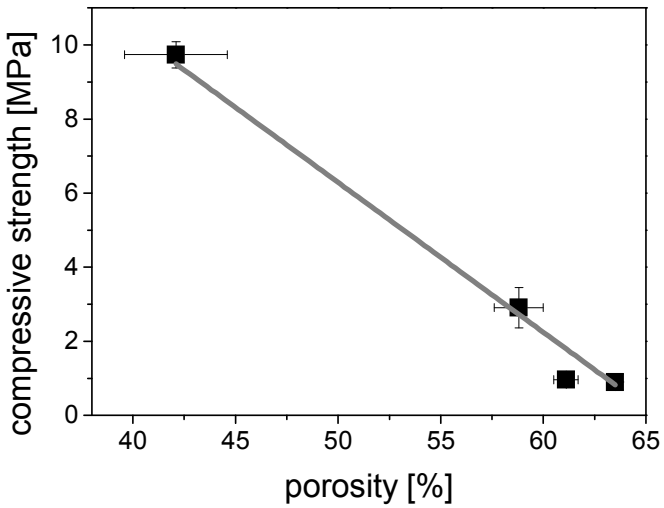

Figure 30: Correlation of porosity vs. compressive strength of the CPC reference and the CPC/silica gel composite with different water to TEOS ratios X (3, 9, 15).

The reason is probably related to changes of the crystal shape and the silica gel morphology with increasing X (Figure 25). The result is a composite material with a bimodal pore size distribution, where the bigger pores between the cement crystals

are subsequently filled with silica gel. With X ≤ 9 spherical structures could be observed (Figure 25 d & e) as a result of the high silica content which forms spheres during the composite setting to minimize surface tension. The load is then not only counteracted by the physical entanglement of the cement crystals, but also by the chemically bound silica gel. In addition it was shown for vancomycin, that this size distribution is able to control the release of biological active agents. Vancomycin was chosen as model drug in this study since it shows only physical interactions with calcium phosphate matrices [380] and it mostly retains its pharmaceutical activity after encapsulation in silica gel [381] as well as in CPCs [273;382]. As shown in Figure 22 c the composite has pores in the range of the size of vancomycin (5.5 nm² [383]) to encapsulate the antibiotic and release it not until the material is resorbed. Surprisingly, the kinetic behavior is not changed by the insertion of the silica gel in the composite. All analyzed cements deliver vancomycin in a comparable way: a burst release in the first two days followed by a first-order kinetic. The release curves show the same trend, but differ in the amount of the initial burst release (Figure 24), which is due to the adapted pore sizes of the carrier composite material.

The above mentioned morphology properties could be one reason for the good cell response of the CPC/silica gel composite with X = 3, which had the best cell proliferation and activity values in comparison to the brushite reference and the composites with lower silica gel content (X = 9 and 15). HA was used as an additional reference, because it is known for good cell response in vitro [384-386], which could be confirmed here (Figure 28). Possible influencing factors on the cell response, which are affected by the material system, could be either the pH, the cement morphology or the adsorption and release of nutrient ions. The brushite reference used for cell experiments was produced without citric acid as it was recently shown by Jamshidi *et al.* that the formation of a dicalcium phosphate-citrate complex within the cements inhibits cell attachment to the cement surface.[230] All cements discs used for in vitro testing were washed only once in 3 mL for 24 h resulting in a pH of the solutions of 5.8 – 6.7. Although the washing solution of pure brushite (H_2O) had a nearly neutral pH of 6.5, a high cell apoptosis level was observed on these surfaces similar to the CPC/silica gel composites with high X (9 and 15). Only at X = 3, composite samples were found to provide a high cell growth and activity similar to HA. The explanation for the completely different cell behavior of the materials is probably related to ionic changes of the cell culture medium in

contact with the samples (Figure 28). One reason to use silica gel as co-material in this system was the well known fact that silicon is an important source in bone mineralization [387-389] and Si substituted CaPs show superior biological performance [390-391]. By consideration of this, all materials should show good cell response, since every sample released silicon (Figure 29 c) above the medium silicon concentration (note: the silicon in the reference cements derives probably from the agate mill devices during CPC powder fabrication). However, no direct correlation between Si-release and cell response could be observed, since the Si-release of all composites was nearly equal independent of their biological performance. This is in correspondence with a review article from M. Bohner on silica-substituted calcium phosphate ceramics, in which he suggested that the beneficial effect of Si-substitution may often stem from additionally caused topographical or chemical changes of the material rather than from Si-release.[392] This also likely appears in our study, whereas besides a change of morphology (Figure 25) and an increasing monetite content (Figure 27), a strong influence of some composites on the phosphate and magnesium level in the cell culture medium was observed (Figure 29 b and d). Values over 100 % indicate an ion release of the cement samples, whereas below 100 % ion adsorption by the cement samples or ion consumption by the cells took place. It is conspicuous that only in the cell medium with lower phosphor concentration (< 1500 % in relation to fresh cell medium) cell activity and proliferation could be observed. Klammert *et al.* measured comparable phosphate concentrations for printed brushite, monetite [163] and struvite [393] with good cell response of MG63. In the cell medium of the cements, which showed no cell response, the phosphor concentration was much higher (> 2500 % in relation to fresh cell medium). Maybe this concentration exceeds a critical value and is cytotoxic for the cells. One additional hint supporting this hypothesis is the positive cell activity and proliferation on brushite on day 2, where the phosphate concentration is under the critical value (about 1200 % in relation to fresh cell medium). On the 6th day the concentration rises and cell apoptosis appears. Another critical parameter seems to be the magnesium concentration in the media. While pure brushite and the composites with X = 9 and 15 quantitatively adsorbed magnesium ions from the cell medium, HA and the composites with X = 3 adsorbed less magnesium ions such that Mg^{2+} is still available in the medium in concentrations above 3 $mg \cdot L^{-1}$. This could be the crucial factor for the benefical cell activity and proliferation on these cements since

magnesium is known to influence the mineralization as well as the matrix metabolism of bone cells [394]. The difference in calcium and phosphate ions content could be explained by the oversaturation in the cell medium whereby lower soluble calcium phosphates are precipitated [395]. For example brushite transforms into octacalcium phosphate [245] an hydroxyapatite [137;139] with a higher Ca/P ratio, which leaves free phosphate ions in solution due to stoichiometric reasons.

4.4 Conclusion

The porosity properties of calcium phosphate cement and silica gel could be combined by a dual setting composite approach, which was successful to both slow down the release rate of biological agents such as vancomycin and to increase the mechanical properties by an order of magnitude. A further effect was the formation of monetite instead of brushite by the competitive water uptake during setting. This is beneficial regarding the in vivo behavior, where brushite is known to form reprecipitates of insoluble hydroxyapatite.[151] In contrast monetite has a lower solubility, did not show a HA transformation and is known to be osteoconductive and resorbable in vivo.[166;396] The relatively high solubility of the low temperature formed silica matrix (approx. 2.3 - 4.4 % in two weeks) will at the same time ensure a fast degradation of this second component similar to the degradation of the calcium phosphate matrix. The limiting parameter for a good cell response of the composites seemed to be the ion adsorption (Mg^{2+}) and release (HPO_4^{2-}, SiO_4^{4-}) properties of the cements.

Chapter 5

Self-densifying dual setting calcium phosphate cement: Brushite and fibroin

Parts of Chapter 5 were used in a publication manuscript, which is however not submitted or published by the time of the submission of this thesis.

Calcium phosphate cements (CPC) are a clinically applied material class for bone replacement, however the low fracture toughness restricts the use of CPC to non-load-bearing defects.[3;16] Recent approaches to improve the mechanical performance of CPC for load-bearing applications were focused on the addition of fibers to the cement matrix [18-19] or the modification of the cement with polymeric additives. The latter may be either non-reactive compounds such as collagen [255-256], hyaluronic acid [296;397-398] or chitosan [399-401] or the polymers chemically interfere with the inorganic cement components [297]. Most prominent examples are compounds with a high density of carboxylic groups such as polyacrylic acid [22;402] or poly(methyl vinyl ether maleic acid) [24] as well as polymers which contain phosphate groups like polyvinyl phosphonates [21] or polyphosphazenes [219]. During setting, a deprotonating of the organic acid occurs, followed by the formation of intra- or inter-chained bonding of Ca^{2+} - acid chelates. Another reinforcement mechanism utilizes the simultaneous polymerization reaction of dissolved monomers [28-30]. This forms a hydrogel matrix within several minutes, in which the embedded cement particles are subsequently converted into the setting product by a continuous dissolution – precipitation reaction. This dual setting strategy benefits from the possibility of a high polymer loading of the cement as well as practically unchanged rheological properties of the fresh cement paste.[16]

In the current study, we extended the dual setting concept by combining a brushite ($CaHPO_4 \cdot 2\ H_2O$) forming cement paste with an aqueous solution of the biopolymer silk fibroin (SF) as the second component. SF shows a typical random coil conformation in aqueous solution with negligible intermolecular bindings [403]. Fibroin gelation is known to be affected by several parameters such as concentration [404], pH [405], sheer forces [406-407], temperature [408] and ionic strength [404]. The gelation is a two-step reaction, whereas initially weak interchain interactions like hydrogen bonding, hydrophobic and electrostatic interactions dominate, followed by the formation of more thermodynamically stable secondary β-sheet protein structures.[409] These crystalline structures are irreversible intermolecular structures, which largely influence the chemical and mechanical properties of silk fibroin.[408;410]

Several of the SF gelation initiating factors are favoured by the brushite cement setting conditions such as the pH drop and high ionic strength at an initial stage of

setting. Here, we hypothesised that by the combination of the cement powder with the aqueous silk fibroin solution both the cement setting reaction and the fibroin gelation will simultaneously occur to build up an interpenetrating fibroin – brushite composite with combined properties of the elastic polymer and the rigid cement (Figure 31).

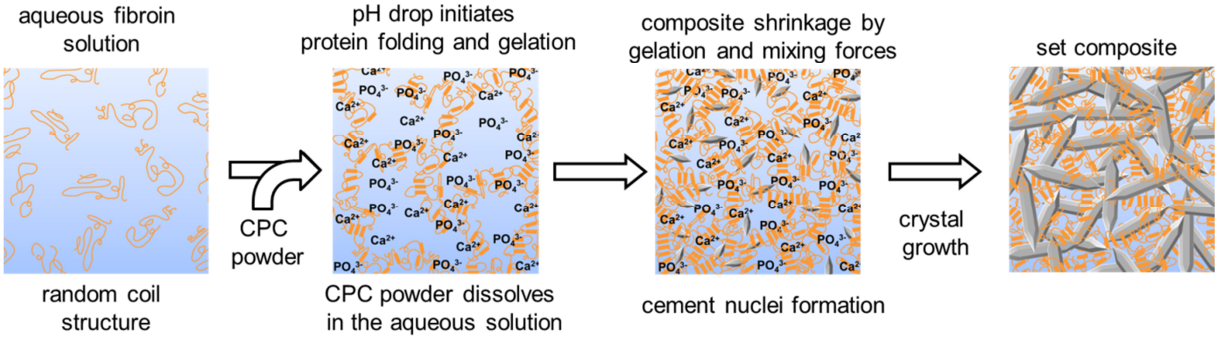

Figure 31: Schematical model of the dual setting reactions of fibroin and brushite cement

5.1 Materials and methods

β-TCP was prepared by sintering $CaHPO_4$ (Baker, Renningen, Germany) and $CaCO_3$ (Merck, Darmstadt, Germany) in a molar ratio of 2:1 for 5 h at 1050 °C. The sintered cakes were crushed and sieved with 100 µm pore size-mesh followed by ball milling in a planetary ball mill (Retsch, Haan, Germany) for 60 min at 200 rpm. Brushite cements were produced by mixing β-TCP powder in an equimolar ratio with monocalcium phosphate anhydrous ($Ca(H_2PO_4)_2$, MCPA, Aldrich, Steinheim, Germany) in a coffee grinder for 30 sec. SF solution was produced by dissolving silk cocoons from *Bombyx mori*. Briefly, silk was degummed by boiling the cocoons 3 times in 0.02 M Na_2CO_3 for 1 h and rinsed with distilled water to remove sericin. After drying the washed silk was dissolved in 9 M LiBr at 60 °C and afterwards dialyzed against distilled water using a dialyzing tube with a cut off of 3.5 kDa for 2 days. This resulted in a 4 wt.-% aqueous SF solution as determined by weighing the remaining solid after drying. Finally, this solution was concentrated by PEG (20 kDa)-dialysis. The cement pastes were formed by manually mixing CPC powder and the aqueous SF solution with a concentration between 4 and 16 wt.-% at powder to liquid ratios (PLR) of either 0.5 $g \cdot mL^{-1}$ or 1.0 $g \cdot mL^{-1}$. The samples were transferred for 24 h into a water bath with 100 % relative humidity and 37 °C for setting. As reference, the CPC powder was mixed with water and treated similar to the composite material.

Cement characterization

Porosity characteristics were measured by mercury (Hg) porosimetry (PASCAL 140/440, Porotec GmbH, Hofheim, Germany). A contact angle of 141.3° and a surface tension of 480 $mN \cdot mm^{-1}$ of mercury were used for calculation. The accuracy of measurement was about 1 % for the detection of the volume and ca. 0.25 % for the pressure. The errors for the pore size and the total porosity were than calculated by the maximum error law. Fourier Transform Infrared Spectroscopy (FT-IR; Nicolet is10, Thermo Scientific, Waltham, MA) was used to quantify the secondary structure of fibroin by determining the area under the corresponding gauss curves of the different vibrational band assigned to the Amide I region of *B. Mori* Silk fibroin.[408] Spectra were recorded in a range from 400 to 4000 cm^{-1} with a resolution 4 cm^{-1}. X-ray diffraction (XRD) patterns of samples were recorded using monochromatic CuK_{α} radiation (D5005, Siemens, Karlsruhe, Germany). Data were collected from 2θ = 10 - 40° with a step size of 0.02° and a normalized count time of 3 $sec \cdot step^{-1}$. The phase composition was checked by means of JCPDS reference patterns for brushite (PDF Ref. 09-0077), monetite (PDF Ref. 09-0080) and β-TCP (PDF Ref. 09-0169). A crossbeam scanning electron microscope CB 340 (Zeiss, Oberkochen, Germany) was used to analyse the surfaces of the ceramic monoliths. Samples were imaged using an accelerating voltage of 1 kV. For mechanical analysis, the CPC/SFS composites were produced with different fibroin (4, 8 or 16 wt.-% in solution) and CPC contents (PLR = 0.5 or 1 $g \cdot mL^{-1}$). Five samples were measured for each parameter after storage in water or drying at 37 °C overnight. Mechanical testing was performed using a static mechanical testing machine (440, Zwick, Ulm, Germany) and a 2.5 kN load cell. For compression tests, cuboid samples (12 x 6 x 6 mm^3) were loaded parallel to their long axis and tested at a constant cross head displacement rate of 1 $mm \cdot min^{-1}$ under water. The 3-point bending test was performed under wet and dry conditions with a support span of 20 mm. These samples (7.5 x 2.5 x 30 mm^3) were loaded with a displacement rate of 1 $mm \cdot min^{-1}$. A cyclic load test was done under the same conditions, but with a speed of 1 Hz per cycle. A nail penetration test was performed with a commercial steel nail ($Ø_{nail} \approx 1.3$ mm, $Ø_{nailpoint} \approx 0.3$ mm), which penetrated the sample (height = 15 mm) by a constant cross head displacement rate of 10 $mm \cdot min^{-1}$ until the nail was inserted in the wood underneath the sample.

In vitro cytocompatibility testing

The osteoblastic cell line MG 63 (ATCC no. CRL-1427, Rockville, MD) was cultured at 37 °C and 5 % CO_2 in Dulbecco's Modified Eagle's Medium (DMEM, Invitrogen Life Technologies, Karlsruhe, Germany). The culture medium was supplemented with 10 % fetal calf serum, 100 U·mL penicillin, and 100 mg·mL streptomycin (all from Invitrogen Life Technologies). The medium was changed in fixed intervals of 2 days. During the experiments cells were cultivated on brushite (PLR = 1 g·mL) or CPC/SF composite (concentration of SF solution: 4, 8 and 16 wt.-%; PLR = 1 g·mL). Before testing, every cement disk (Ø = 15 mm, h = 2 mm) was washed for 4 d in 2 ml PBS at 37 °C with a daily change of PBS. Samples were then placed in quadruplicate into the wells of a 24-well plate and covered with cell suspension (10^5 cells·well^{-1}). The cytocompatibility tests of the cement surfaces were performed by means of cell counting and determination of cell activity after 2, 6, 10, and 14 days in culture on all surfaces as described in detail elsewhere.[373] Briefly, cell proliferation was analyzed by cell counting using a CASY 1 TTC cell analyzer (Schärfe System, Reutlingen, Germany), while cell viability was analyzed using the cell proliferation reagent WST 1 (Roche Diagnostics, Mannheim, Germany). For each method and sample, four readings were recorded and the mean values and standard deviations were calculated.

Ion concentrations (Ca^{2+}, Mg^{2+} and phosphate) in the cell culture medium were determined by inductively coupled plasma mass spectrometry (ICP-MS, Varian, Darmstadt, Germany). The quantitative measurement was carried out against standard solutions (Merck, Darmstadt, Germany) containing defined concentrations of all ions of interest.

5.2 Results

While the SF solutions had a basic pH of 8.9 ± 0.2, composites with brushite cement powder set at an acid pH ranging from 2.2 - 4.8 (Figure 32a). By mixing both components, the SF solution started to gel within seconds and the composite became sticky and rubber-like until the cement phase was set (Figure 32b).

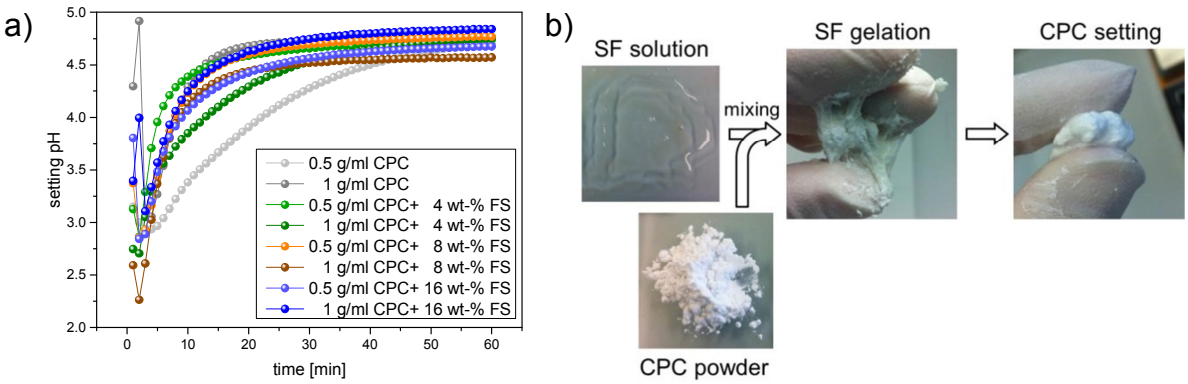

Figure 32: a) Setting pH of pure CPC and CPC/fibroin composites (PLR = 0.5 & 1 g·mL^{-1}) with a concentration of the aqueous SF solutions of 4, 8 and 16 wt.-% and b) images of the setting reaction.

The fibroin shrinks during the gelation, which resulted in an ejection of cement liquid. By this mechanism, the pure SF solution showed a volume reduction of two-thirds. Cements formed at PLR of 0.5 - 1.0 g·mL^{-1} were highly porous constructs with porosity values up to 77 %. With an increasing SF content in the composites the porosity was reduced to 45 % for the 0.5 and 1 g·mL^{-1} CPC + 16 wt.-% SF composites. For the composites produced with a PLR of 1 g·mL^{-1} the theoretical and measured porosity values are nearly the same, whereby for the 0.5 g·mL^{-1} composites the differences are enlarged (Figure 33).

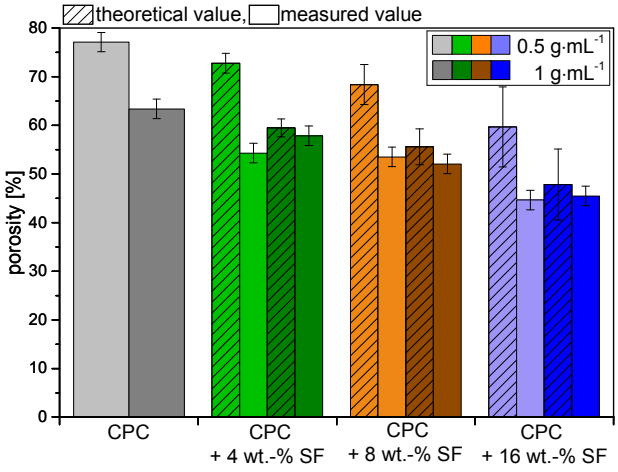

Figure 33: Porosity of pure CPC and CPC/fibroin composites (PLR = 0.5 & 1 g·mL^{-1}) with a concentration of the aqueous SF solutions of 4, 8 and 16 wt.-% SF, whereby the blank bars give the measured values and the striped bars the theoretical porosity values without self-densifying behavior.

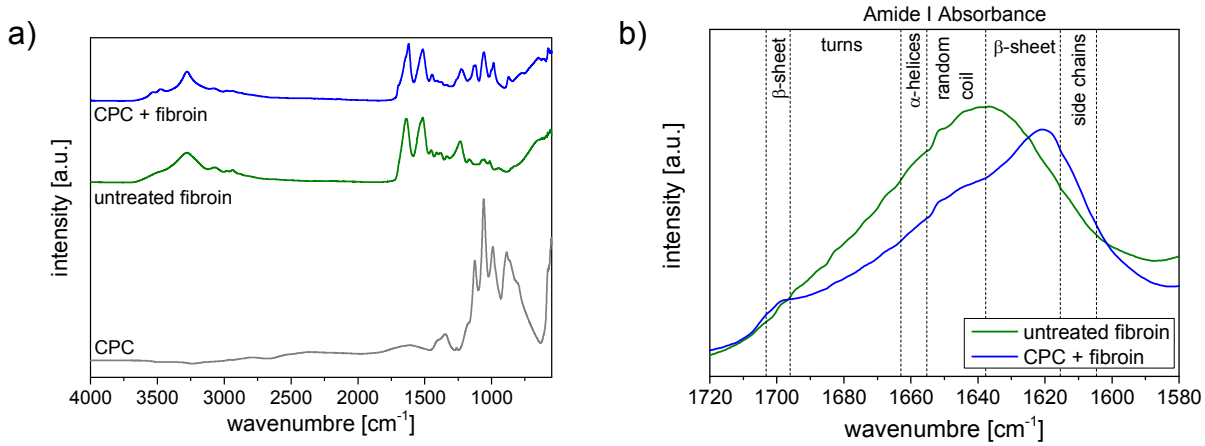

Figure 34: FT-IR spectra of pure set CPC, untreated SF and the CPC/SF composite in a range of a) 4000 – 550 cm^{-1} and b) the amide I absorbance (1720 – 1580 cm^{-1})

FT-IR spectra of the CPC/SF composite showed a shift of the Amide I absorbance region to lower wavenumbers in comparison to the untreated fibroin (Figure 34). This indicates a higher β-sheet secondary structure of the fibroin by the combination with CPC. The β-sheet content increased from 32.3 ± 0.3 % to 41.2 ± 1.1 %, whereas the random coil content decreased from 29.8 ± 0.1 % to 24.8 ± 1.3 %. Thereby the SF becomes insoluble in water and the mechanical strength is improved.[410-411]

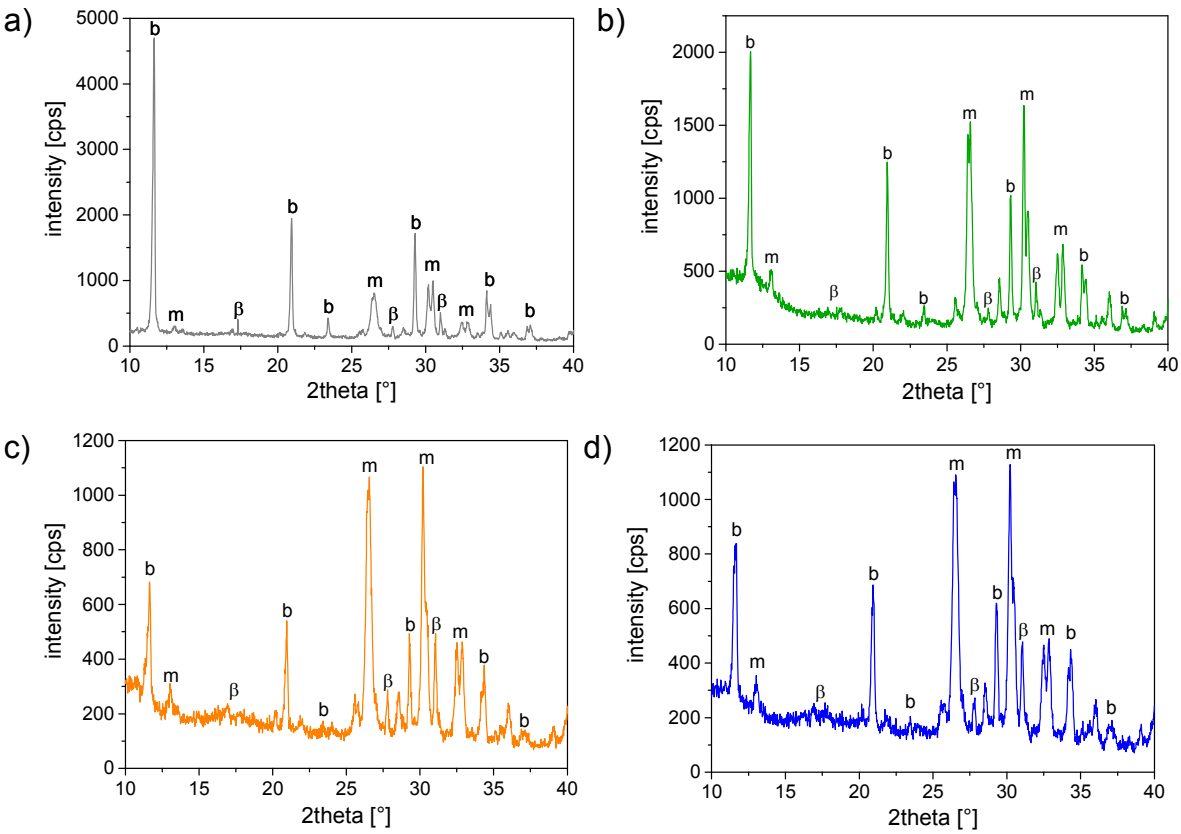

Figure 35: XRD patterns of pure a) CPC and CPC/SF composites (PLR = 1 $g \cdot mL^{-1}$), where the aqueous SF solutions had a concentration of b) 4, c) 8 and d) 16 wt.-%. B indicates typical brushite peaks, β indicates typical β-TCP peaks and m indicates typical monetite peaks.

For all materials, brushite ($CaHPO_4 \cdot 2\,H_2O$) or monetite ($CaHPO_4$) could be approved as the cement setting product by XRD analysis (Figure 35). Only small peaks of the raw material β-TCP could be observed, which indicates an almost full conversion of the cement raw powder into the setting product. The monetite content increased and the overall intensity of the diffraction patterns subsequently decreased with an increasing SF content in the composite. The baseline displacement in the region between 10° and 20° resulted from the crystalline ß-sheet structure of the SF.

The CPC references (PLR = 0.5 & 1 $g \cdot mL^{-1}$) showed the typical brittle behavior during compression tests and fractured below a strain of 5 % under wet conditions. In contrast, the CPC/SF composites did not entirely fail and even at a compression of 65 %, no complete cracking was observed (Figure 36 b).

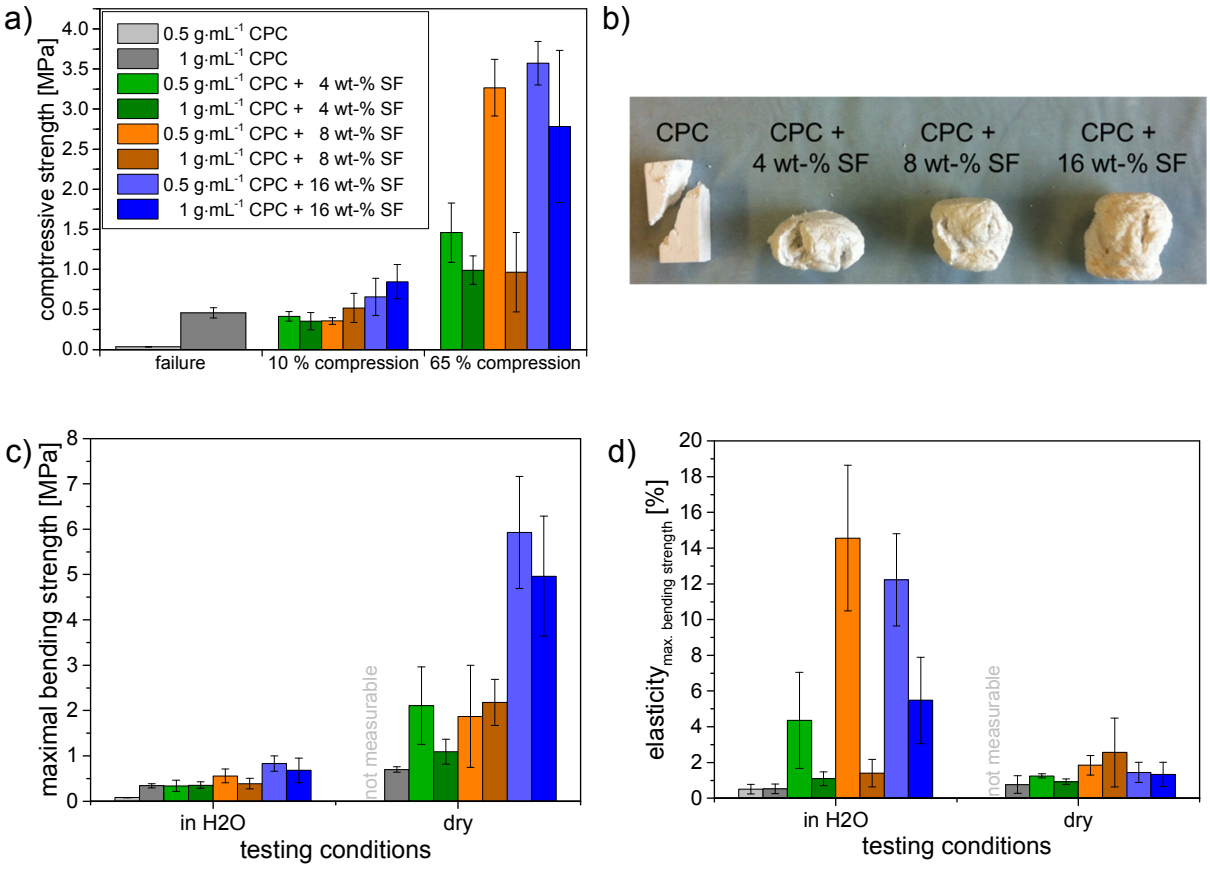

Figure 36: a) Compressive strength by a compression of 10 and 65 % tested under water (n=5), b) image of the testing samples after testing, c) maximal bending strength in 3-point bending test and d) elasticity of pure CPC and CPC/fibroin composites (PLR = 0.5 & 1 $g \cdot mL^{-1}$), where the aqueous SF solutions had a concentration of 4, 8 and 16 wt.-%. 3-point bending testing was performed either in water or under dry conditions (n=4).

With an increasing SF content in the system the fractures were significantly reduced and the materials seem to have a certain content of recilience.

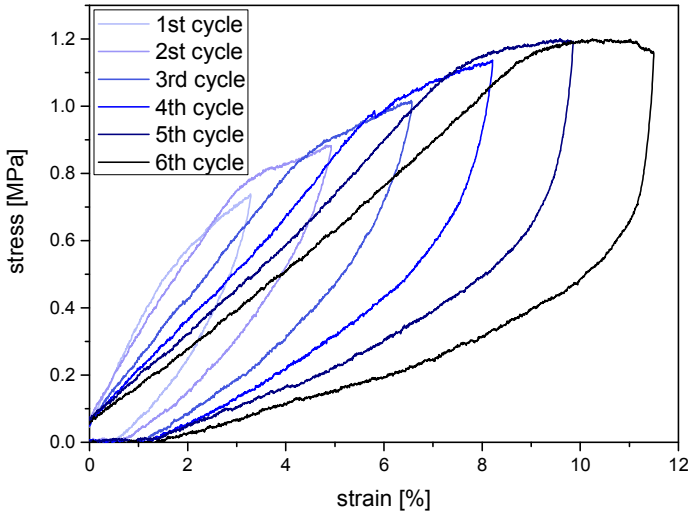

Figure 37: Stress-strain diagram during cyclic load with increasing strain of CPC/SF composite (PLR = 0.5 g·mL^{-1}; 16 wt.-% SF).

At the same time, the mechanical performance of the CPC/SF composites depends on the testing conditions (Figure 36 c & d).The fibroin is plasticized by water under wet conditions, whereby the elasticity of the material increased with a simultaneous loss of strength. Under dry conditions the composites showed a brittle character similar to the reference CPC, but with improved bending strength up to 8 times higher for the CPC with a PLR of 0.5 g·mL^{-1} and 8 wt.-% SF composite (5.9 ± 1.2 MPa) in comparison to the 1 g·mL^{-1} CPC (0.7 ± 0.1 MPa) (Figure 36 c). The 0.5 g·mL^{-1} CPC was too weak for measurements. The bending behavior of the highly flexible CPC with a PLR of 0.5 g·mL^{-1} and 16 wt.-% SF was additionally analyzed by a cyclic load with increasing strain per cycle (Figure 37) showing an increasing bending stress with every cycle. During the unloading phase, the stress declines faster than the strain resulting in a typical stress-strain-hysteresis. The remaining strain in the unloaded state was found to be 15.7 ± 1.8 % of the maximal strain per cycle.

Figure 38a shows the curves of the nail penetration test of pure CPC and CPC/SF composites (PLR = 1 g·mL^{-1}). The CPC reference breaks by a nail penetration depth of approximately 3.5 mm (Figure 38 b), whereas the composites can be nailed onto a piece of wood without any instable crack growth. Especially the composites with ≥ 8 wt.-% SF resist a crack development and can be penetrated without any damage (Figure 38 c). The composites with ≥ 8 wt.-% were in addition sliceable in the wet state and could be cut into complex geometries (Figure 38 e).

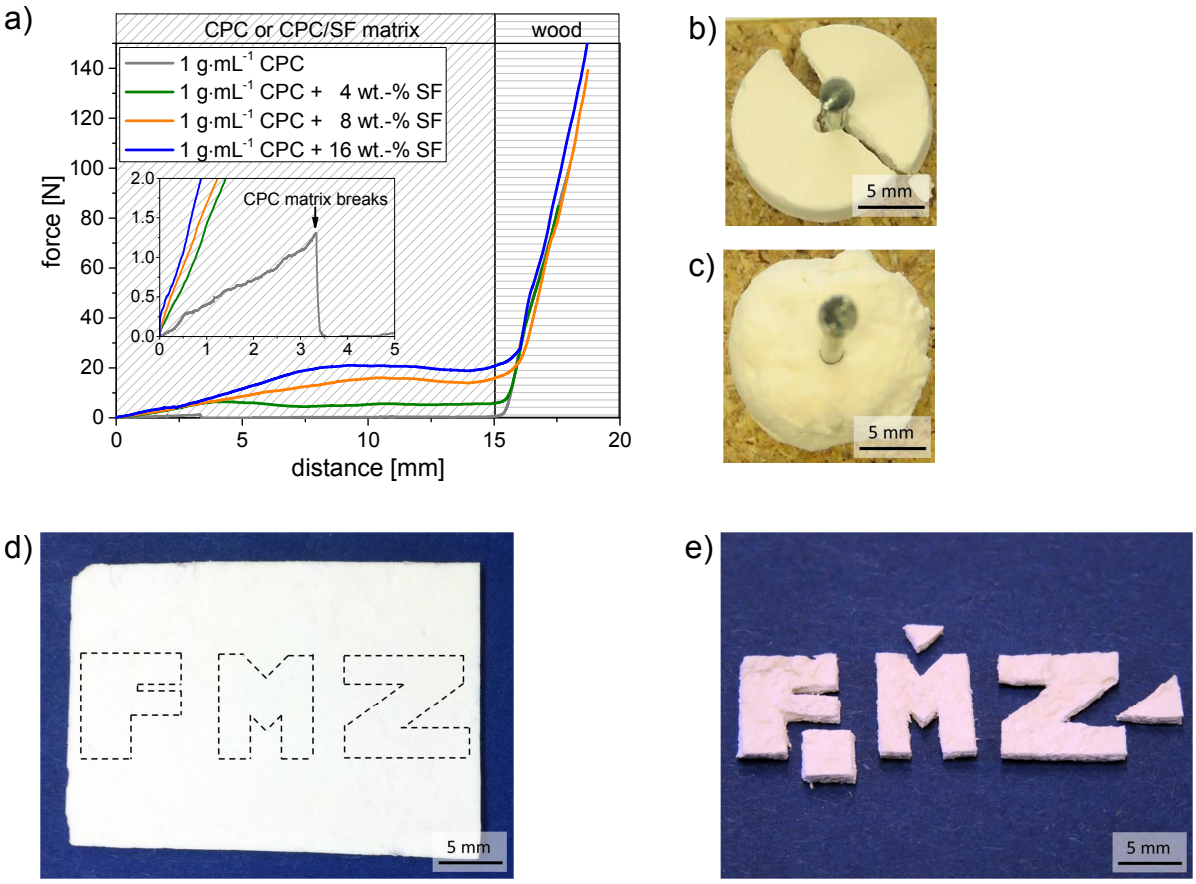

Figure 38: a) Nail penetration test diagram of pure CPC and CPC/SF composites (PLR = 1 g·mL^{-1}), where the aqueous SF solution had a concentration of 4, 8 and 16 wt.-% and images of b) 1 g/ml CPC and c) 1 g/ml CPC + 8 wt.-% SF samples after nail penetration test; Image of CPC + 8 wt.-% SF d) plate and afterwards e) the cut geometry.

In vitro cytocompatibility

Figure 39 shows cell number, cell activity and the resulting activity per cell of MG-63 cells grown on the surfaces of CPC (brushite, PLR = 1 g·mL^{-1}) and the CPC/SF composites (PLR = 1 g·mL^{-1}). Prior to cell seeding, all samples were washed in PBS buffer (pH 7.4) leading to a pH of 6.6 ± 0.1 of the washing solution after the 4th day. Obviously the cell proliferation on the CPC/SF composites surfaces increased over the time period of 14 days, whereas the cell number on the CPC reference remained constant until day 10 and decreased on day 14 (Figure 39 a).

Here, the WST 1 test indicated complete cell apoptosis on the CPC reference surface. In contrast, the activity on CPC/SF composites rose with an increasing SF content and cultivation time (Figure 39b). Additionally, the activity per cell seemed to depend on the SF concentration with an increasing cell activity at higher SF content.

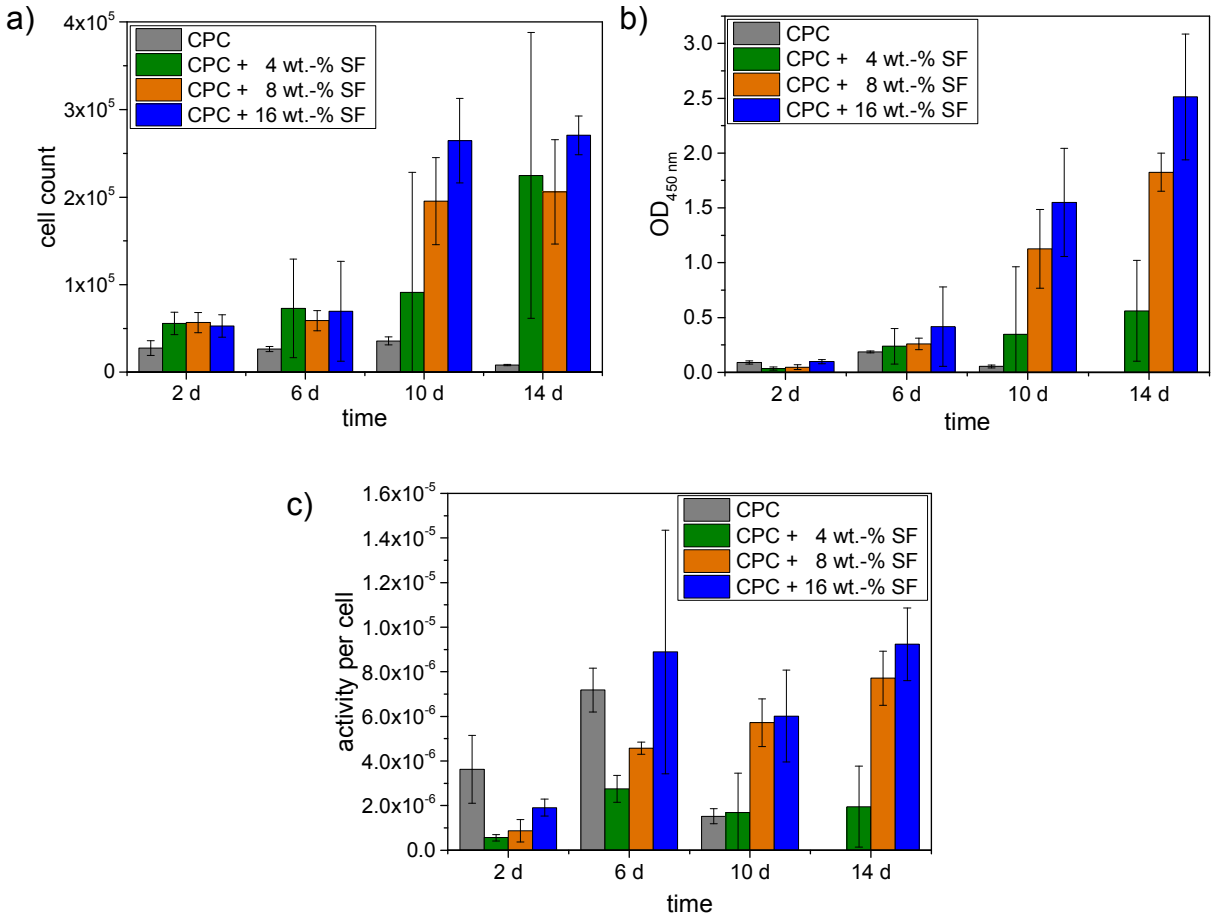

Figure 39: a) Proliferation, b) cell activity and c) activity per cell of osteoblast-like MG-63 cells cultivated on pure CPC and CPC/SF composites (PLR = 1 g·mL^{-1}), where the aqueous SF solution had a concentration of 4, 8 and 16 wt.-% over 14 (n=4).

SEM images of the materials surfaces before and after cell cultivation (Figure 40) showed smaller cement crystals with an increasing SF content and crystals seemed to be subsequently stronger embedded in the SF matrix (Figure 40 a, c, e & g). Obviously the cell layer after 14 days cultivation is denser with the highest SF content in the composite and the cells showed the typical active spread shape (Figure 40 h). With a decreasing SF content in the composite more and more spherical, inactive cells were observed on the surface. In contrast, on the CPC reference surface no cells could be found. Here the morphology of the crystals changed from a boulder like structure to thin plates during the cultivation time of 14 days (Figure 40 a & b).

Figure 41 shows the calcium, phosphor (as phosphate) and magnesium ion release of the materials during the cell cultivation as well as the surface composition of the CPC and CPC/SF composites after cultivation. Distinctly, magnesium and calcium ions are absorbed from DMEM by all materials, whereas phosphate is released into DMEM.

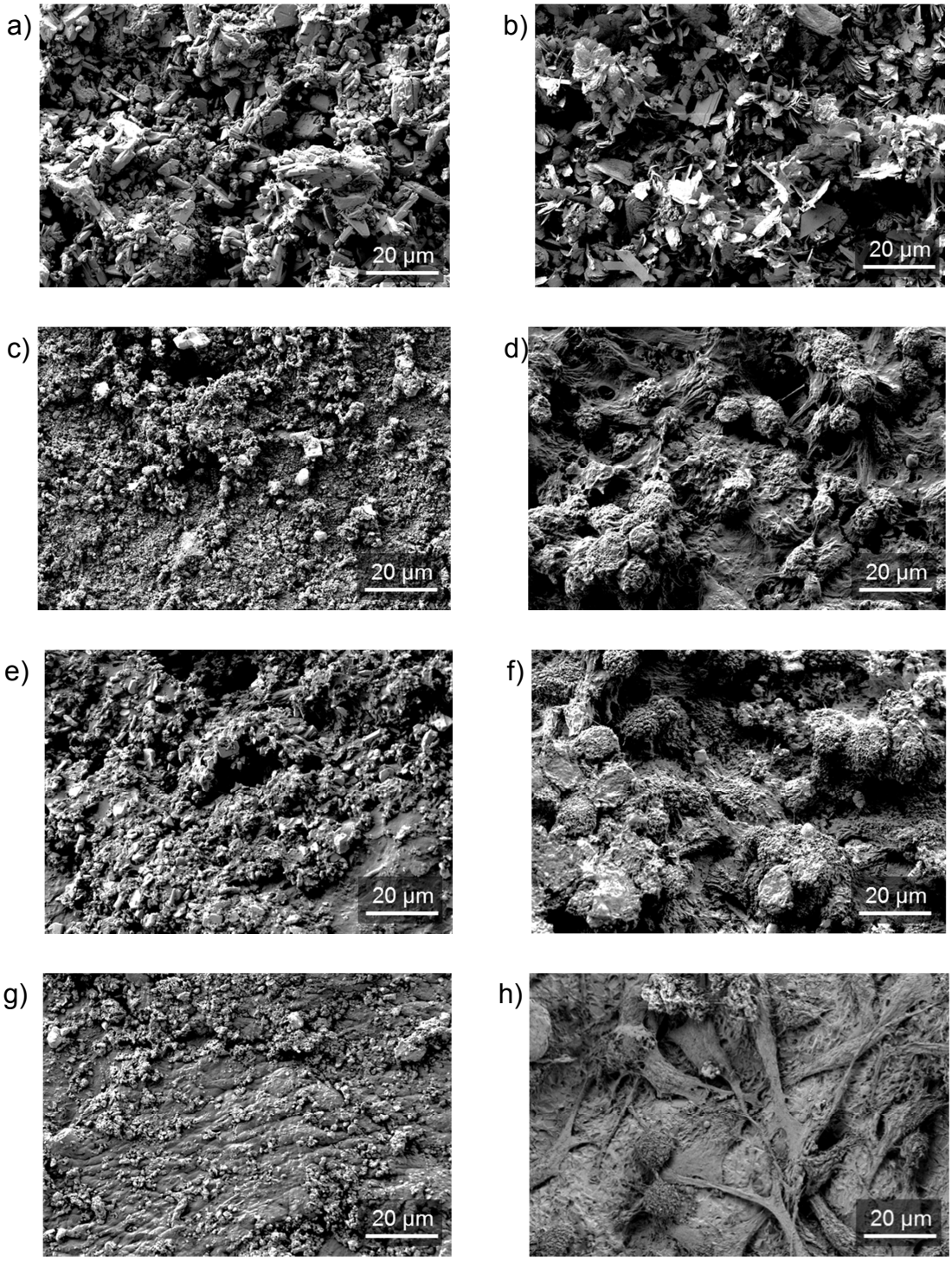

Figure 40: SEM images of a/b) CPC-reference and CPC/SF composites (PLR = 1 g·mL^{-1}), where the aqueous SF solutions had a concentration of c/d) 4, e/f) 8 and g/d) 16 wt.-% before (a, c, e & g) and after 14 days of MG-63 cell cultivation (b, d, f & g).

The SF content in the material seemed to correlate with the attenuation of the ion adsorption as well as the phosphate release. The latter was about twice as high for the CPC reference compared to the composites after day 6 and magnesium ions were almost completely removed by the fibroin free cement. The brushite phase on the CPC reference surface was practically completely dissolved after 14 days in

DMEM and the XRD pattern showed only a negligible peak for brushite (Figure 41 d). The main peaks indicated the presence of the cement raw material β-TCP, the side-product monetite (see also Figure 35a) and hydroxyapatite (HA). HA is known to be a reprecipitation product of brushite at physiological pH *in vitro* and *in vivo*.[137;139;242] Monetite became the dominant calcium phosphate phase for the composites on the material surfaces with minor amounts of residual β-TCP raw material, but no HA reprecipitates were observed.

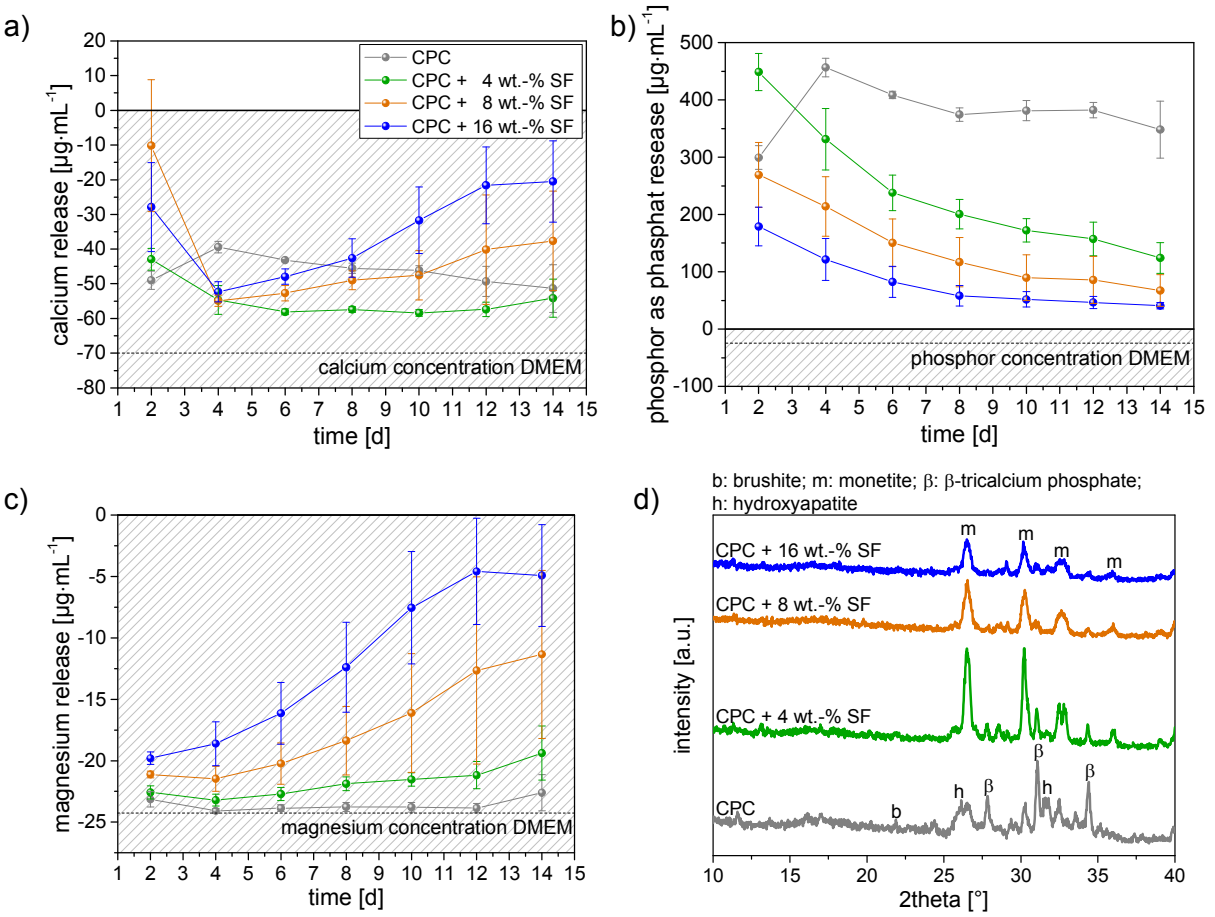

Figure 41: a) Calcium, b) phosphor as phosphate and c) magnesium release of CPC and CPC/SF composites in DMEM during the cell cultivation period of 14 days (shaded area indicates ion adsorption of the medium by the cement monoliths); d) XRD patterns of the cement surfaces after 14 d of cell cultivation. B indicates typical brushite peaks, β indicates typical β-TCP peaks, h indicates typical HA peaks and m indicates typical monetite peaks.

5.3 Discussion

The final mechanical strength of set CPC matrices depends on various parameters, such as the degree of cement conversion [67], cement porosity [17], kind of setting product [48], crystal size [371] or the use of filler particles [372].

Due to their brittle behavior and their compared to polymeric cements low mechanical performance, CPC are indicated only to non- or low-load bearing applications such as defects in craniomaxillofacial surgery [231]. Most approaches for a reinforcement of CPC are based on an optimization of the above mentioned parameters as well as on the addition of fibers [18] to increase bending strength and work of fracture due to fiber pull-out and energy dissipating mechanisms. However, fiber reinforcement has a detrimental effect on the rheological and injection properties of CPC and the fibers used in many studies are of a non-degradable nature.[18-19] This study aimed to improve the mechanical performance and to reduce the brittleness of CPC by combining the cement with silk fibroin as reinforcing phase. SF as the polymer phase is able to promote bone regeneration by providing nucleation sides for mineral deposition [412-413], has excellent mechanical properties [414], and is cheap in comparison to other biopolymers due to its large-scale production for textile industry [415]. Although a couple of studies before created calcium phosphate – silk fibroin composites [416-418], to the best of our knowledge, there is no study about a dual setting system of CPC combined with an aqueous SF solution. Here such a system of a brushite forming cement and the biodegradable SF with improved mechanical as well as biological properties in comparison to the pure CPC could successfully developed.

The combination of calcium phosphates with silk fibroin causes excellent osteogenic properties.[419-422] These composites are mainly processed at low calcium phosphates concentrations. Usually, a calcium solution and a phosphate solution are added to an aqueous SF solution, whereby the SF works as an organic template for the crystal growth during calcium phosphate precipitation.[421;423-426] Depending on the pH of the solution, this reaction either forms nanocrystalline HA or at lower pH ≤ 4, brushite is formed.[427-428] The latter has excellent biological properties and shows a better resorption profile *in vivo* [176;245] due to its higher solubility compared to HA under physiological conditions [141;429]. The main focus of these studies was to mimic the well-ordered structure of natural bone on a nanoscale level

composed of collagen fibrils and HA crystals.[412] For the manufacturing of pores, granular sodium chloride particles were added to the gel during synthesis, whose are leached out after drying.[413;421]

The materials described above are pre-set implants with a predefined size and shape. Here, a CaP-SF cement system with the advantage of a free moldability to any defect geometry and in situ setting property to finally form a hardened implant was developed. The key feature of this dual setting approach is a simultaneously occurring cement reaction and SF gelation, which is different to the few previous studies dealing with SF modified hydroxyapatite forming CPC, where the fibroin phase was only added as non-reactive filler to the cement matrix.[430-431] Mechanistically, SF gelation is induced by the pH decrease from 8.9 ± 0.2 to 2.7 ± 0.5 after adding the cement powder. This low pH favors the transformation of random coil to β-sheet fibroin structure according to FT-IR analysis (Figure 34) and by that gelation. The hydrophobic β-sheet-forming blocks are linked by small hydrophilic segments or spacers to build up the typically silk fibroin block copolymer. This crystalline structure is responsible for insolubility, high strength and thermal stability of SF.[432] In addition, the ionic strength in the system is increased by the dissolved CPC powder and the free phosphate ions present in the cement paste are inducing the fibroin gelation similar to the natural spinning process of *Bombyx mori*. Here, the spinning solution is acidified (pH 4.8 - 5.2) by epithelial cells containing a vesicular proton pump.[433]

By combining the cement powder and the SF hydrogel in a dual setting system in an unreacted state, much higher concentrations of both components can be used to form homogenous interpenetrating matrices on a microscopic level. This aspect is especially very important for the mechanical properties, whereas the polymeric SF phase is located in the gaps between the entangled cement crystals reinforcing the matrix. Additionally, the SF solution contracts during gelation leading to a self-densifying of the cement paste and hence closer packed crystals of the CPC precursor phase. This self-densifying behavior is proofed by the fact, that the measured porosities are lower than the theoretical porosities, determined with the assumption that the SF reduces the porosity of the cement matrix only by its volume (Figure 33). All these parameters additionally decrease the composite porosity in comparison to the pure CPC resulting in higher strength values.[17]

A key parameter for the porosity of CPCs is the PLR during mixing. Since the polymeric monomers are usually dissolved in the liquid cement phase, the PLR of the system can be retained at the same ratio as the CPC reference.[28] Similar to other studies [424;430;434], we observed improved mechanical properties by the combination of cement with SF both for elasticity and strength values. The compressive and the bending strength were about 8 times higher than the concerning CPC reference (Figure 36). The combination of high strength and elasticity results in an excellent toughness.[410;414;435] While the composites showed typical ductile fracture behavior under dry conditions, wet testing maintained the mobility of the SF chains, which results in a softening of the SF matrix and a higher elasticity of the whole composite.[436] Thereby the composites can be nailed onto a sheet of wood without fracture and can be cut into complex geometries in wet state (Figure 38). During cyclic loading, the remaining strain in the unloaded state demonstrates the plastic behavior of the composite. Additionally the Young`s modulus decreases with every cycle, which indicates a cyclic damage of the ductile CPC matrix, whereas the SF matrix is stable and retained the shape of the composite (Figure 37). For future applications this mechanism may be used for a self-healing concept, where the damaged CPC matrix could be repaired by bone remodeling or CaP deposition from body fluids.

Surprisingly, the CPC/fibroin composites produced with lower PLR of 0.5 $g \cdot mL^{-1}$ showed better mechanical performances than those with a PLR of 1 $g \cdot mL^{-1}$, even at a similar CPC:SF weight ratio. As the SF contracts during gelation as described above, the fibroin might be pre-stressed since SF relaxation is prevented by the embedded cement crystals. With a higher crystal content in the system, this pre-stress effect is likely increased, whereas the measurable strength decreases, since the analyzed stress starts from a higher level. Even with a compression of 65 %, no complete rupture was observed for the CPC/SF composites (Figure 36 a). The elastic SF matrix within the composite supports the brittle CPC matrix and maintains the bulk composite, even if the CPC matrix failed. This cohesion is likely an advantage for medical applications, since no small particles will splint by an overload causing potential blood-vessel blocking near the implantation side.

The combination of CPC powder with the SF solution continuously formed more monetite instead of brushite as product of the setting reaction correlating with the SF

content in the composite (Figure 35). Although the precipitation of monetite is thermodynamically favored, brushite is the common product of acidic CPC systems, because of kinetic reasons.[159-160] In comparison to brushite, monetite shows a lower solubility under physiological conditions [151], but resorbs faster *in vivo* since monetite does not transform into insoluble HA at physiological pH [161-162]. Monetite is only formed under highly acidic pH conditions, water-deficient environment or by adding metal ions disrupting brushite crystal growth.[126;160;437-438] In CPC/SF composites, the precipitation of the calcium phosphate phase is prolonged by the reduced diffusion rate caused by the additional hydrogel in the system compared to the CPC reference. In addition, it was observed, that cement liquid is partially squeezed out of the composite in a high percentage prior the cement setting. This continuously decreased the water content in the composite with an increasing SF amount, which in turn results in an insufficient water concentration for brushite formation. This effect might be supported by a high affinity of the SF hydrogel to water due to the fact that fibroin hydrogels show a swelling behavior in water [439-442].

The XRD patterns of the composites (Figure 35 c - d) showed an expanded baseline displacement in the 2-Theta region between 10° and 20° resulting from the crystalline β-sheet structure of the SF.[404-405;443] With an increasing SF content in the composite, the intensity of the XRD peaks subsequently decreased indicating a rising amorphous fraction and the peaks are broadened resulting from smaller crystals of the CPC setting product. As described above, SF is commonly used as a template for synthesis of nanocrystalline calcium phosphates, since crystal growth is retarded in a SF matrix by a reduced diffusion rated.[412] This was analyzed here by calculate the crystal size d by applying the Scherrer equation (14):

$$d = \frac{k \cdot \lambda}{\beta \cdot \cos(\Theta)} \tag{14}$$

where K is the dimensionless shape factor, λ the X-ray wavelength, β is the full width at half maximum of the characteristic peak and θ the diffraction angle. The SEM images (Figure 40 a, c, e & f) as well as the determination of the crystal sizes (Figure 42) confirmed a down scaling of the crystals by the addition of an increasing amount of SF to the composite.

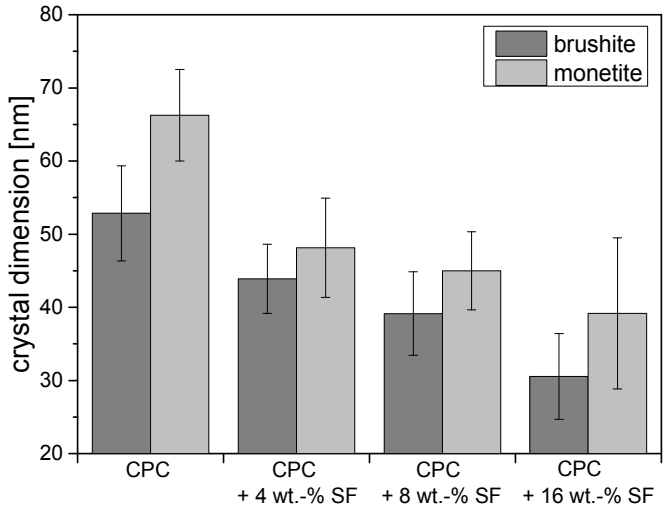

Figure 42: Dimension of brushite and monetite crystals calculated by the Scherrer equation in pure CPC and CPC/SF composites, where the aqueous SF solutions had a concentration of 4, 8 and 16 wt.-%.

Regarding *in vitro* cell tests, the proliferation and activity of the seeded MG-63 cells are obviously improved in correlation with an increasing SF content in the composite over a time period of 14 days (Figure 39). The cell proliferation and activity depends on a multiplicity number of parameters like pH, ion concentration in the surrounding medium, morphology and the mechanical properties of the substrate. SF is known to be a useful substrate for the cultivation of the cell line MG-63 and stimulates the osteoblastogenic gene expression.[444-445] Shi et al. observed an improved MG-63 cell growth with a minimization of the HA particle size and explained it by an enhanced interfacial adhesion due to the better penetration ability.[446] Here, a reduced particle dimension accompanied with better cell response were also found (Figure 39 & Figure 42). The reduced deviation of ion concentrations referred to fresh DMEM is likely another crucial factor for the improved cell behavior with an increasing SF content (Figure 39). Both the magnesium ion adsorption and the phosphate release are reduced at higher SF concentrations, which might be explained by the observed phase transformation from brushite into monetite by SF addition. The solubility of monetite in water at physiological pH (41.07 $mg \cdot L^{-1}$) is half the value of brushite (85.20 $mg \cdot L^{-1}$).[38;240] Hence, the phosphate release of the composites even with 16 wt.-% SF should be less than half of the brushite phosphate release due to preferred monetite precipitation in the composites (Figure 35). Actually, the phosphate release is reduced by 75 % for the CPC + 16 wt.-% after day 4, which is likely caused by the SF hydrogel in the CPC pores retarding ion diffusion and which also explains the decreased ion adsorption (Ca^{2+}, Mg^{2+}). Following this, a

potentially cytotoxic ion level (phosphate, Ca^{2+}, Mg^{2+}) is more and more minimized by the higher SF content in comparison to the CPC reference. Zhang *et al.* mentioned the necessity of the optimal concentration range by soluble factor release of resorbable ceramics for osteogenetic differentiation, cell growth and proliferiation.[447] Tamini *et al.* compared brushite and autoclaved brushite resulting in monetite *in vitro* and *in vivo*. Cell culture on monetite showed improved initial osteogenic gene expression than on brushite. The authors attributed this to the physical properties like an increased specific surface area and lower solubility, whereby the ion concentrations pass no cytotoxic level.[165] Additionally, the transformation of brushite into HA (Figure 41 d) causes crystalline reprecipitates on the cell seeded surfaces. Sporadically, it could be observed that single cells were covered by these depositions, which likely results in cell apoptosis.

5.4 Conclusion

Mineral cements forming the secondary phosphates brushite or monetite instead of HA are of a high clinical interest due to their higher bone remodeling capacity compared to HA forming cements, which degrades only slowly within years *in vivo* solely by osteoclastic activity.[118;237-238] As a natural polymer, SF is degraded proteolytically [411;448-449], whereas degradation time ranges from several days to months [449-451] with influencing parameters such as structure, morphology, mechanical and biological conditions.[411] This study demonstrated the possibility to create dual setting cements based on SF and secondary CPC with highly improved fracture resistance and self-densifying capacity. The *in vitro* degradation of the CPC phase in such composites is clearly slowed down by the incorporation of SF (Figure 41). This opens the possibility for further studies to either adapt the degradation behavior of both phases or to further retard SF degradation, such that the SF matrix remains over a longer time and works as a temporarily stable scaffold template during bone remodelling.

Chapter 6

General discussion and outlook

Three different dual setting systems on the basis of calcium phosphate cement were developed in this thesis (Figure 43).

In advancement of earlier studies, where an α-TCP cement was combined with 2-hydroxyethyl methacrylate (HEMA) [28;452], HEMA was replaced in a first approach by NCO-sP(EO-*stat*-PO) to avoid the need of a radical initiator system for the polymerization reaction, which may have detrimental effects on cytocompatibility by initiating cell apoptosis. Here, crosslinking of the hydrogel was designed to be an autocatalytic process after adding the aqueous cement liquid according to Figure 15 with a simultaneous formation of the HA matrix.

The next step was to achieve a biodegradable system by replacing low soluble HA forming cement. Brushite cement was chosen to accelerate degradation due to the higher solubility of brushite under physiological conditions [240] with a high bone remodeling capacity [140-141;241-242]. Furthermore, the secondary phase was exchanged by more degradable materials such as silica sol or silk fibroin. While silica is known to have a positive effect on bone mineralization [387-389], the biopolymer fibroin persuades by its extraordinary mechanical performance [414], biocompatibility [453] and high availability [415].

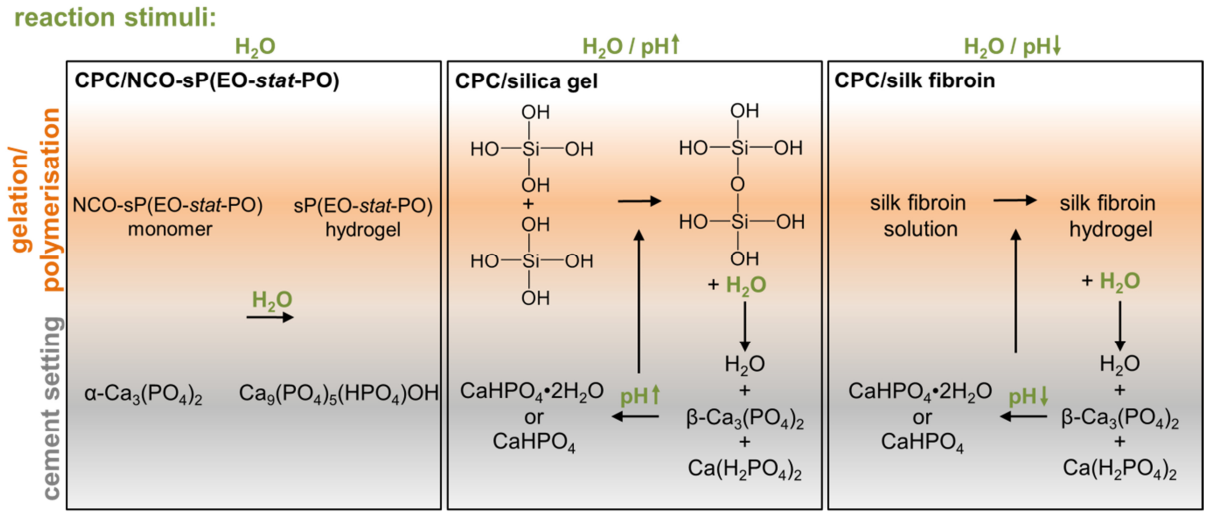

Figure 43: Overview of the dual setting systems developed in this thesis.

6.1 Dual setting system: Combination of unequal materials

The most challenging parameter for the development of a dual setting cement system is the simultaneous formation of a second polymeric or hydrogel phase from low molecular compounds along with the inorganic setting reaction of the cement. While this concept is advantageous compared to traditionally polymer modified cements in terms of mostly unaltered rheological properties, the practical realization is highly demanding due to the different material natures and reaction conditions (Figure 14).

As in most cases the monomer solution represents the cement liquid, it is crucial that the monomer solution is water-based to enable a sufficient cement reactivity by dissolution of the raw powder. Additionally, the viscosity of the monomer solution must be low enough to obtain a homogeneous paste after blending with the cement raw powder without the formation of particle agglomerates, but at the same time the monomer concentration has to be high enough for a noticeable reinforcement effect. The direct dissolution of the calcium phosphate raw powder in the cement liquid results in a beneficial viscosity reduction and the paste shows a thixotropic liquefaction by the external load of the spatula [261] simplifying the homogenization of the paste. Kinetically, the cement precipitation and the polymer crosslinking should start after the mixing and molding period of the cement paste for a better workability.

In most cases of dual setting cements, both setting reactions start almost simultaneously, however the polymerization/gelation of the reinforcing matrix is commonly much faster and completed with less than one hour, whereas the final setting of CPC can last for days.[68] The already formed polymeric matrix additionally retards the precipitation and growth of the cement crystals due to an impaired diffusion. This results in prolonged conversion times in comparison to the pure CPC, which can be analyzed by time-dependent XRD measurements (Figure 20).[452] The reduced conversion rate can theoretically result in lower strength values of the composite in comparison to the pure CPCs due to flaws and irregularities in the entangled cement matrix, especially in the first days, when the CPC conversion is not completed as observed for the CPC/NCO-sP(EO-*stat*-PO) composite (Figure 19).For the other two systems, the porosity reduction seems to compensate the retarded cement conversion, as no strength decrease was found during the investigated time period. However, the reduced CPC precipitation rate may also cause positive side-effects, e.g. the remaining cement raw powder in the set CPC is thought to be able to

adjust the degradation time of the composite. While HA is almost insoluble under physiological conditions, remaining α-TCP is leached out of the CPC matrix (Table 3) due to the higher solubility leaving pores for a better cell ingrowth. β-TCP in case of a brushite forming CPC has a detrimental effect and remains as a framework at the implantation side after brushite dissolution, which is known to be sometimes too fast for bone remodeling [142-143]. Furthermore, the formation of monetite instead of brushite is favored by the slow setting reaction [127;155-156], resulting in a new cement type with altered properties like cell response and degradation ability (chapter 0 and 0). Additionally, the hydrogel works as a template for crystal growth, whereby the crystals are generally smaller due to a diffusion barrier mechanism in comparison to the free spatial growth possibility in water. Smaller CPC crystals can dissolve faster and more easily accessible by osteoclasts for active dissolution [446].

Another challenging requirement in the development of the composite cements from this thesis was the interdependent starting of both setting reactions after mixing, without any further external trigger to ensure a fast hardening within a suitable surgical time frame. Here, the probably most simple system were CPC/NCO-sP(EO-*stat*-PO) composites, where both reactions started by the addition of water, whereby the cement setting and gelation of the other two systems (fibroin and silica sol) were catalyzing each other (Figure 43).

For CPC/silica gel cements, basic principles of the sol-gel-process were applied. The latter is a two-step reaction: First the precursor is hydrolyzed, followed by the polycondensation to form a Si-O-Si network.[454] The high dependency of the hydrolysis and condensation on the pH was exploited here to firstly stabilize the pre-hydrolyzed TEOS sol at acidic conditions (pH ~ 1 - 2 by HCl addition) and then to initiate the gelation reaction by the pH raise during cement setting (Figure 44). Since silica condensation released water as by-product, this in turn accelerated CPC setting.

In contrast, fibroin gelation is initiated by the initial pH drop of the brushite cement setting reaction, since the aqueous SF solution is stable at neutral pH and the cement setting runs in an acid range (pH ~ 2 - 3) as discussed in detail in chapter 5.3.

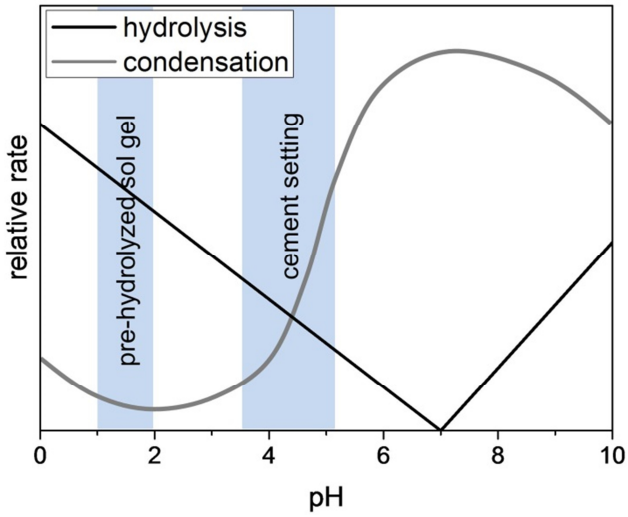

Figure 44: pH dependent hydrolysis and condensation curve of the sol gel process with the pH regions of the pre-hydrolyzed sol gel and the cement setting (modified from [378]).

6.2 Comparison with other cement reinforcing strategies

Despite all the beneficial properties of calcium phosphate cements for biomedical application and the intensive research in this field, such cements still suffer from insufficient mechanical properties in comparison to natural bone limiting their use to non- or low-bearing defects.

As described in detail in chapter 2.3, there are several strategies to improve the mechanical properties and fracture behavior of mineral biocements by intrinsic and extrinsic modifications (Figure 11) with advantages and disadvantages of the different methods. Here, this thesis focused on the relatively novel approach of a dual setting system.

The more commonly used simple mixing of a reactive phase and a non-reactive filler material (e.g. dissolved polymer or calcium phosphate particles), the viscosity increases and the concentrations of the different components have to be reduced to maintain processability of the cement paste. Usually, this results in a higher porosity of the set cement compared to the non-modified cement and therefore in a strength decrease [17]. For example, the mineralization of the NCO-sP(EO-*stat*-PO) hydrogels by adding non-reactive HA particles was possible only to an extend of ~ 50 wt.-%, whereby the mineral content could be increased up to 75 wt.-% by applying a dual setting system (Table 5). In addition, the formation of an entangled cement structure by the cement setting reaction resulted in a further mechanical reinforcement

compared to simply adding inorganic filler. This was demonstrated by incorporation of non-reactive β-TCP particles instead of the HA forming reactant α-TCP. Here, the compressive strength was 30times higher due to the cement setting reaction and the entanglement of the newly precipitated crystals within the hydrogel.

As mentioned above, cement porosity (mostly determined by the PLR used for cement mixing) is one of the most influencing parameters for the mechanical performance of the set cement. An easy way to reduce porosity is to compact the fresh cement paste prior to setting to eject an excess of cement liquid by filter-pressing. Various compacting methods are established in construction industry such as vibration compacting [455], compression compacting by roller [456] or self-compacting materials, which are compacted by their own weight or the use of superplasticizers [457]. In literature, CPCs have been compacted by uniaxial compression to squeeze out the exceeded water amount and minimize the porosity of the set cement with largely improved strength values.[17;112] However, compacted cement implants for biomedical applications have to be prefabricated and loose the beneficial free moldability and *in situ* hardening in the body. In the case of a dual setting cement, the additional polymeric phase is normally located in the gaps between the CPC crystals and reduces the cement porosity by its volume resulting in a strength improvement (Figure 25 and Figure 40). Especially, the here developed system of brushite and silk fibroin showed a self-densifying effect due to the SF shrinkage during setting resulting in an additional compaction mechanism while maintaining the ability to be molded or injected for minimal invasive surgery.

To avoid the typical instable and brittle fracture behavior of cements and to create more stable and mild crack growth, cements are commonly reinforced by fibers, whereby the energy of the external load can be absorbed by both fiber extension and pull out (chapter 2.3.2). Since the external applied force is transferred to the fibers via the matrix/fiber interface, it has to be maximized in terms of adhesion as well as mechanical interlocking.[19] Especially, the latter can be realized by increasing the fiber surface through an adequate length to diameter aspect ratio. Although the theoretical absorbable energy rises with an elongation of the inserted fibers, the workability slopes dramatically at the same time and prohibits injection of the cement paste.[292] Contrary, dual setting systems show a much higher interface between the CPC and the secondary matrix since they are in contact on a microscopic level,

which enables a maximum adhesion area of the two components. Additionally, the extensibility is not limited by the fiber length since the secondary matrix is continuously integrated in the composite. Furthermore, by largely maintaining the rheological properties of the dual setting cement paste, they can still be injected even with high amounts of the reinforcing phase.

Clearly, it should be possible to combine the dual setting system with several of the other reinforcing strategies like the combination of dual setting system and compacting in the case of the CPC/SF composite. For example a better interaction between fiber and cement matrix is imaginable, since the monomers of the secondary phase could be functionalized with binding motives both to the fibers as well as to the CPC matrix to work additional as linker.

6.3 Further applications with controllable reaction start

The main focus of this work was first to develop material systems, where the setting reactions of the two components were catalyzing each other to simultaneously form interpenetrating networks with an improvement of the mechanical properties like elasticity and fracture behavior. Furthermore the combination of mineral cements with a polymeric phase opens a wide range of possible applications and properties, which were partially broached by the here developed systems like the degradation adaption or the improved release of pharmaceutical agents. However, although other aspects like ready-to-use pastes, 3D plotting or the encapsulation of living cells are ambitious, these aspects should be clearly the focus of further experiments. Consequently, it would be of high interest to create set-on-demand pastes to control the start of the reaction at a precise time point to allow the above mentioned applications.

The crosslinking of the NCO-sP(EO-*stat*-PO) in water occurs fast within seconds for high polymer concentrations (≥ 50 wt.-%). Even with lower NCO-sP(EO-*stat*-PO) concentrations, the working window is just between 1 - 3 minutes for homogeneously mixing and applying the paste. Here, the isocyanate groups of NCO-sP(EO-*stat*-PO) might be blocked to avoid the undesired polymerization before complete composite mixing.[458-459] This blockage should be removable by the cement setting parameters to ensure the crosslinking parallel to the CPC matrix formation. In this context, the formation of a poly(carbamoyl sulfate) (PCS) seems to be a promising

method. PCS are formed by the addition of sodium hydrogen sulfite ($NaHSO_3$) to the NCO-sP(EO-*stat*-PO) solution according to equation (15) .[460]

$$R(\text{-}NCO)_n + n\ HSO_3^-\ Na^+ \leftrightarrow R(\text{-}NH\text{-}CO\text{-}SO_3^-\ Na^+)_n \qquad (15)$$

This complex is stable at room temperature and an acidic pH and can be decomposed with increasing pH and temperature.[461] Vorlop *et al.* described an unblocking with an accompanied gelation for a pH between 7 and 10 [462], which would be in the setting pH range of HA cements based on α-TCP hydrolysis. Therefore it is imaginable to improve the workability of the CPC/NCO-sP(EO-*stat*-PO) composite by the blocking of the isocyanate for a better handling and the automatic unblocking by the CPC setting reaction.

Furthermore, it may be also possible to create a ready-to-use paste on the base of α-TCP powder and NCO-sP(EO-*stat*-PO). Such ready-to-use or premixed pastes are of high clinical interest for minimal invasive applications like vertebroplasty, osteoporosis caused bone defect filling or implant fixation [463-464]. The pastes can be used directly without a mixing step of the cement liquid and powder, which results in advantageous features like reduced processing time, less contamination risk and a higher reproducibility.[465] The common approach is based on mixing the CPC raw powder with a water-free liquid and adjusting anti wash-out properties and setting time by adding gelling agents (e.g. chitosan or cellulose derivates) and reaction accelerators.[466] The pastes are stable under sealed conditions and harden not until they were exposed to the wet implantation side. There, the water-miscible liquid (mostly glycerol or poly(ethylene glycol) based [466-469]) is exchanged by aqueous body fluids and the dissolution/precipitation reaction is initiated. Heinemann *et al.* developed such a premixed CPC paste on the base of oil with retained setting time, mechanical properties and biocompatibility (Figure 45).[465]

For all this systems the water-free liquid acts only as an auxiliary material to transfer the CPC powder in the right pasty condition for injection and is washed out afterwards without any further function.

In the case of the CPC/NCO-sP(EO-*stat*-PO) composite it may be possible to develop a ready-to-use paste, whereby the polymeric phases remains in the implanted material to combine the benefits of a pre-mixed paste and a dual setting system. The presence of water initiates the CPC setting as well as the NCO-sP(EO-

stat-PO) crosslinking. Since NCO-sP(EO-*stat*-PO) monomers are a honey like fluid, the α-TCP powder can be blended under water-free conditions with the monomer to obtain a homogeneous paste, which should be stable in a sealed container and will likely show no phase separation due to the high viscosity of the NCO-sP(EO-*stat*-PO) monomer. With the injection of the paste into the implantation side both reactions should start by the diffusion of body fluids within the paste combining the elastic polymer and the brittle cement properties.

Figure 45: Ready-to-use CPC paste on the base of oil (Miglyol 812) (modified and reproduced from [273] with permission from Elsevier).

Furthermore, such CPC ready-to-use pastes are interesting for 3D plotting applications. 3D plotting is an additive manufacturing (AM) method, where a construct is manufactured through a layer-by-layer structure according to a computer-aided design.[470-471] Thereby, it is possible to build up patient-specific implants without the need and preparation of molds. In addition, the method has the potential to create defined interconnective pore systems within the construct to allow nutrients supply and vascularization. In comparison to other AM methods like stereolithography or laser sintering, 3D plotting offers the ability to incorporate and encapsulate biological agents [472] and even living cells [473] in the implant due to the mild processing conditions. For the fabrication, a viscous or pasty material is extruded through an moving nozzle (x,y-axis) by a continuous flow dispensing the strands according to the computer design and manufacture the scaffold layer-by-layer through movement in the z-direction in an gaseous or liquid environment (Figure 46 a).[474]

3D plotting of CPC pastes is challenging, since the paste must be rheological stable during the plotting process without cement setting or phase separation by filter pressing. Furthermore, paste viscosity must be low enough for a workable extrusion, but high enough to remain the strand structure after plotting without flowing away to

enable the deposition of the next layer. By the usage of the above mentioned oil based ready-to-use paste [465] Lode *et al.* demonstrated the construction of CPC scaffolds with different geometries by 3D plotting with adequate mechanical properties (Figure 46 b).[475]

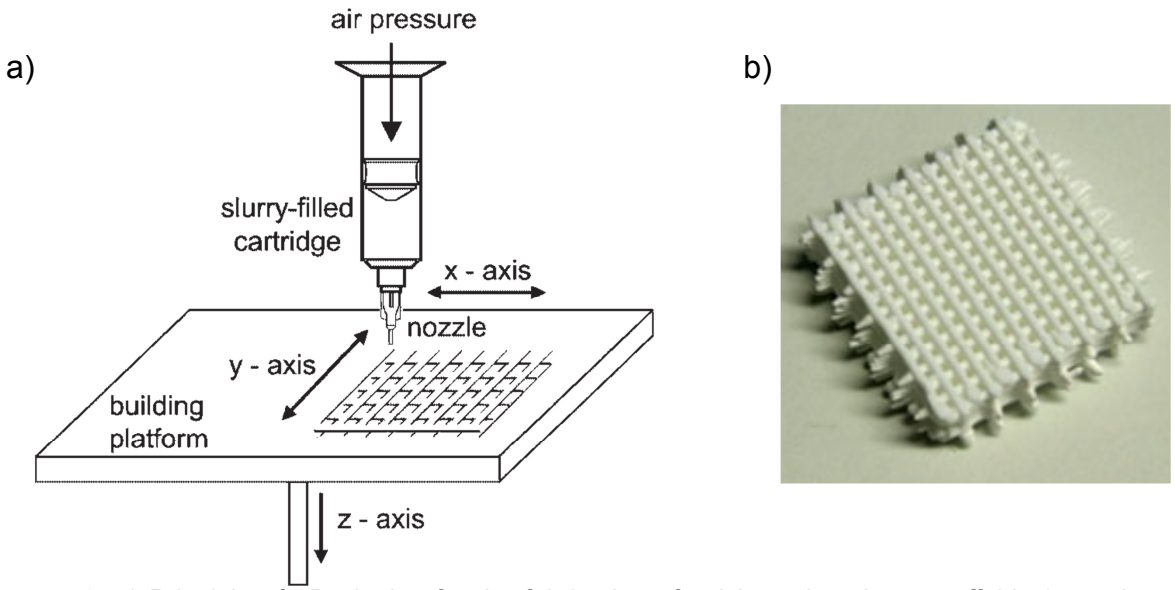

Figure 46: a) Principle of 3D plotting for the fabrication of calcium phosphate scaffolds (reproduced from [476] with permission from John Wiley and Sons) and b) a 3D plotted scaffold of a ready-to-use CPC paste on the base of oil (Miglyol 812) (reproduced from [475] with permission from John Wiley and Sons).

3D plotting should be also realizable with the above mentioned conceivable ready-to-use paste on the base of the composition of CPC and NCO-sP(EO-*stat*-PO). Here it is important to work under water-free conditions, for example in a glovebox to avoid the cement setting reaction until the end of the plotting process.

Especially, 3D plotting of the CPC/SF composite would be a promising and continuative approach for the dual setting system, since it is possible to entrap cells in SF hydrogels [407;477] to generate a three dimensional cell-material construct for tissue engineering. The SF gelation in the here developed CPC/SF system was initiated by the pH drop in an acid range due to the cement setting reaction, which occurred directly after mixing (Figure 31). To delay the SF gelation in the paste, the pH must remain in a neutral range to stabilize the aqueous SF solution. This can be realized by changing the cement system from an acidic type to a neutral pH setting cement. The pH shift to a milder value would be beneficial for both an extension of the paste shelf-life as well as for cell encapsulation.

One possibility may be to use α-TCP, which set into HA apatite under neutral conditions like it was used for the CPC/NCO-sP(EO-*stat*-PO) composite.[97] Problematically could be the starting cement reaction directly by the contact with the water of the SF solution. One big requirement for a feasible plotting paste are constant rheological properties of the paste during the plotting process to enable a workability without the need of parameter adjustment or even nozzle blocking. The immediate incipient cement setting reactions will cause formation of crystal agglomerates and hardening within the paste cartridge, whereby the timeframe may be too short for a practical plotting process. Furthermore, by the long-time stability of HA *in vivo* (chapter 2.2.1), the intended degradation of the composite is questionable.

Certainly, the use of magnesium phosphate cement (MPC) presents a promising alternative as mineral phase in the cement/SF system for the design of a plottable paste. Magnesium phosphates occur in physiological and pathological mineralized tissue [478-479] and are known to be biocompatible [384;395]. Since magnesium has a smaller ionic radius it can coordinate water molecules in a higher amount than calcium. Consequently, a much higher diversity of magnesium phosphate phases than calcium phosphates are possible.[480] The commonly magnesium sources for a MPC are magnesium oxide (MgO) [481] or farringtonite ($Mg_3(PO_4)_2$).[245] Especially the latter is widely investigated as cement raw powder for biomedical applications. By combining farringtonite with an acidic monocalcium phosphate, newberyite ($MgHPO_4 \cdot 3H_2O$) is formed by a dissolution and precipitation reaction as new magnesium phosphate phase.[395]

At neutral conditions farringtonite is almost insoluble in pure water (Table 11), which enables the possibility to prepare a ready-to-use paste with an aqueous solution. Consequently, a storable paste might be realized by the combination of farringtonite powder and an aqueous SF solution due to the absence of a pH change or increased ionic strength (chapter 0). After the fabrication of the green body by plotting the MPC/SF paste, the cement setting as well as the fibroin gelation can be initiated by the addition of an ammonium phosphate source. Farringtonite reacts by the combination with diammonium hydrogen phosphate (DAHP) into struvite (equation (16)) [393] or a mixture of struvite and newberyite (equation (17)) [482-483].

$$Mg_3(PO_4)_2 + (NH_4)_2HPO_4 + 36\ H_2O \rightarrow 6\ MgNH_4PO_4 \cdot 6H_2O + H_3PO_4 \qquad (16)$$

$$Mg_3(PO_4)_2 + (NH_4)_2HPO_4 + 15\ H_2O \rightarrow 2\ MgNH_4PO_4{\cdot}6H_2O + MgHPO_4{\cdot}3H_2O \quad (17)$$

Simultaneously to the cement reaction the fibroin gelation will be initiated by the addition of DAHP. DAHP is a kosmotropic salt according to the Hofmeister series.

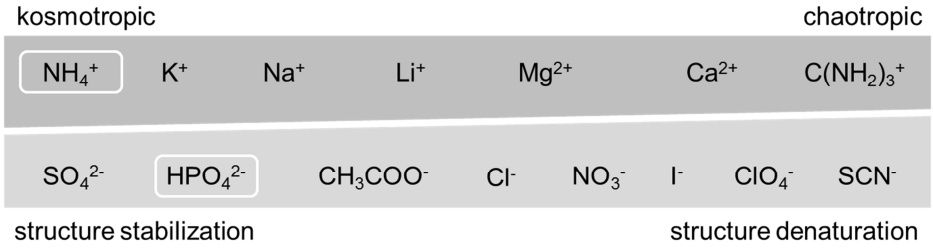

Figure 47: The Hofmeister series (modified from [484])

It favors the hydrophobic effect of the proteins in the aqueous solution and lead to protein folding due to the facilitated hydrophobic interactions and thereby to gelation.[485]

Lee *et al.* were able to produce three dimensional scaffolds with complex geometries with a MPC paste by plotting a green body with a post-hardening step in DAHP solution.[483] For a better workability, the authors used hydroxypropyl methyl cellulose (HPMC) as thickening agent. Contrary to HPMC, the SF would not only work as an additive for a better workability during the plotting process, but will also remain in the composite as reinforcing matrix to improve the mechanical properties.

Table 11: Composition and solubility constant of magnesium phosphates.

Compound	Formula	Mg/P ratio	-log (K_{sp}) at 37 °C	calculated solubility [mg·L^{-1}]
Trimagnesium phosphate anhydrate (farringtonite)	$Mg_3(PO_4)_2$	1.5	27.7 [486]	0.3
Dimagnesium phosphate trihydrate (newberyite)	$MgHPO_4{\cdot}3H_2O$	1.0	5.8 [487]	232.8
Magnesium ammonium phosphate hexahydrate (struvite)	$MgNH_4PO_4{\cdot}6H_2O$	1.0	12.7 [482]	14.6

The overall degradation of struvite *in vitro* is even higher than the brushite degradation [488], which is at first sight a positive property. Nevertheless, it can cause cell delamination by medium changes *in vitro* or an overreaching degradation rate *in vivo* like discussed for brushite. Most likely the additional SF phase will act as a diffusion barrier and hence retard the degradation kinetics like observed for other

dual setting systems. Consequently, it should be possible to adjust the degradation rate of the composite by the SF concentration.

MPCs are promising bone replacement materials due to their high compressive strength (newberyite: ~30 MPa [228]; struvite: ~60 MPa [489]), biocompatibility [384;395] and *in vivo* behavior [176;245]. Furthermore, struvite forming MGCs set in a neutral pH range [384;490], which is beneficial for cell encapsulation. Soltmann *et al.* were able to embed living microorganisms (*Rhodococcus ruber* and *Saccharomyces cerevisiae*) in a MPC with remaining biocatalytic activity.[491] For the more complex entrapment of eukaryotic cells due to their lower resistance level against osmotic stress, temperature and pH, the additional SF hydrogel in the here discussed application form may work as a suitable extracellular matrix environment.

7 References

1. H.-M. Ludwig and W. Zhang, *Research review of cement clinker chemistry*. Cem. Concr. Res., **2015**. 78: p. 24-37.
2. K. L. Scrivener and A. Nonat, *Hydration of cementitious materials, present and future*. Cem. Concr. Res., **2011**. 41(7): p. 651-665.
3. S. V. Dorozhkin, *Calcium orthophosphate cements for biomedical application*. J. Mater. Sci., **2008**. 43(9): p. 3028-3057.
4. S. P. Shah and C. Ouyang, *Mechanical Behavior of Fiber-Reinforced Cement-Based Composites*. J. Am. Ceram. Soc., **1991**. 74(11): p. 2727-2953.
5. D. D. L. Chung, *Cement reinforced with short carbon fibers: a multifunctional material*. Composites, Part B, **2000**. 31(6): p. 511-526.
6. R. Narayan Swamy, *Polymer reinforcement of cement systems*. J. Mater. Sci., **1979**. 14(7): p. 1521-1553.
7. J. B. Kardon, *Polymer-modified concrete: review*. J. Mater. Civ. Eng., **1997**. 9(2): p. 85-92.
8. D. D. L. Chung, *Use of polymers for cement-based structural materials*. J. Mater. Sci., **2004**. 39(9): p. 2973-2978.
9. K. Kendall, A. J. Howard, J. D. Birchall, P. L. Pratt, B. A. Proctor and S. A. Jefferis, *The relation between porosity, microstructure and strength, and the approach to advanced cement-based materials [and discussion]*. Philos. Trans. R. Soc., A, **1983**. 310(1511): p. 139-153.
10. J. D. Birchall, A. J. Howard and K. Kendall, *Flexural strength and porosity of cements*. Nature, **1981**. 289: p. 388-390.
11. K. Wille, A. E. Naaman, S. El-Tawil and G. J. Parra-Montesinos, *Ultra-high performance concrete and fiber reinforced concrete: achieving strength and ductility without heat curing*. Mater. Struct., **2012**. 45(3): p. 309-324.
12. K. Wille, A. E. Naaman and G. J. Parra-Montesinos, *Ultra-high performance concrete with compressive strength exceeding 150 MPa (22 ksi): A simpler way*. ACI Mater. J., **2011**. 108(1): p. 46-54.
13. J. D. Birchall, A. J. Howard and K. Kendall, *A cement spring*. J. Mater. Sci. Lett., **1982**. 1(3): p. 125-126.
14. B. W. Darvell and R. C. T. Wu, *"MTA"—an Hydraulic Silicate Cement: review update and setting reaction*. Dent. Mater., **2011**. 27(5): p. 407-422.
15. A. Rao, A. Rao and R. Shenoy, *Mineral trioxide aggregate—a review*. J. Clin. Pediatr. Dent., **2009**. 34(1): p. 1-8.
16. M. Geffers, J. Groll and U. Gbureck, *Reinforcement strategies for load-bearing calcium phosphate biocements*. Materials, **2015**. 8(5): p. 2700-2717.
17. J. E. Barralet, T. Gaunt, A. J. Wright, I. R. Gibson and J. C. Knowles, *Effect of porosity reduction by compaction on compressive strength and microstructure of calcium phosphate cement*. J. Biomed. Mater. Res., **2002**. 63(1): p. 1-9.
18. C. Canal and M. P. Ginebra, *Fibre-reinforced calcium phosphate cements: a review*. J. Mech. Behav. Biomed. Mater., **2011**. 4(8): p. 1658-1671.
19. R. Krüger and J. Groll, *Fiber reinforced calcium phosphate cements–On the way to degradable load bearing bone substitutes?* Biomaterials, **2012**. 33(25): p. 5887-5900.
20. Y. E. Greish, J. D. Bender, S. Lakshmi, P. W. Brown, H. R. Allcock and C. T. Laurencin, *Low temperature formation of hydroxyapatite-poly(alkyl oxybenzoate)phosphazene composites for biomedical applications*. Biomaterials, **2005**. 26(1): p. 1-9.
21. Y. E. Greish and P. W. Brown, *Chemically formed HAp-Ca poly(vinyl phosphonate) composites*. Biomaterials, **2001**. 22(8): p. 807-816.
22. A. O. Majekodunmi and S. Deb, *Poly(acrylic acid) modified calcium phosphate cements: the effect of the composition of the cement powder and of the molecular*

weight and concentration of the polymeric acid. J. Mater. Sci.: Mater. Med., **2007**. 18(9): p. 1883-8.
23. A. O. Majekodunmi, S. Deb and J. W. Nicholson, *Effect of molecular weight and concentration of poly(acrylic acid) on the formation of a polymeric calcium phosphate cement*. J. Mater. Sci.: Mater. Med., **2003**. 14(9): p. 747-52.
24. Y. Matsuya, J. M. Antonucci, S. Matsuya, S. Takagi and L. C. Chow, *Polymeric calcium phosphate cements derived from poly (methyl vinyl ether-maleic acid)*. Dent. Mater., **1996**. 12(1): p. 2-7.
25. K. Miyazaki, T. Horibe, J. M. Antonucci, S. Takagi and L. C. Chow, *Polymeric calcium phosphate cements: analysis of reaction products and properties*. Dent. Mater., **1993**. 9(1): p. 41-45.
26. A. Sugawara, J. M. Antonucci, S. Takagi, L. C. Chow and M. Ohashi, *Formation of hydroxyapatite in hydrogels from tetracalcium phosphate/dicalcium phosphate mixtures*. J. Nihon Univ. Sch. Dent., **1989**. 31(1): p. 372-381.
27. K. E. Watson, K. S. Tenhuisen and P. W. Brown, *The formation of hydroxyapatite–calcium polyacrylate composites*. J. Mater. Sci.: Mater. Med., **1999**. 10(4): p. 205-213.
28. T. Christel, M. Kuhlmann, E. Vorndran, J. Groll and U. Gbureck, *Dual setting α-tricalcium phosphate cements*. J. Mater. Sci.: Mater. Med., **2013**. 24(3): p. 573-581.
29. L. A. Dos Santos, R. G. Carrodeguas, A. O. Boschi and A. C. De Arruda, *Dual-Setting Calcium Phosphate Cement Modified with Ammonium Polyacrylate*. Artif. Organs, **2003**. 27(5): p. 412-418.
30. L. A. Dos Santos, R. G. Carrodeguas, A. O. Boschi and A. C. Fonseca de Arruda, *Fiber-enriched double-setting calcium phosphate bone cement*. J. Biomed. Mater. Res., Part A, **2003**. 65(2): p. 244-250.
31. J. Wang, C. S. Liu, Y. F. Liu and S. Zhang, *Double-Network Interpenetrating Bone Cement via in situ Hybridization Protocol*. Adv. Funct. Mater., **2010**. 20(22): p. 3997-4011.
32. W. D. Kingery, *II, Cold-Setting Properties*. J. Am. Ceram. Soc., **1950**. 33(8): p. 242-246.
33. R. Z. LeGeros, A. Chohayeb and A. Shulman, *Apatitic calcium phosphates: possible dental restorative materials*. J. Dent. Res., **1982**. 61(1): p. 343-347.
34. W. E. Brown and L. C. Chow, *Combinations of sparingly soluble calcium phosphates in slurries and pastes as mineralizers and cements*. **1986**, U.S. Patent No. 4,612,053.
35. W. E. Brown and L. C. Chow, *A new calcium phosphate, water-setting cement*. Cem. Res. Prog., **1987**. p. 351-379.
36. W. E. Brown and L. C. Chow, *Dental resptorative cement pastes*. **1985**, U.S. Patent No. 4,518,430.
37. S. V. Dorozhkin, *Self-setting calcium orthophosphate formulations: cements, concretes, pastes and putties*. Int. J. Mater. Chem., **2011**. 1(1): p. 1-48.
38. J. C. Elliott, *Structure and chemistry of the apatites and other calcium orthophosphates*. **2013**: Elsevier.
39. J. T. Zhang, W. Z. Liu, V. Schnitzler, F. Tancret and J. M. Bouler, *Calcium phosphate cements for bone substitution: Chemistry, handling and mechanical properties*. Acta Biomaterialia, **2014**. 10(3): p. 1035-1049.
40. E. Fernandez, F. J. Gil, M. P. Ginebra, F. C. Driessens, J. A. Planell and S. M. Best, *Calcium phosphate bone cements for clinical applications. Part II: precipitate formation during setting reactions*. J. Mater. Sci.: Mater. Med., **1999**. 10(3): p. 177-83.
41. T. M. Gregory, E. C. Moreno and W. E. Brown, *Solubility of CaHP04· 2H20 in the System Ca(OH)2 -H3P04 -H20 at 5, 15, 25, and 37.5 °C* J. Res. Nat. Bur. Stand., **1970**. 74A(4): p. 461-475.
42. J. R. Sutter, H. McDowell and W. E. Brown, *Solubility study of calcium hydrogen phosphate. Ion-pair formation*. Inorg. Chem., **1971**. 10(8): p. 1638-1643.
43. M. S. Tung, N. Eidelman, B. Sieck and W. E. Brown, *Octacalcium Phosphate Solubility Product from 4 to 37 °C* J. Res. Nat. Bur. Stand., **1988**. 93(5): p. 613-624.

44. B. O. Fowler and S. Kuroda, *Changes in heated and in laser-irradiated human tooth enamel and their probable effects on solubility*. Calcif. Tissue Int., **1986**. 38(4): p. 197-208.
45. T. M. Gregory, E. C. Moreno, J. M. Patel and W. E. Brown, *Solubility of ß-Ca3(PO4)2 in the System Ca(OH)2-H3PO4-H2O at 5, 15, 25, and 37 °C*. J. Res. Nat. Bur. Stand., **1974**. 78A(6): p. 667-674.
46. H. McDowell, T. M. Gregory and W. E. Brown, *Solubility of Ca5(PO4)3OH in the System Ca(OH)2-H3PO4-H2O at 5, 15, 25 and 37 °C*. J. Res. Nat. Bur. Stand., **1977**. 81A(2): p. 273-281.
47. W. C. Chen, J. H. Lin and C. P. Ju, *Transmission electron microscopic study on setting mechanism of tetracalcium phosphate/dicalcium phosphate anhydrous-based calcium phosphate cement*. J. Biomed. Mater. Res., Part A, **2003**. 64(4): p. 664-71.
48. M. Bohner, *Calcium orthophosphates in medicine: from ceramics to calcium phosphate cements*. Injury, **2000**. 31: p. D37-D47.
49. G. Vereecke and J. Lemaître, *Calculation of the solubility diagrams in the system Ca(OH)2-H3PO4-KOH-HNO3-CO2-H2O*. J. Cryst. Growth, **1990**. 104(4): p. 820-832.
50. M. P. Ginebra, E. Fernandez, F. C. M. Driessens, M. G. Boltong, J. Muntasell, J. Font and J. A. Planell, *The effects of temperature on the behaviour of an apatitic calcium phosphate cement*. J. Mater. Sci.: Mater. Med., **1995**. 6(12): p. 857-860.
51. F. C. M. Driessens, M. G. Boltong, E. A. P. D. Maeyer, R. M. H. Verbeeck and R. Wenz, *Effect of temperature and immersion on the setting of some calcium phosphate cements*. J. Mater. Sci.: Mater. Med., **2000**. 11(7): p. 453-457.
52. L. M. Grover, U. Gbureck, A. M. Young, A. J. Wright and J. E. Barralet, *Temperature dependent setting kinetics and mechanical properties of ß-TCP-pyrophosphoric acid bone cement*. J. Mater. Chem., **2005**. 15(46): p. 4955-4962.
53. S. J. Zawacki, P. B. Koutsoukos, M. H. Salimi and G. H. Nancollas, *The growth of calcium phosphates*. ACS Symp. Ser., **1986**. 323: p. 650-662.
54. K. Ishikawa, Y. Miyamoto, M. Takechi, Y. Ueyama, K. Suzuki, M. Nagayama and T. Matsumura, *Effects of neutral sodium hydrogen phosphate on setting reaction and mechanical strength of hydroxyapatite putty*. J. Biomed. Mater. Res., **1999**. 44(3): p. 322-329.
55. M. T. Fulmer and P. W. Brown, *Effects of Na2HPO4 and NaH2PO4 on hydroxyapatite formation*. J. Biomed. Mater. Res., **1993**. 27(8): p. 1095-1102.
56. L. C. Chow, M. Markovic and S. Takagi, *Formation of hydroxyapatite in cement systems: Effects of phosphate*. Phosphorus, Sulfur Silicon Relat. Elem., **1999**. 144(1): p. 129-132.
57. K. A. R. Hassan, *The Microelectrophoretic Behavior of Sparingly Soluble Salts*. **1984**: State University of New York.
58. M. Bohner, J. Lemaitre and T. A. Ring, *Effects of sulfate, pyrophosphate, and citrate ions on the physicochemical properties of cements made of β-tricalcium phosphate-phosphoric acid-water mixtures*. J. Am. Ceram. Soc., **1996**. 79(6): p. 1427-1434.
59. M. Bohner, H. P. Merkle, P. Van Landuyt, G. Trophardy and J. Lemaitre, *Effect of several additives and their admixtures on the physico-chemical properties of a calcium phosphate cement*. J. Mater. Sci.: Mater. Med., **2000**. 11(2): p. 111-116.
60. M. P. Ginebra, F. C. M. Driessens and J. A. Planell, *Effect of the particle size on the micro and nanostructural features of a calcium phosphate cement: a kinetic analysis*. Biomaterials, **2004**. 25(17): p. 3453-3462.
61. M. P. Hofmann, *Physikalische Charakterisierung von Calciumphosphat-Pulvern zur Einstellung von Prozessparametern für die Herstellung von Knochenzement*, in *Department for functional materials in medicine and dentistry*. **2003**, University of Würzburg: Würzburg, Germany.
62. M. Otsuka, Y. Matsuda, Y. Suwa, J. L. Fox and W. I. Higuchi, *Effect of particle size of metastable calcium phosphates on mechanical strength of a novel self-setting bioactive calcium phosphate cement*. J. Biomed. Mater. Res., **1995**. 29(1): p. 25-32.

63. S. Takagi, L. Chow and K. Ishikawa, *Formation of hydroxyapatite in new calcium phosphate cements*. Biomaterials, **1998**. 19(17): p. 1593-1599.
64. H. Monma and T. Kanazawa, *The Hydration of alpha-Tricalcium Phosphate*. J. Ceram. Soc. Jpn., **1976**. 84: p. 209-2013.
65. M.-P. Ginebra, E. Fernández, F. C. Driessens and J. A. Planell, *Modeling of the Hydrolysis of α-Tricalcium Phosphate*. J. Am. Ceram. Soc., **1999**. 82(10): p. 2808-2812.
66. U. Gbureck, J. E. Barralet, L. Radu, H. G. Klinger and R. Thull, *Amorphous α-Tricalcium Phosphate: Preparation and Aqueous Setting Reaction*. J. Am. Ceram. Soc., **2004**. 87(6): p. 1126-1132.
67. U. Gbureck, O. Grolms, J. E. Barralet, L. M. Grover and R. Thull, *Mechanical activation and cement formation of β-tricalcium phosphate*. Biomaterials, **2003**. 24(23): p. 4123-4131.
68. K. Hurle, J. Neubauer, M. Bohner, N. Doebelin and F. Goetz-Neunhoeffer, *Effect of amorphous phases during the hydraulic conversion of α-TCP into calcium-deficient hydroxyapatite*. Acta Biomater., **2014**. 10(9): p. 3931-3941.
69. B. H. O'Connor and M. D. Raven, *Application of the Rietveld refinement procedure in assaying powdered mixtures*. Powder Diffr., **1988**. 3(01): p. 2-6.
70. M. Bohner, A. K. Malsy, C. L. Camiré and U. Gbureck, *Combining particle size distribution and isothermal calorimetry data to determine the reaction kinetics of α-tricalcium phosphate–water mixtures*. Acta Biomater., **2006**. 2(3): p. 343-348.
71. T. J. Brunner, M. Bohner, C. Dora, C. Gerber and W. J. Stark, *Comparison of amorphous TCP nanoparticles to micron-sized α-TCP as starting materials for calcium phosphate cements*. J. Biomed. Mater. Res., Part B, **2007**. 83B(2): p. 400-407.
72. D. D. Lee, C. Rey and M. Aiolova, *Synthesis of reactive amorphous calcium phosphates*. **1997**, US 5676976 A.
73. P. W. Brown and R. I. Martin, *An analysis of hydroxyapatite surface layer formation*. J. Phys. Chem. B, **1999**. 103(10): p. 1671-1675.
74. J. L. Lacout, E. Mejdoubi and M. Hamad, *Crystallization mechanisms of calcium phosphate cement for biological uses*. J. Mater. Sci.: Mater. Med., **1996**. 7(6): p. 371-374.
75. J. P. Schmitz, J. O. Hollinger and S. B. Milam, *Reconstruction of bone using calcium phosphate bone cements: A critical review*. J. Oral Maxillofac. Surg., **1999**. 57(9): p. 1122-1126.
76. D. D. Weiss, M. A. Sachs and C. R. Woodard, *Calcium phosphate bone cements: a comprehensive review*. J. Long-Term Eff. Med. Implants, **2003**. 13(1): p.
77. J. C. Le Huec, T. Schaeverbeke, D. Clement, J. Faber and A. Le Rebeller, *Influence of porosity on the mechanical resistance of hydroxyapatite ceramics under compressive stress*. Biomaterials, **1995**. 16(2): p. 113-118.
78. L. C. Chow, *Development of self-setting calcium phosphate cements*. J. Ceram. Soc. Jpn., **1991**. 99(1154): p. 954-964.
79. K. Ishikawa, S. Takagi, L. C. Chow and Y. Ishikawa, *Properties and mechanisms of fast-setting calcium phosphate cements*. J. Mater. Sci.: Mater. Med., **1995**. 6(9): p. 528-533.
80. Y. Fukase, E. D. Eanes, S. Takagp, L. C. Chow and W. E. Brown, *Setting reactions and compressive strengths of calcium phosphate cements*. J. Dent. Res., **1990**. 69(12): p. 1852-1856.
81. C. Liu, W. Shen, Y. Gu and L. Hu, *Mechanism of the hardening process for a hydroxyapatite cement*. J. Biomed. Mater. Res., **1997**. 35(1): p. 75-80.
82. U. Posset, E. Löcklin, R. Thull and W. Kiefer, *Vibrational spectroscopic study of tetracalcium phosphate in pure polycrystalline form and as a constituent of a self-setting bone cement*. J. Biomed. Mater. Res., **1998**. 40(4): p. 640-645.

83. M. Kouassi, P. Michaïlesco, A. Lacoste-Armynot and P. Boudeville, *Antibacterial effect of a hydraulic calcium phosphate cement for dental applications*. J. Endod., **2003**. 29(2): p. 100-103.
84. H. El Briak, D. Durand, J. Nurit, S. Munier, B. Pauvert and P. Boudeville, *Study of a hydraulic dicalcium phosphate dihydrate/calcium oxide-based cement for dental applications*. J. Biomed. Mater. Res., **2002**. 63(4): p. 447-453.
85. S. Matsuya, S. Takagi and L. C. Chow, *Effect of mixing ratio and pH on the reaction between Ca4 (PO4) 2O and CaHPO4*. J. Mater. Sci.: Mater. Med., **2000**. 11(5): p. 305-311.
86. K. Ishikawa, S. Takagi, L. C. Chow and K. Suzuki, *Reaction of calcium phosphate cements with different amounts of tetracalcium phosphate and dicalcium phosphate anhydrous*. J. Biomed. Mater. Res., **1999**. 46(4): p. 504-510.
87. P. W. Brown and M. T. Fulmer, *Kinetics of hydroxyapatite formation at low temperature*. J. Am. Ceram. Soc., **1991**. 74(5): p. 934-940.
88. K. S. TenHuisen and P. W. Brown, *The formation of hydroxyapatite-ionomer cements at 38 C*. J. Dent. Res., **1994**. 73(3): p. 598-606.
89. U. Gbureck, J. E. Barralet, M. P. Hofmann and R. Thull, *Mechanical activation of tetracalcium phosphate*. J. Am. Ceram. Soc., **2004**. 87(2): p. 311-313.
90. U. Gbureck, R. Thull and J. E. Barralet, *Alkali ion substituted calcium phosphate cement formation from mechanically activated reactants*. J. Mater. Sci.: Mater. Med., **2005**. 16(5): p. 423-427.
91. G. Berger, R. Gildenhaar and U. Ploska, *Rapid resorbable, glassy crystalline materials on the basis of calcium alkali orthophosphates*. Biomaterials, **1995**. 16(16): p. 1241-1248.
92. D. Jörn, R. Gildenhaar, G. Berger, M. Stiller and C. Knabe. *Behaviour of calcium alkali orthophosphate cements under simulated implantation conditions*. in *Key Eng. Mater.* **2009**. Trans Tech Publ.
93. G. Berger, R. Gildenhaar, J. Pauli and H. Marx. *Preparation and characterization of new self-setting calcium phosphate cements based on alkali containing orthophosphates*. in *Key Eng. Mater.* **2005**. Trans Tech Publ.
94. R. Gildenhaar, G. Berger, E. Lehmann and C. Knabe. *Development of alkali containing calcium phosphate cements*. in *Key Eng. Mater.* **2007**. Trans Tech Publ.
95. F. C. M. Driessens, M. G. Boltong, E. A. P. De Maeyer, R. Wenz, B. Nies and J. A. Planell, *The Ca/P range of nanoapatitic calcium phosphate cements*. Biomaterials, **2002**. 23(19): p. 4011-4017.
96. L. Yubao, Z. Xingdong and K. De Groot, *Hydrolysis and phase transition of alpha-tricalcium phosphate*. Biomaterials, **1997**. 18(10): p. 737-741.
97. K. S. TenHuisen and P. W. Brown, *Formation of calcium-deficient hydroxyapatite from α-tricalcium phosphate*. Biomaterials, **1998**. 19(23): p. 2209-2217.
98. F. C. Driessens, M. G. Boltong, J. A. Planell, O. Bermudez, M. P. Ginebra and E. Fernandez, *A new apatitic calcium phosphate bone cement: preliminary results*. Bioceram., **1993**. 6: p. 469-473.
99. M. T. Fulmer, R. I. Martin and P. W. Brown, *Formation of calcium deficient hydroxyapatite at near-physiological temperature*. J. Mater. Sci.: Mater. Med., **1992**. 3(4): p. 299-305.
100. M. P. Ginebra, E. Fernandez, E. De Maeyer, R. M. H. Verbeeck, M. G. Boltong, J. Ginebra, F. C. M. Driessens and J. A. Planell, *Setting reaction and hardening of an apatitic calcium phosphate cement*. J. Dent. Res., **1997**. 76(4): p. 905-912.
101. C. L. Camire, U. Gbureck, W. Hirsiger and M. Bohner, *Correlating crystallinity and reactivity in an alpha-tricalcium phosphate*. Biomaterials, **2005**. 26(16): p. 2787-94.
102. M. P. Ginebra, E. Fernandez, M. G. Boltong, F. C. Driessens and J. A. Planell, *Influence of the particle size of the powder phase in the setting and hardening behaviour of a calcium phosphate cement*. Bioceram., **1997**. 10: p. 481-484.
103. C. Durucan and P. W. Brown, *Reactivity of α-tricalcium phosphate*. J. Mater. Sci., **2002**. 37(5): p. 963-969.

104. C. Liu and W. Shen, *Effect of crystal seeding on the hydration of calcium phosphate cement*. J. Mater. Sci.: Mater. Med., **1997**. 8(12): p. 803-807.
105. Q. Yang, T. Troczynski and D.-M. Liu, *Influence of apatite seeds on the synthesis of calcium phosphate cement*. Biomaterials, **2002**. 23(13): p. 2751-2760.
106. M.-P. Ginebra, C. Canal, M. Espanol, D. Pastorino and E. B. Montufar, *Calcium phosphate cements as drug delivery materials*. Adv. Drug Delivery Rev., **2012**. 64(12): p. 1090-1110.
107. C. Liu, H. Shao, F. Chen and H. Zheng, *Effects of the granularity of raw materials on the hydration and hardening process of calcium phosphate cement*. Biomaterials, **2003**. 24(23): p. 4103-4113.
108. E. B. Montufar, T. Traykova, C. Gil, I. Harr, A. Almirall, A. Aguirre, E. Engel, J. A. Planell and M. P. Ginebra, *Foamed surfactant solution as a template for self-setting injectable hydroxyapatite scaffolds for bone regeneration*. Acta Biomater., **2010**. 6(3): p. 876-885.
109. N. Nezafati, F. Moztarzadeh, S. Hesaraki and M. Mozafari, *Synergistically reinforcement of a self-setting calcium phosphate cement with bioactive glass fibers*. Ceram. Int., **2011**. 37(3): p. 927-934.
110. A. R. Calafiori, G. Di Marco, G. Martino and M. Marotta, *Preparation and characterization of calcium phosphate biomaterials*. J. Mater. Sci.: Mater. Med., **2007**. 18(12): p. 2331-2338.
111. R. I. Martin and P. W. Brown, *Mechanical properties of hydroxyapatite formed at physiological temperature*. J. Mater. Sci.: Mater. Med., **1995**. 6(3): p. 138-143.
112. U. Gbureck, J. E. Barralet, K. Spatz, L. M. Grover and R. Thull, *Ionic modification of calcium phosphate cement viscosity. Part I: hypodermic injection and strength improvement of apatite cement*. Biomaterials, **2004**. 25(11): p. 2187-2195.
113. J. E. Barralet, M. P. Hofmann, L. M. Grover and U. Gbureck, *High-Strength Apatitic Cement by Modification with α-Hydroxy Acid Salts*. Adv. Mater., **2003**. 15(24): p. 2091-2094.
114. J. Henkel, M. A. Woodruff, D. R. Epari, R. Steck, V. Glatt, I. C. Dickinson, P. F. M. Choong, M. A. Schuetz and D. W. Hutmacher, *Bone regeneration based on tissue engineering conceptions—a 21st century perspective*. Bone Res., **2013**. 1(3): p. 216.
115. A. J. Wagoner Johnson and B. A. Herschler, *A review of the mechanical behavior of CaP and CaP/polymer composites for applications in bone replacement and repair*. Acta Biomater., **2011**. 7(1): p. 16-30.
116. B. Bourgeois, O. Laboux, L. Obadia, O. Gauthier, E. Betti, E. Aguado, G. Daculsi and J. M. Bouler, *Calcium-deficient apatite: A first in vivo study concerning bone ingrowth*. J. Biomed. Mater. Res., Part A, **2003**. 65(3): p. 402-408.
117. J. Lu, M. Descamps, J. Dejou, G. Koubi, P. Hardouin, J. Lemaitre and J. P. Proust, *The biodegradation mechanism of calcium phosphate biomaterials in bone*. J. Biomed. Mater. Res., **2002**. 63(4): p. 408-412.
118. S. Wenisch, J. P. Stahl, U. Horas, C. Heiss, O. Kilian, K. Trinkaus, A. Hild and R. Schnettler, *In vivo mechanisms of hydroxyapatite ceramic degradation by osteoclasts: fine structural microscopy*. J. Biomed. Mater. Res., Part A, **2003**. 67(3): p. 713-718.
119. D. L. Alge, W. S. Goebel and T. M. Chu, *In vitro degradation and cytocompatibility of dicalcium phosphate dihydrate cements prepared using the monocalcium phosphate monohydrate/hydroxyapatite system reveals rapid conversion to HA as a key mechanism*. J. Biomed. Mater. Res., Part B, **2012**. 100(3): p. 595-602.
120. S. V. Dorozhkin, *Calcium Orthophosphates in Nature, Biology and Medicine*. Materials, **2009**. 2(2): p. 399.
121. E. S. Sanzana, M. Navarro, F. Macule, S. Suso, J. A. Planell and M. P. Ginebra, *Of the in vivo behavior of calcium phosphate cements and glasses as bone substitutes*. Acta Biomater., **2008**. 4(6): p. 1924-1933.
122. A. A. Mirtchi, J. Lemaitre and E. Munting, *Calcium phosphate cements: action of setting regulators on the properties of the beta-tricalcium phosphate-monocalcium phosphate cements*. Biomaterials, **1989**. 10(9): p. 634-8.

123. A. A. Mirtchi, J. Lemaitre and N. Terao, *Calcium phosphate cements: Study of the β-tricalcium phosphate—monocalcium phosphate system*. Biomaterials, **1989**. 10(7): p. 475-480.
124. S. V. Dorozhkin, *Calcium Orthophosphates: Applications in Nature, Biology, and Medicine*. **2012**: Pan Stanford Publishing.
125. S. V. Dorozhkin, *Calcium orthophosphates*. J. Mater. Sci., **2007**. 42(4): p. 1061-1095.
126. M. Bohner and U. Gbureck, *Thermal reactions of brushite cements*. J. Biomed. Mater. Res., Part B, **2008**. 84(2): p. 375-385.
127. M. Bohner, P. Van Landuty, H. P. Merkle and J. Lemaitre, *Composition effects on the pH of a hydraulic calcium phosphate cement*. J. Mater. Sci.: Mater. Med., **1997**. 8(11): p. 675-681.
128. J. Lemaitre, A. A. Mirtchi and A. Mortier, *Calcium phosphate cements for medical use: State of the art and perspectives of development*. Silic. Ind., **1987**. 9: p. 141-146.
129. H. Andrianjatovo, F. Jose and J. Lemaitre, *Effect of β-TCP granularity on setting time and strength of calcium phosphate hydraulic cements*. J. Mater. Sci.: Mater. Med., **1996**. 7(1): p. 34-39.
130. C. Pittet, P.-D. Grasso and J. Lemaître. *Influence of raw powder granulometry on the mechanical properties of a calcium phosphate bone cement*. in *Key Eng. Mater.* **2001**. Trans Tech Publ.
131. U. Gbureck, S. Dembski, R. Thull and J. E. Barralet, *Factors influencing calcium phosphate cement shelf-life*. Biomaterials, **2005**. 26(17): p. 3691-3697.
132. M. Bohner, *Reactivity of calcium phosphate cements*. J. Mater. Chem., **2007**. 17(38): p. 3980-3986.
133. M. Bohner, T. J. Brunner and W. J. Stark, *Controlling the reactivity of calcium phosphate cements*. J. Mater. Chem., **2008**. 18(46): p. 5669-5675.
134. A. A. Mirtchi, J. Lemaître and E. Hunting, *Calcium phosphate cements: action of setting regulators on the properties of the β-tricalcium phosphate-monocalcium phosphate cements*. Biomaterials, **1989**. 10(9): p. 634-638.
135. P. Frayssinet, L. Gineste, P. Conte, J. Fages and N. Rouquet, *Short-term implantation effects of a DCPD-based calcium phosphate cement*. Biomaterials, **1998**. 19(11): p. 971-977.
136. M. H. Alkhraisat, F. T. Marino, J. R. Retama, L. B. Jerez and E. Lopez-Cabarcos, *Beta-tricalcium phosphate release from brushite cement surface*. J. Biomed. Mater. Res., Part A, **2008**. 84(3): p. 710-7.
137. B. R. Constantz, B. M. Barr, I. C. Ison, M. T. Fulmer, J. Baker, L. McKinney, S. B. Goodman, S. Gunasekaren, D. C. Delaney and J. Ross, *Histological, chemical, and crystallographic analysis of four calcium phosphate cements in different rabbit osseous sites*. J. Biomed. Mater. Res., **1998**. 43(4): p. 451-461.
138. S. Rousseau and J. Lemaitre, *Long-term aging of brushite cements in physiological conditions: an in vitro study*. Eur. Cells Mater., **2003**. 5(2): p. 83.
139. L. M. Grover, J. C. Knowles, G. J. P. Fleming and J. E. Barralet, *In vitro ageing of brushite calcium phosphate cement*. Biomaterials, **2003**. 24(23): p. 4133-4141.
140. J. M. Kuemmerle, A. Oberle, C. Oechslin, M. Bohner, C. Frei, I. Boecken and B. von Rechenberg, *Assessment of the suitability of a new brushite calcium phosphate cement for cranioplasty–an experimental study in sheep*. J. Cranio-Maxillofac. Surg., **2005**. 33(1): p. 37-44.
141. F. Theiss, D. Apelt, B. Brand, A. Kutter, K. Zlinszky, M. Bohner, S. Matter, C. Frei, J. A. Auer and B. Von Rechenberg, *Biocompatibility and resorption of a brushite calcium phosphate cement*. Biomaterials, **2005**. 26(21): p. 4383-4394.
142. L. M. Grover, U. Gbureck, A. J. Wright, M. Tremayne and J. E. Barralet, *Biologically mediated resorption of brushite cement in vitro*. Biomaterials, **2006**. 27(10): p. 2178-2185.
143. M. Ikenaga, P. Hardouin, J. Lemaitre, H. Andrianjatovo and B. Flautre, *Biomechanical characterization of a biodegradable calcium phosphate hydraulic cement: a*

comparison with porous biphasic calcium phosphate ceramics. J. Biomed. Mater. Res., **1998**. 40(1): p. 139-144.
144. M. Bohner, F. Theiss, D. Apelt, W. Hirsiger, R. Houriet, G. Rizzoli, E. Gnos, C. Frei, J. Auer and B. Von Rechenberg, *Compositional changes of a dicalcium phosphate dihydrate cement after implantation in sheep*. Biomaterials, **2003**. 24(20): p. 3463-3474.
145. B. Flautre, C. Maynou, J. Lemaitre, P. Van Landuyt and P. Hardouin, *Bone colonization of β–TCP granules incorporated in brushite cements*. J. Biomed. Mater. Res., **2002**. 63(4): p. 413-417.
146. K. Ohura, M. Bohner, P. Hardouin, J. Lemaître, G. Pasquier and B. Flautre, *Resorption of, and bone formation from, new β-tricalcium phosphate-monocalcium phosphate cements: An in vivo study*. J. Biomed. Mater. Res., **1996**. 30(2): p. 193-200.
147. E. Charrière, S. Terrazzoni, C. Pittet, P. Mordasini, M. Dutoit, J. Lemaître and P. Zysset, *Mechanical characterization of brushite and hydroxyapatite cements*. Biomaterials, **2001**. 22(21): p. 2937-2945.
148. C. Pittet and J. Lemaitre, *Mechanical characterization of brushite cements: A Mohr circles' approach*. J. Biomed. Mater. Res., **2000**. 53(6): p. 769-780.
149. J. E. Barralet, L. M. Grover and U. Gbureck, *Ionic modification of calcium phosphate cement viscosity. Part II: hypodermic injection and strength improvement of brushite cement*. Biomaterials, **2004**. 25(11): p. 2197-2203.
150. M. P. Hofmann, A. R. Mohammed, Y. Perrie, U. Gbureck and J. E. Barralet, *High-strength resorbable brushite bone cement with controlled drug-releasing capabilities*. Acta Biomater., **2009**. 5(1): p. 43-49.
151. F. Tamimi, Z. Sheikh and J. E. Barralet, *Dicalcium phosphate cements: Brushite and monetite*. Acta Biomater., **2012**. 8(2): p. 474-487.
152. J. Nurit, J. Margerit, A. Terol and P. Boudeville, *pH-metric study of the setting reaction of monocalcium phosphate monohydrate/calcium oxide-based cements*. J. Mater. Sci. Mater. Med., **2002**. 13(11): p. 1007-14.
153. P. Van Landuyt, C. Lowe and J. Lemaître, *Optimization of setting time and mechanical strength of beta-TCP/MCPM cements*. **1997**. p. 477-480.
154. M. P. Hofmann, A. M. Young, U. Gbureck, S. N. Nazhat and J. E. Barralet, *FTIR-monitoring of a fast setting brushite bone cement: effect of intermediate phases*. J. Mater. Chem., **2006**. 16(31): p. 3199-3206.
155. A. Wereszczak, E. Lara-Curzio and M. Mizuno, *Advances in Bioceramics and Biocomposites II, Ceramic Engineering and Science Proceedings*. **2009**: Wiley.
156. M. Bohner, H. P. Merkle and J. Lemai, *In vitro aging of a calcium phosphate cement*. J. Mater. Sci.: Mater. Med., **2000**. 11(3): p. 155-162.
157. T. R. Desai, S. B. Bhaduri and A. C. Tas, *A self-setting, monetite (CaHPO 4) cement for skeletal repair*. Adv. Bioceram. Biocompos. II, **2007**. 27: p. 61-69.
158. L. G. Galea, M. Bohner, J. Lemaître, T. Kohler and R. Müller, *Bone substitute: Transforming β-tricalcium phosphate porous scaffolds into monetite*. Biomaterials, **2008**. 29(24–25): p. 3400-3407.
159. G. Cama, B. Gharibi, M. S. Sait, J. C. Knowles, A. Lagazzo, S. Romeed, L. Di Silvio and S. Deb, *A novel method of forming micro-and macroporous monetite cements*. J. Mater. Chem. B, **2013**. 1(7): p. 958-969.
160. E. Şahin and M. Çiftçioğlu, *Monetite promoting effect of NaCl on brushite cement setting kinetics*. J. Mater. Chem. B, **2013**. 1(23): p. 2943-2950.
161. F. Tamimi, J. Torres, C. Kathan, R. Baca, C. Clemente, L. Blanco and E. Lopez Cabarcos, *Bone regeneration in rabbit calvaria with novel monetite granules*. J. Biomed. Mater. Res., Part A, **2008**. 87(4): p. 980-5.
162. U. Gbureck, T. Hölzel, U. Klammert, K. Würzler, F. A. Müller and J. E. Barralet, *Resorbable dicalcium phosphate bone substitutes prepared by 3D powder printing*. Adv. Funct. Mater., **2007**. 17(18): p. 3940-3945.

163. U. Klammert, T. Reuther, C. Jahn, B. Kraski, A. C. Kübler and U. Gbureck, *Cytocompatibility of brushite and monetite cell culture scaffolds made by three-dimensional powder printing*. Acta Biomater., **2009**. 5(2): p. 727-734.
164. M. Alshaaer, H. Cuypers, H. Rahier and J. Wastiels, *Production of monetite-based Inorganic Phosphate Cement (M-IPC) using hydrothermal post curing (HTPC)*. Cem. Concr. Res., **2011**. 41(1): p. 30-37.
165. F. Tamimi, D. L. Nihouannen, H. Eimar, Z. Sheikh, S. Komarova and J. E. Barralet, *The effect of autoclaving on the physical and biological properties of dicalcium phosphate dihydrate bioceramics: Brushite vs. monetite*. Acta Biomater., **2012**. 8(8): p. 3161-3169.
166. F. Tamimi, J. Torres, D. Bassett, J. E. Barralet and E. L. Cabarcos, *Resorption of monetite granules in alveolar bone defects in human patients*. Biomaterials, **2010**. 31(10): p. 2762-2769.
167. F. Tamimi, J. Torres, U. Gbureck, E. Lopez-Cabarcos, D. C. Bassett, M. H. Alkhraisat and J. E. Barralet, *Craniofacial vertical bone augmentation: a comparison between 3D printed monolithic monetite blocks and autologous onlay grafts in the rabbit*. Biomaterials, **2009**. 30(31): p. 6318-6326.
168. M. Montazerolghaem, M. Karlsson Ott, H. Engqvist, H. Melhus and A. J. Rasmusson, *Resorption of monetite calcium phosphate cement by mouse bone marrow derived osteoclasts*. Mater. Sc.i Eng. C, Mater. Biol. Appl., **2015**. 52: p. 212-8.
169. M. Mathew, W. E. Brown, L. W. Schroeder and B. Dickens, *Crystal structure of octacalcium bis (hydrogenphosphate) tetrakis (phosphate) pentahydrate, Ca8 (HP04) 2 (PO4) 4· 5H2O*. J. Crystallogr. Spectrosc. Res., **1988**. 18(3): p. 235-250.
170. P. Steuer, J.-C. Voegel and F. J. G. Cuisinier, *First experimental evidence for human dentine crystal formation involving conversion of octacalcium phosphate to hydroxyapatite*. Acta Crystallogr., Sect. D: Biol. Crystallogr., **1998**. 54(6): p. 1377-1381.
171. R. Z. LeGeros, G. Daculsi, I. Orly, T. Abergas and W. Torres, *Solution-mediated transformation of octacalcium phosphate (OCP) to apatite*. Scanning Microsc., **1989**. 3(1): p. 129-37; discussion 137-8.
172. J. L. Meyer and E. D. Eanes, *A thermodynamic analysis of the secondary transition in the spontaneous precipitation of calcium phosphate*. Calcif. Tissue Res., **1978**. 25(1): p. 209-216.
173. M. S. Tung and W. E. Brown, *The role of octacalcium phosphate in subcutaneous heterotopic calcification*. Calcif. Tissue Int., **1985**. 37(3): p. 329-331.
174. I. Ajaxon, C. Öhman and C. Persson, *Long-Term In Vitro Degradation of a High-Strength Brushite Cement in Water, PBS, and Serum Solution*. BioMed Res. Int., **2015**. 2015: p.
175. Z. Sheikh, Y. L. Zhang, L. M. Grover, G. E. Merle, F. Tamimi and J. E. Barralet, *In vitro degradation and in vivo resorption of dicalcium phosphate cement based grafts*. Acta Biomater., **2015**. 26: p. 338-346.
176. U. Klammert, A. Ignatius, U. Wolfram, T. Reuther and U. Gbureck, *In vivo degradation of low temperature calcium and magnesium phosphate ceramics in a heterotopic model*. Acta Biomater., **2011**. 7(9): p. 3469-3475.
177. N. Temizel, G. Girisken and A. C. Tas, *Accelerated transformation of brushite to octacalcium phosphate in new biomineralization media between 36.5 C and 80 C*. Mater. Sci. Eng., C, **2011**. 31(5): p. 1136-1143.
178. M. Markovic and L. C. Chow, *An octacalcium phosphate forming cement*. J. Res. Natl. Inst. Stand. Technol., **2010**. 115(4): p. 257.
179. I. V. Fadeeva, S. M. Barinov, D. Ferro, V. S. Komlev and L. I. Shvorneva, *Hydrolysis of dicalcium phosphate dihydrate in a sodium acetate solution*. Dokl. Chem., **2013**. 447(2): p. 303-305.
180. S. Graham and P. W. Brown, *The low temperature formation of octacalcium phosphate*. J. Cryst. Growth, **1993**. 132(1): p. 215-225.

181. E. Boanini, S. Panzavolta, K. Rubini, M. Gandolfi and A. Bigi, *Effect of strontium and gelatin on the reactivity of α-tricalcium phosphate*. Acta Biomater., **2010**. 6(3): p. 936-942.
182. H. Monma, A. Makishima, M. Mitomo and T. Ikegami, *Hydraulic Properties of the Tricalcium Phosphate-Dicalcium Phosphate Mixture*. J. Ceram. Soc. Jpn., **1988**. 96(1116): p. 878-880.
183. O. Bermúdez, M. G. Boltong, F. C. M. Driessens and J. A. Planell, *Development of an octocalcium phosphate cement*. J. Mater. Sci.: Mater. Med., **1994**. 5(3): p. 144-146.
184. H. Imaizumi, M. Sakurai, O. Kashimoto, T. Kikawa and O. Suzuki, *Comparative study on osteoconductivity by synthetic octacalcium phosphate and sintered hydroxyapatite in rabbit bone marrow*. Calcif. Tissue Int., **2006**. 78(1): p. 45-54.
185. S. Kamakura, Y. Sasano, M. Nakamura, O. Suzuki, H. Ohki, M. Kagayama and K. Motegi, *Initiation of alveolar ridge augmentation in the rat mandible by subperiosteal implantation of octacalcium phosphate*. Arch. Oral Biol., **1996**. 41(11): p. 1029-1038.
186. T. Kikawa, O. Kashimoto, H. Imaizumi, S. Kokubun and O. Suzuki, *Intramembranous bone tissue response to biodegradable octacalcium phosphate implant*. Acta Biomater., **2009**. 5(5): p. 1756-1766.
187. F. Barrere, C. M. Van Der Valk, R. A. J. Dalmeijer, C. A. Van Blitterswijk, K. De Groot and P. Layrolle, *In vitro and in vivo degradation of biomimetic octacalcium phosphate and carbonate apatite coatings on titanium implants*. J. Biomed. Mater. Res., Part A, **2003**. 64(2): p. 378-387.
188. A. Bigi, B. Bracci, F. J. G. Cuisinier, R. Elkaim, M. Fini, I. Mayer, I. N. Mihailescu, G. Socol, L. Sturba and P. Torricelli, *Human osteoblast response to pulsed laser deposited calcium phosphate coatings*. Biomaterials, **2005**. 26(15): p. 2381-2389.
189. P. Habibovic, C. M. Van der Valk, C. A. Van Blitterswijk, K. De Groot and G. Meijer, *Influence of octacalcium phosphate coating on osteoinductive properties of biomaterials*. J. Mater. Sci.: Mater. Med., **2004**. 15(4): p. 373-380.
190. O. Suzuki, M. Nakamura, Y. Miyasaka, M. Kagayama and M. Sakurai, *Bone formation on synthetic precursors of hydroxyapatite*. Tohoku J. Exp. Med., **1991**. 164(1): p. 37-50.
191. O. Suzuki, S. Kamakura, T. Katagiri, M. Nakamura, B. Zhao, Y. Honda and R. Kamijo, *Bone formation enhanced by implanted octacalcium phosphate involving conversion into Ca-deficient hydroxyapatite*. Biomaterials, **2006**. 27(13): p. 2671-2681.
192. R. M. Shelton, Y. Liu, P. R. Cooper, U. Gbureck, M. J. German and J. E. Barralet, *Bone marrow cell gene expression and tissue construct assembly using octacalcium phosphate microscaffolds*. Biomaterials, **2006**. 27(14): p. 2874-2881.
193. Y. Liu, P. R. Cooper, J. E. Barralet and R. M. Shelton, *Influence of calcium phosphate crystal assemblies on the proliferation and osteogenic gene expression of rat bone marrow stromal cells*. Biomaterials, **2007**. 28(7): p. 1393-1403.
194. T. Anada, T. Kumagai, Y. Honda, T. Masuda, R. Kamijo, S. Kamakura, N. Yoshihara, T. Kuriyagawa, H. Shimauchi and O. Suzuki, *Dose-dependent osteogenic effect of octacalcium phosphate on mouse bone marrow stromal cells*. Tissue Eng., Part A, **2008**. 14(6): p. 965-978.
195. Y. Z. Chen, X. Y. Lu and G. D. Liu, *A novel root-end filling material based on hydroxyapatite, tetracalcium phosphate and polyacrylic acid*. Int. Endod. J., **2013**. 46(6): p. 556-64.
196. H. Liu, H. Li, W. Cheng, Y. Yang, M. Zhu and C. Zhou, *Novel injectable calcium phosphate/chitosan composites for bone substitute materials*. Acta Biomater., **2006**. 2(5): p. 557-565.
197. A. Yokoyama, S. Yamamoto, T. Kawasaki, T. Kohgo and M. Nakasu, *Development of calcium phosphate cement using chitosan and citric acid for bone substitute materials*. Biomaterials, **2002**. 23(4): p. 1091-1101.
198. K. Achelhi, S. Masse, G. Laurent, A. Saoiabi, A. Laghzizil and T. Coradin, *Role of carboxylate chelating agents on the chemical, structural and textural properties of*

hydroxyapatite. Dalton transactions (Cambridge, England : 2003), **2010**. 39(44): p. 10644-51.
199. J.-H. C. Lin, C.-P. Ju, K.-L. Lin and I.-C. Wang, *Process for producing fast-setting, bioresorbable calcium phosphate cements*. **2005**, Google Patents.
200. K. Miyazaki, T. Horibe, J. M. Antonucci, S. Takagi and L. C. Chow, *Polymeric calcium phosphate cements: setting reaction modifiers*. Dent. Mater., **1993**. 9(1): p. 46-50.
201. R. Bhowmik, K. S. Katti and D. Katti, *Molecular dynamics simulation of hydroxyapatite–polyacrylic acid interfaces*. Polymer, **2007**. 48(2): p. 664-674.
202. K. S. TenHuisen and P. W. Brown, *The formation of hydroxyapatite-ionomer cements at 38 degrees C*. J. Dent. Res., **1994**. 73(3): p. 598-606.
203. W. C. Chen, C. P. Ju, J. C. Wang, C. C. Hung and J. H. Chern Lin, *Brittle and ductile adjustable cement derived from calcium phosphate cement/polyacrylic acid composites*. Dent Mater, **2008**. 24(12): p. 1616-22.
204. S. Hesaraki, D. Sharifi, R. Nemati and N. Nezafati, *Preparation and characterisation of calcium phosphate cement made by poly (acrylic/itaconic) acid*. Adv. Appl. Ceram., **2009**. 108(2): p. 106-110.
205. D. C. Smith, *Development of glass-ionomer cement systems*. Biomaterials, **1998**. 19(6): p. 467-478.
206. M. L. Porter, A. Bertó, C. M. Primus and I. Watanabe, *Physical and chemical properties of new-generation endodontic materials*. J. Endod., **2010**. 36(3): p. 524-528.
207. B. Bujoli, J.-M. Bouler, J. Guicheux, O. Gauthier and P. Janvier, *Calcium Phosphates / Biphosphonates Combinations…Towards a Therapeutic Synergy*. Key Eng. Mater., **2008**. 377: p. 99-110.
208. R. F. Sognnaes, J. H. Shaw and R. Bogoroch, *Radiotracer studies on bone, cementum, dentin and enamel of rhesus monkeys*. Am. J. Physiol., **1955**. 180: p. 408-420.
209. Y. E. Greish and P. W. Brown, *Formation and properties of hydroxyapatite-calcium poly(vinyl phosphonate) composites*. J. Am. Ceram. Soc., **2002**. 85(7): p. 1738-1744.
210. M. J. Phillips, P. Duncanson, K. Wilson, J. A. Darr, D. V. Griffith.s and I. U. Rehman, *Surface modification of bioceramics by grafting of tailored allyl phosphonic acid*. Adv. Appl. Ceram., **2005**. 104(5): p. 261-267.
211. H. W. Choi, H. J. Lee, K. J. Kim, H.-M. Kim and S. C. Lee, *Surface modification of hydroxyapatite nanocrystals by grafting polymers containing phosphonic acid groups*. J. Colloid. Interface Sci., **2006**. 304(1): p. 277-281.
212. N. Pramanik, S. Mohapatra, P. Bhargava and P. Pramanik, *Chemical synthesis and characterization of hydroxyapatite (HAp)-poly (ethylene co vinyl alcohol) (EVA) nanocomposite using a phosphonic acid coupling agent for orthopedic applications*. Mater. Sci. Eng., C, **2009**. 29(1): p. 228-236.
213. J. Allock, *Chemistry and Applications of Polyphosphazenes*. **2003**: John Wiley & Sons Canada, Limited.
214. A. K. Andrianov, *Polyphosphazenes for Biomedical Applications*. **2009**: Wiley.
215. C. T. Laurencin, S. F. El-Amin, S. E. Ibim, D. A. Willoughby, M. Attawia, H. R. Allcock and A. A. Ambrosio, *A highly porous 3-dimensional polyphosphazene polymer matrix for skeletal tissue regeneration*. J. Biomed. Mater. Res., **1996**. 30(2): p. 133-138.
216. C. T. Laurencin, M. E. Norman, H. M. Elgendy, S. F. El-Amin, H. R. Allcock, S. R. Pucher and A. A. Ambrosio, *Use of polyphosphazenes for skeletal tissue regeneration*. J. Biomed. Mater. Res., **1993**. 27(7): p. 963-973.
217. Y. E. Greish, J. D. Bender, S. Lakshmi, P. W. Brown, H. R. Allcock and C. T. Laurencin, *Composite formation from hydroxyapatite with sodium and potassium salts of polyphosphazene*. J. Mater. Sci.: Mater. Med., **2005**. 16(7): p. 613-620.
218. Y. E. Greish, J. D. Bender, S. Lakshmi, P. W. Brown, H. R. Allcock and C. T. Laurencin, *Formation of hydroxyapatite-polyphosphazene polymer composites at physiologic temperature*. J. Biomed. Mater. Res., Part A, **2006**. 77A(2): p. 416-425.

219. Y. E. Greish, P. W. Brown, J. D. Bender, H. R. Allcock, S. Lakshmi and C. T. Laurencin, *Hydroxyapatite-polyphosphazane composites prepared at low temperatures*. J. Am. Ceram. Soc., **2007**. 90(9): p. 2728-2734.
220. K. S. Tenhuisen, P. W. Brown, C. S. Reed and H. R. Allcock, *Low temperature synthesis of a self-assembling composite: hydroxyapatite-poly[bis(sodium carboxylatophenoxy)phosphazene]*. J. Mater. Sci.: Mater. Med., **1996**. 7(11): p. 673-682.
221. E. Graf and J. W. Eaton, *Antioxidant functions of phytic acid*. Free Radicals Biol. Med., **1990**. 8(1): p. 61-69.
222. S. Hirabayashi, T. Hirasawa, A. Kohno and H. Usui, *Studies on primers combined chelating agent with metallic ion for tooth-bonding I. Effects of primer combined phytic acid and tin(II) fluoride.* J. Jpn. Soc. Dent. Mater. Dev., **1993**. 12: p. 435-444.
223. Y. Horiguchi, A. Yoshikawa, K. Oribe and M. Aizawa, *Fabrication of chelate-setting hydroxyapatite cements from four kinds of commercially-available powder with various shape and crystallinity and their mechanical property*. J. Ceram. Soc. Jpn., **2008**. 116(1349): p. 50-55.
224. T. Konishi, Y. Horiguchi, M. Mizumoto, M. Honda, K. Oribe, H. Morisue, K. Ishii, Y. Toyama, M. Matsumoto and M. Aizawa, *Novel chelate-setting calcium-phosphate cements fabricated with wet-synthesized hydroxyapatite powder*. J. Mater. Sci.: Mater. Med., **2013**. 24(3): p. 611-21.
225. T. Konishi, S. Takahashi, Z. Zhuang, K. Nagata, M. Mizumoto, M. Honda, Y. Takeuchi, H. Matsunari, H. Nagashima and M. Aizawa, *Biodegradable beta-tricalcium phosphate cement with anti-washout property based on chelate-setting mechanism of inositol phosphate*. J Mater Sci Mater Med, **2013**. 24(6): p. 1383-94.
226. T. Konishi, M. Mizumoto, M. Honda, Y. Horiguchi, K. Oribe, H. Morisue, K. Ishii, Y. Toyama, M. Matsumoto and M. Aizawa, *Fabrication of novel biodegradable α-tricalcium phosphate cement set by chelating capability of inositol phosphate and its biocompatibility*. J. Nanomater., **2013**. 2013: p. 4.
227. Z. Sheikh, M. Geffers, T. Christel, J. E. Barralet and U. Gbureck, *Chelate setting of alkali ion substituted calcium phosphates*. Ceram. Int., **2015**. 41(8): p. 10010-10017.
228. T. Christel, S. Christ, J. E. Barralet, J. Groll and U. Gbureck, *Chelate bonding mechanism in a novel magnesium phosphate bone cement*. J. Am. Ceram. Soc., **2015**. 98(3): p. 694-697.
229. S. Meininger, C. Blum, M. Schamel, J. E. Barralet, J. Groll, A. Ignatius and U. Gbureck, *In vitro performance of brushite cements with different setting modifiers* **in preparation**. p.
230. P. Jamshidi, R. H. Bridson, A. J. Wright and L. M. Grover, *Brushite cement additives inhibit attachment to cell culture beads*. Biotechnol. Bioeng., **2013**. 110(5): p. 1487-1494.
231. M. Bohner, U. Gbureck and J. Barralet, *Technological issues for the development of more efficient calcium phosphate bone cements: a critical assessment*. Biomaterials, **2005**. 26(33): p. 6423-6429.
232. L. C. Chow, *Calcium phosphate cements*. Monogr. Oral Sci., **2001**. 18: p. 148-163.
233. G. H. Nancollas and S. J. Zawacki, *Calcium phosphate mineralization*. Connect. Tissue Res., **1989**. 21(1-4): p. 239-246.
234. J. Zhang, W. Liu, V. Schnitzler, F. Tancret and J.-M. Bouler, *Calcium phosphate cements for bone substitution: Chemistry, handling and mechanical properties*. Acta Biomater., **2014**. 10(3): p. 1035-1049.
235. M. Bohner, *Design of ceramic-based cements and putties for bone graft substitution*. Eur. Cells Mater., **2010**. 20(1): p. 3-10.
236. D. Apelt, F. Theiss, A. O. El-Warrak, K. Zlinszky, R. Bettschart-Wolfisberger, M. Bohner, S. Matter, J. A. Auer and B. Von Rechenberg, *In vivo behavior of three different injectable hydraulic calcium phosphate cements*. Biomaterials, **2004**. 25(7): p. 1439-1451.

237. A. C. Tas, *The use of physiological solutions or media in calcium phosphate synthesis and processing*. Acta Biomater., **2014**. 10(5): p. 1771-1792.
238. C. Großardt, A. Ewald, L. M. Grover, J. E. Barralet and U. Gbureck, *Passive and active in vitro resorption of calcium and magnesium phosphate cements by osteoclastic cells*. Tissue Eng., Part A, **2010**. 16(12): p. 3687-3695.
239. R. Detsch, H. Mayr and G. Ziegler, *Formation of osteoclast-like cells on HA and TCP ceramics*. Acta Biomater., **2008**. 4(1): p. 139-148.
240. B. M. Holzapfel, J. C. Reichert, J.-T. Schantz, U. Gbureck, L. Rackwitz, U. Nöth, F. Jakob, M. Rudert, J. Groll and D. W. Hutmacher, *How smart do biomaterials need to be? A translational science and clinical point of view*. Adv. Drug Delivery Rev., **2013**. 65(4): p. 581-603.
241. F. Tamimi, J. Torres, E. Lopez-Cabarcos, D. C. Bassett, P. Habibovic, E. Luceron and J. E. Barralet, *Minimally invasive maxillofacial vertical bone augmentation using brushite based cements*. Biomaterials, **2009**. 30(2): p. 208-216.
242. G. Penel, N. Leroy, P. Van Landuyt, B. Flautre, P. Hardouin, J. Lemaitre and G. Leroy, *Raman microspectrometry studies of brushite cement: in vivo evolution in a sheep model*. Bone, **1999**. 25(2): p. 81S-84S.
243. M. Bohner and J. Lemaitre, *Can bioactivity be tested in vitro with SBF solution?* Biomaterials, **2009**. 30(12): p. 2175-2179.
244. X. Lu and Y. Leng, *Theoretical analysis of calcium phosphate precipitation in simulated body fluid*. Biomaterials, **2005**. 26(10): p. 1097-1108.
245. B. Kanter, M. Geffers, A. Ignatius and U. Gbureck, *Control of in vivo mineral bone cement degradation*. Acta Biomater., **2014**. 10(7): p. 3279-3287.
246. U. Gbureck, K. Spatz, R. Thull and J. E. Barralet, *Rheological enhancement of mechanically activated α-tricalcium phosphate cements*. J. Biomed. Mater. Res., Part B, **2005**. 73(1): p. 1-6.
247. S. V. Dorozhkin, *Calcium orthophosphate-based biocomposites and hybrid biomaterials*. J. Mater. Sci., **2009**. 44(9): p. 2343-2387.
248. A. S. Von Gonten, J. R. Kelly and J. M. Antonucci, *Load-bearing behavior of a simulated craniofacial structure fabricated from a hydroxyapatite cement and bioresorbable fiber-mesh*. J. Mater. Sci.: Mater. Med., **2000**. 11(2): p. 95-100.
249. T. R. Blattert, L. Jestaedt and A. Weckbach, *Suitability of a calcium phosphate cement in osteoporotic vertebral body fracture augmentation: a controlled, randomized, clinical trial of balloon kyphoplasty comparing calcium phosphate versus polymethylmethacrylate*. Spine, **2009**. 34(2): p. 108-114.
250. G. Maestretti, C. Cremer, P. Otten and R. P. Jakob, *Prospective study of standalone balloon kyphoplasty with calcium phosphate cement augmentation in traumatic fractures*. Eur. Spine J., **2007**. 16(5): p. 601-610.
251. S. M. Tarsuslugil, R. M. O'Hara, N. J. Dunne, F. J. Buchanan, J. F. Orr, D. C. Barton and R. K. Wilcox, *Development of calcium phosphate cement for the augmentation of traumatically fractured porcine specimens using vertebroplasty*. J. Biomech., **2013**. 46(4): p. 711-715.
252. I. A. Grafe, M. Baier, G. Noldge, C. Weiss, K. Da Fonseca, J. Hillmeier, M. Libicher, G. Rudofsky, C. Metzner, P. Nawroth, P. J. Meeder and C. Kasperk, *Calcium-phosphate and polymethylmethacrylate cement in long-term outcome after kyphoplasty of painful osteoporotic vertebral fractures*. Spine, **2008**. 33(11): p. 1284-1290.
253. P. F. Heini, *[Vertebroplasty: an update: value of percutaneous cement augmentation after randomized, placebo-controlled trials]*. Orthopade, **2010**. 39(7): p. 658-64.
254. K. Kiyasu, R. Takemasa, M. Ikeuchi and T. Tani, *Differential blood contamination levels and powder–liquid ratios can affect the compressive strength of calcium phosphate cement (CPC): a study using a transpedicular vertebroplasty model*. Eur. Spine J., **2013**. 22(7): p. 1643-1649.

255. J. L. Moreau, M. D. Weir and H. H. K. Xu, *Self-setting collagen-calcium phosphate bone cement: Mechanical and cellular properties*. J. Biomed. Mater. Res., Part A, **2009**. 91(2): p. 605-613.
256. W. Schneiders, A. Reinstorf, A. Biewener, A. Serra, R. Grass, M. Kinscher, J. Heineck, S. Rehberg, H. Zwipp and S. Rammelt, *In vivo effects of modification of hydroxyapatite/collagen composites with and without chondroitin sulphate on bone remodeling in the sheep tibia*. J. Orthop. Res., **2009**. 27(1): p. 15-21.
257. F. Tamimi, B. Kumarasami, C. Doillon, U. Gbureck, D. Le Nihouannen, E. L. Cabarcos and J. E. Barralet, *Brushite–collagen composites for bone regeneration*. Acta Biomater., **2008**. 4(5): p. 1315-1321.
258. R. M. O'Hara, J. F. Orr, F. J. Buchanan, R. K. Wilcox, D. C. Barton and N. J. Dunne, *Development of a bovine collagen–apatitic calcium phosphate cement for potential fracture treatment through vertebroplasty*. Acta Biomater., **2012**. 8(11): p. 4043-4052.
259. L. A. Dos Santos, L. C. De Oliveira, E. C. da Silva Rigo, R. G. Carrodéguas, A. O. Boschi and A. C. Fonseca de Arruda, *Fiber reinforced calcium phosphate cement*. Artif. Organs, **2000**. 24(3): p. 212-216.
260. M. Espanol, R. A. Perez, E. B. Montufar, C. Marichal, A. Sacco and M. P. Ginebra, *Intrinsic porosity of calcium phosphate cements and its significance for drug delivery and tissue engineering applications*. Acta Biomater., **2009**. 5(7): p. 2752-2762.
261. M. Geffers, J. E. Barralet, J. Groll and U. Gbureck, *Dual-setting brushite–silica gel cements*. Acta Biomater., **2015**. 11: p. 467-476.
262. J. Engstrand, C. Persson and H. Engqvist, *The effect of composition on mechanical properties of brushite cements*. J. Mech. Behav. Biomed. Mater., **2014**. 29: p. 81-90.
263. M. P. Ginebra, J. A. Delgado, I. Harr, A. Almirall, S. Del Valle and J. A. Planell, *Factors affecting the structure and properties of an injectable self-setting calcium phosphate foam*. J. Biomed. Mater. Res., Part A, **2007**. 80(2): p. 351-361.
264. E. F. Burguera, F. Guitian and L. C. Chow, *A water setting tetracalcium phosphate–dicalcium phosphate dihydrate cement*. J. Biomed. Mater. Res., Part A, **2004**. 71(2): p. 275-282.
265. J. Unosson, C. Persson and H. Engqvist, *An evaluation of methods to determine the porosity of calcium phosphate cements*. J. Biomed. Mater. Res., Part B, **2015**. 103(1): p. 62-71.
266. M. Bohner and G. Baroud, *Injectability of calcium phosphate pastes*. Biomaterials, **2005**. 26(13): p. 1553-1563.
267. J. E. Barralet, M. Tremayne, K. J. Lilley and U. Gbureck, *Modification of calcium phosphate cement with α-hydroxy acids and their salts*. Chem. Mater., **2005**. 17(6): p. 1313-1319.
268. T. Gu, H. Shi and J. Ye, *Reinforcement of calcium phosphate cement by incorporating with high-strength β-tricalcium phosphate aggregates*. J. Biomed. Mater. Res., Part B, **2012**. 100(2): p. 350-359.
269. S. Gravius, D. C. Wirtz, R. Marx, U. Maus, S. Andereya, R. Müller-Rath and T. Mumme, *[Mechanical in vitro testing of fifteen commercial bone cements based on polymethylmethacrylate]*. Z. Ortho. Unfallchirugie, **2006**. 145(5): p. 579-585.
270. L. C. Chow, S. Hirayama, S. Takagi and E. Parry, *Diametral tensile strength and compressive strength of a calcium phosphate cement: effect of applied pressure*. J. Biomed. Mater. Res., **2000**. 53(5): p. 511-517.
271. K. Ishikawa and K. Asaoka, *Estimation of ideal mechanical strength and critical porosity of calcium phosphate cement*. J. Biomed. Mater. Res., **1995**. 29(12): p. 1537-1543.
272. R. P. Del Real, J. G. C. Wolke, M. Vallet-Regı and J. A. Jansen, *A new method to produce macropores in calcium phosphate cements*. Biomaterials, **2002**. 23(17): p. 3673-3680.
273. E. Vorndran, M. Geffers, A. Ewald, M. Lemm, B. Nies and U. Gbureck, *Ready-to-use injectable calcium phosphate bone cement paste as drug carrier*. Acta Biomater., **2013**. 9(12): p. 9558-9567.

274. M. A. Lopez-Heredia, K. Sariibrahimoglu, W. Yang, M. Bohner, D. Yamashita, A. Kunstar, A. A. Van Apeldoorn, E. M. Bronkhorst, R. P. F. Lanao and S. C. G. Leeuwenburgh, *Influence of the pore generator on the evolution of the mechanical properties and the porosity and interconnectivity of a calcium phosphate cement*. Acta Biomater., **2012**. 8(1): p. 404-414.
275. G. Cama, F. Barberis, R. Botter, P. Cirillo, M. Capurro, R. Quarto, S. Scaglione, E. Finocchio, V. Mussi and U. Valbusa, *Preparation and properties of macroporous brushite bone cements*. Acta Biomater., **2009**. 5(6): p. 2161-2168.
276. J. Unosson, E. B. Montufar, H. Engqvist, M. P. Ginebra and C. Persson, *Brushite foams—the effect of Tween® 80 and Pluronic® F-127 on foam porosity and mechanical properties*. J. Biomed. Mater. Res., Part B, **2016**. 104(1): p. 67-77.
277. G. Dewith and A. J. Corbijn, *Metal fibre reinforced hydroxy-apatite ceramics*. J. Mater. Sci., **1989**. 24(9): p. 3411-3415.
278. J. Rösler, H. Harders and M. Bäker, *Mechanisches Verhalten der Werkstoffe*. **2006**: Springer.
279. W. D. Callister and D. G. Rethwisch, *Materials science and engineering: an introduction*. Vol. 7. **2007**: Wiley New York.
280. A. M. Brandt, *Cement-based composites: materials, mechanical properties and performance*. **2009**: CRC Press.
281. H. H. K. Xu, F. C. Eichmiller and P. R. Barndt, *Effects of fiber length and volume fraction on the reinforcement of calcium phosphate cement*. J. Mater. Sci.: Mater. Med., **2001**. 12(1): p. 57-65.
282. H. H. K. Xu, F. C. Eichmiller and A. A. Giuseppetti, *Reinforcement of a self-setting calcium phosphate cement with different fibers*. J. Biomed. Mater. Res., **2000**. 52(1): p. 107-114.
283. Y. Zhang and H. H. K. Xu, *Effects of synergistic reinforcement and absorbable fiber strength on hydroxyapatite bone cement*. J. Biomed. Mater. Res., Part A, **2005**. 75(4): p. 832-840.
284. H. H. K. Xu, J. B. Quinn, S. Takagi, L. C. Chow and F. C. Eichmiller, *Strong and macroporous calcium phosphate cement: effects of porosity and fiber reinforcement on mechanical properties*. J. Biomed. Mater. Res., **2001**. 57(3): p. 457-466.
285. H. H. K. Xu and J. B. Quinn, *Calcium phosphate cement containing resorbable fibers for short-term reinforcement and macroporosity*. Biomaterials, **2002**. 23(1): p. 193-202.
286. H. H. K. Xu and C. G. Simon, *Self-hardening calcium phosphate cement–mesh composite: Reinforcement, macropores, and cell response*. J. Biomed. Mater. Res., Part A, **2004**. 69(2): p. 267-278.
287. H. H. K. Xu, J. B. Quinn, S. Takagi and L. C. Chow, *Synergistic reinforcement of in situ hardening calcium phosphate composite scaffold for bone tissue engineering*. Biomaterials, **2004**. 25(6): p. 1029-1037.
288. N. J. S. Gorst, Y. Perrie, U. Gbureck, A. L. Hutton, M. P. Hofmann, L. M. Grover and J. E. Barralet, *Effects of fibre reinforcement on the mechanical properties of brushite cement*. Acta Biomater., **2006**. 2(1): p. 95-102.
289. P. Zhao, K. N. Sun, T. R. Zhao and X. H. Ren. *Effect of CNTs on property of calcium phosphate cement*. in *Key Eng. Mater.* **2007**. Trans Tech Publ.
290. F. A. Müller, U. Gbureck, T. Kasuga, Y. Mizutani, J. E. Barralet and U. Lohbauer, *Whisker-Reinforced Calcium Phosphate Cements*. J. Am. Ceram. Soc., **2007**. 90(11): p. 3694-3697.
291. H. H. K. Xu, F. C. Eichmiller and A. A. Giuseppetti, *Calcium-phosphate cement reinforcement: Effect of fiber type, length and fraction*. J. Dent. Res., **2000**. 79: p. 357-361.
292. S. Maenz, E. Kunisch, M. Mühlstädt, A. Böhm, V. Kopsch, J. Bossert, R. W. Kinne and K. D. Jandt, *Enhanced mechanical properties of a novel, injectable, fiber-reinforced brushite cement*. J. Mech. Behav. Biomed. Mater., **2014**. 39: p. 328-338.

293. M. D. Weir, H. H. K. Xu and C. G. Simon, *Strong calcium phosphate cement-chitosan-mesh construct containing cell-encapsulating hydrogel beads for bone tissue engineering*. J. Biomed. Mater. Res., Part A, **2006**. 77(3): p. 487-496.
294. R. Krüger, J.-M. Seitz, A. Ewald, F.-W. Bach and J. Groll, *Strong and tough magnesium wire reinforced phosphate cement composites for load-bearing bone replacement*. J. Mech. Behav. Biomed. Mater., **2013**. 20: p. 36-44.
295. I. Khairoun, F. C. M. Driessens, M. G. Boltong, J. A. Planell and R. Wenz, *Addition of cohesion promotors to calcium phosphate cements*. Biomaterials, **1999**. 20(4): p. 393-398.
296. M. H. Alkhraisat, C. Rueda, F. T. Marino, J. Torres, L. B. Jerez, U. Gbureck and E. L. Cabarcos, *The effect of hyaluronic acid on brushite cement cohesion*. Acta Biomater., **2009**. 5(8): p. 3150-3156.
297. R. M. Khashaba, M. Moussa, C. Koch, A. R. Jurgensen, D. M. Missimer, R. L. Rutherford, N. B. Chutkan and J. L. Borke, *Preparation, physical-chemical characterization, and cytocompatibility of polymeric calcium phosphate cements*. Int. J. Biomater., **2011**. 2011: p. 1-13.
298. E. C. S. Rigo, L. A. Dos Santos, L. C. O. Vercik, R. G. Carrodeguas and A. O. Boschi, *α-tricalcium phosphate-and tetracalcium phosphate/dicalcium phosphate-based dual setting cements*. Lat. Am. Appl. Res., **2007**. 37(4): p. 267-274.
299. G. Ahn, J. Y. Lee, D.-W. Seol, S. G. Pyo and D. Lee, *The effect of calcium phosphate cement–silica composite materials on proliferation and differentiation of pre-osteoblast cells*. Mater. Lett., **2013**. 109: p. 302-305.
300. H. Zhou, T. J. F. Luchini, A. K. Agarwal, V. K. Goel and S. B. Bhaduri, *Development of monetite–nanosilica bone cement: A preliminary study*. J. Biomed. Mater. Res., Part B, **2014**. 102(8): p. 1620-1626.
301. S. Hesaraki, M. Alizadeh, S. Borhan and M. Pourbaghi-Masouleh, *Polymerizable nanoparticulate silica-reinforced calcium phosphate bone cement*. J. Biomed. Mater. Res., Part B, **2012**. 100(6): p. 1627-1635.
302. N. M. F. Van den Vreken, E. De Canck, M. Ide, K. Lamote, P. Van Der Voort and R. M. H. Verbeeck, *Calcium phosphate cements modified with pore expanded SBA-15 materials*. J. Mater. Chem., **2012**. 22(29): p. 14502-14509.
303. M. H. Alkhraisat, C. Rueda, L. B. Jerez, F. T. Mariño, J. Torres, U. Gbureck and E. L. Cabarcos, *Effect of silica gel on the cohesion, properties and biological performance of brushite cement*. Acta Biomater., **2010**. 6(1): p. 257-265.
304. J. Andersson, S. Areva, B. Spliethoff and M. Lindén, *Sol–gel synthesis of a multifunctional, hierarchically porous silica/apatite composite*. Biomaterials, **2005**. 26(34): p. 6827-6835.
305. S. Heinemann, C. Heinemann, R. Bernhardt, A. Reinstorf, B. Nies, M. Meyer, H. Worch and T. Hanke, *Bioactive silica–collagen composite xerogels modified by calcium phosphate phases with adjustable mechanical properties for bone replacement*. Acta Biomater., **2009**. 5(6): p. 1979-1990.
306. A. Sousa, K. C. Souza and E. M. B. Sousa, *Mesoporous silica/apatite nanocomposite: special synthesis route to control local drug delivery*. Acta Biomater., **2008**. 4(3): p. 671-679.
307. I. TIOfS, *Implants for Surgery-Acrylic Resin Cements*. International Standard ISO 5833, **Geneva, Switzerland 2002**. p.
308. G. Lewis, *Injectable bone cements for use in vertebroplasty and kyphoplasty: State-of-the-art review*. J. Biomed. Mater. Res., Part B, **2006**. 76(2): p. 456-468.
309. H.-J. Wilke, U. Mehnert, L. E. Claes, M. M. Bierschneider, H. Jaksche and B. M. Boszczyk, *Biomechanical evaluation of vertebroplasty and kyphoplasty with polymethyl methacrylate or calcium phosphate cement under cyclic loading*. Spine, **2006**. 31(25): p. 2934-2941.
310. C.-C. Lin and A. T. Metters, *Hydrogels in controlled release formulations: network design and mathematical modeling*. Adv. Drug Delivery Rev., **2006**. 58(12): p. 1379-1408.

311. J. M. Harris, *Poly (ethylene glycol) chemistry: biotechnical and biomedical applications*. **2013**: Springer Science & Business Media.
312. C.-C. Lin and K. S. Anseth, *PEG hydrogels for the controlled release of biomolecules in regenerative medicine*. Pharm. Res., **2009**. 26(3): p. 631-643.
313. K. Inoue, *Functional dendrimers, hyperbranched and star polymers*. Prog. Polym. Sci., **2000**. 25(4): p. 453-571.
314. J. Groll and M. Moeller, *Star polymer surface passivation for single-molecule detection*. Methods Enzymol., **2010**. 472: p. 1-18.
315. N. Hadjichristidis, M. Pitsikalis and H. Iatrou, *Polymers with Star-Related Structures*. Macromol. Eng. Precise Synth. Mater. Prop. Appl., **2007**. p. 909-972.
316. G. Lapienis, *Star-shaped polymers having PEO arms*. Prog. Polym. Sci., **2009**. 34(9): p. 852-892.
317. K. B. Keys, F. M. Andreopoulos and N. A. Peppas, *Poly (ethylene glycol) star polymer hydrogels*. Macromolecules, **1998**. 31(23): p. 8149-8156.
318. H. Götz, U. Beginn, C. F. Bartelink, H. J. M. Grünbauer and M. Möller, *Preparation of isophorone diisocyanate terminated star polyethers*. Macromol. Mater. Eng., **2002**. 287(4): p. 223-230.
319. J. Groll, T. Ameringer, J. P. Spatz and M. Moeller, *Ultrathin coatings from isocyanate-terminated star PEG prepolymers: layer formation and characterization*. Langmuir, **2005**. 21(5): p. 1991-1999.
320. J. Groll, Z. Ademovic, T. Ameringer, D. Klee and M. Moeller, *Comparison of Coatings from Reactive Star Shaped PEG-s tat-PPG Prepolymers and Grafted Linear PEG for Biological and Medical Applications*. Biomacromolecules, **2005**. 6(2): p. 956-962.
321. J. Groll, W. Haubensak, T. Ameringer and M. Moeller, *Ultrathin coatings from isocyanate terminated star PEG prepolymers: patterning of proteins on the layers*. Langmuir, **2005**. 21(7): p. 3076-3083.
322. M. V. Beer, C. Rech, P. Gasteier, B. Sauerzapfe, J. Salber, A. Ewald, M. Möller, L. Elling and J. Groll, *The Next Step in Biomimetic Material Design: Poly-LacNAc-Mediated Reversible Exposure of Extra Cellular Matrix Components*. Adv. Healthcare Mater., **2013**. 2(2): p. 306-311.
323. D. Grafahrend, K.-H. Heffels, M. V. Beer, P. Gasteier, M. Möller, G. Boehm, P. D. Dalton and J. Groll, *Degradable polyester scaffolds with controlled surface chemistry combining minimal protein adsorption with specific bioactivation*. Nat. Mater., **2011**. 10(1): p. 67-73.
324. M. V. Beer, C. Rech, S. Diederichs, K. Hahn, K. Bruellhoff, M. Möller, L. Elling and J. Groll, *A hydrogel-based versatile screening platform for specific biomolecular recognition in a well plate format*. Anal. Bioanal. Chem., **2012**. 403(2): p. 517-526.
325. M. V. Beer, K. Hahn, S. Diederichs, M. Fabry, S. Singh, S. J. Spencer, J. Salber, M. Möller, A. G. Shard and J. Groll, *Quantifying ligand–cell interactions and determination of the surface concentrations of ligands on hydrogel films: The measurement challenge*. Biointerphases, **2015**. 10(2): p. 021007.
326. P. Gasteier, A. Reska, P. Schulte, J. Salber, A. Offenhäusser, M. Moeller and J. Groll, *Surface Grafting of PEO-Based Star-Shaped Molecules for Bioanalytical and Biomedical Applications*. Macromol. Biosci., **2007**. 7(8): p. 1010-1023.
327. P. D. Dalton, C. Hostert, K. Albrecht, M. Moeller and J. Groll, *Structure and Properties of Urea-Crosslinked Star Poly [(ethylene oxide)-ran-(propylene oxide)] Hydrogels*. Macromol. Biosci., **2008**. 8(10): p. 923-931.
328. M. Hütten, A. Dhanasingh, R. Hessler, T. Stöver, K.-H. Esser, M. Möller, T. Lenarz, C. Jolly, J. Groll and V. Scheper, *In vitro and in vivo evaluation of a hydrogel reservoir as a continuous drug delivery system for inner ear treatment*. PloS One, **2014**. 9(8): p. e104564.
329. V. Sansalone, S. Naïli and T. Lemaire, *Nanostructure and effective elastic properties of bone fibril*. Bioinspired, Biomimetic Nanobiomater., **2012**. 1(3): p. 154-165.
330. J.-Y. Rho, L. Kuhn-Spearing and P. Zioupos, *Mechanical properties and the hierarchical structure of bone*. Medical engineering & physics, **1998**. 20(2): p. 92-102.

331. J. D. Currey, *Biocomposites: micromechanics of biological hard tissues*. Curr. Opin. Solid State Mater. Sci., **1996**. 1(3): p. 440-445.
332. J. F. Mano, R. A. Sousa, L. F. Boesel, N. M. Neves and R. L. Reis, *Bioinert, biodegradable and injectable polymeric matrix composites for hard tissue replacement: state of the art and recent developments*. Compos. Sci. Technol., **2004**. 64(6): p. 789-817.
333. K. Gkioni, S. C. G. Leeuwenburgh, T. E. L. Douglas, A. G. Mikos and J. A. Jansen, *Mineralization of hydrogels for bone regeneration*. Tissue Eng., Part B, **2010**. 16(6): p. 577-585.
334. C. Cha, S. R. Shin, N. Annabi, M. R. Dokmeci and A. Khademhosseini, *Carbon-based nanomaterials: multifunctional materials for biomedical engineering*. ACS nano, **2013**. 7(4): p. 2891-2897.
335. T. Dvir, B. P. Timko, M. D. Brigham, S. R. Naik, S. S. Karajanagi, O. Levy, H. Jin, K. K. Parker, R. Langer and D. S. Kohane, *Nanowired three-dimensional cardiac patches*. Nat. Nanotechnol., **2011**. 6(11): p. 720-725.
336. R. Fuhrer, E. K. Athanassiou, N. A. Luechinger and W. J. Stark, *Crosslinking metal nanoparticles into the polymer backbone of hydrogels enables preparation of soft, magnetic field-driven actuators with muscle-like flexibility*. Small, **2009**. 5(3): p. 383-388.
337. C.-J. Wu, A. K. Gaharwar, P. J. Schexnailder and G. Schmidt, *Development of biomedical polymer-silicate nanocomposites: a materials science perspective*. Materials, **2010**. 3(5): p. 2986-3005.
338. A. K. Gaharwar, C. P. Rivera, C.-J. Wu and G. Schmidt, *Transparent, elastomeric and tough hydrogels from poly (ethylene glycol) and silicate nanoparticles*. Acta Biomater., **2011**. 7(12): p. 4139-4148.
339. P. J. Schexnailder, A. K. Gaharwar, I. Bartlett, L. Rush, B. L. Seal and G. Schmidt, *Tuning Cell Adhesion by Incorporation of Charged Silicate Nanoparticles as Cross-Linkers to Polyethylene Oxide*. Macromol. Biosci., **2010**. 10(12): p. 1416-1423.
340. A. K. Gaharwar, S. A. Dammu, J. M. Canter, C.-J. Wu and G. Schmidt, *Highly extensible, tough, and elastomeric nanocomposite hydrogels from poly (ethylene glycol) and hydroxyapatite nanoparticles*. Biomacromolecules, **2011**. 12(5): p. 1641-1650.
341. N. Koupaei, A. Karkhaneh and M. Daliri Joupari, *Preparation and characterization of (PCL-crosslinked-PEG)/hydroxyapatite as bone tissue engineering scaffolds*. J. Biomed. Mater. Res., Part A, **2015**. 103(12): p. 3919-3926.
342. D. S. Couto, Z. Hong and J. F. Mano, *Development of bioactive and biodegradable chitosan-based injectable systems containing bioactive glass nanoparticles*. Acta Biomater., **2009**. 5(1): p. 115-123.
343. A. R. Boccaccini, M. Erol, W. J. Stark, D. Mohn, Z. Hong and J. F. Mano, *Polymer/bioactive glass nanocomposites for biomedical applications: a review*. Compos. Sci. Technol., **2010**. 70(13): p. 1764-1776.
344. M. Šupová, *Problem of hydroxyapatite dispersion in polymer matrices: a review*. J. Mater. Sci.: Mater. Med., **2009**. 20(6): p. 1201-1213.
345. A. L. Boskey, *Bone composition: relationship to bone fragility and antiosteoporotic drug effects*. BoneKEy Rep., **2013**. 2: p.
346. J. D. Currey, *The structure and mechanics of bone*. J. Mater. Sci., **2012**. 47(1): p. 41-54.
347. E. C. Achilleos, R. K. Prud'homme, K. N. Christodoulou, K. R. Gee and I. G. Kevrekidis, *Dynamic deformation visualization in swelling of polymer gels*. Chem. Eng. Sci., **2000**. 55(17): p. 3335-3340.
348. N. A. Peppas, R. M. Ottenbrite, K. Park and T. Okano, *Biomedical applications of hydrogels handbook*. **2010**: Springer Science & Business Media.
349. D. Lickorish, J. A. M. Ramshaw, J. A. Werkmeister, V. Glattauer and C. R. Howlett, *Collagen–hydroxyapatite composite prepared by biomimetic process*. J. Biomed. Mater. Res., Part A, **2004**. 68(1): p. 19-27.

350. T. Taguchi, A. Kishida and M. Akashi, *Hydroxyapatite Formation on/in Poly (vinyl alcohol) Hydrogel Matrices Using a Novel Alternate Soaking Process*. Chem. Lett., **1998**. (8): p. 711-712.
351. C. Zhong and C. C. Chu, *Biomimetic mineralization of acid polysaccharide-based hydrogels: towards porous 3-dimensional bone-like biocomposites*. J. Mater. Chem., **2012**. 22(13): p. 6080-6087.
352. E. E. Wilson, A. Awonusi, M. D. Morris, D. H. Kohn, M. M. J. Tecklenburg and L. W. Beck, *Three structural roles for water in bone observed by solid-state NMR*. Biophys. J., **2006**. 90(10): p. 3722-3731.
353. M. Nordin and V. H. Frankel, *Basic biomechanics of the musculoskeletal system*. **2001**: Lippincott Williams & Wilkins.
354. C. Durucan and P. W. Brown, *α-Tricalcium phosphate hydrolysis to hydroxyapatite at and near physiological temperature*. J. Mater. Sci.: Mater. Med., **2000**. 11(6): p. 365-371.
355. E. Fernandez, M. P. Ginebra, M. G. Boltong, F. C. M. Driessens, J. A. Planell, J. Ginebra, E. A. P. De Maeyer and R. M. H. Verbeeck, *Kinetic study of the setting reaction of a calcium phosphate bone cement*. J. Biomed. Mater. Res., **1996**. 32(3): p. 367-374.
356. M. P. Ginebra, E. Fernández, M. G. Boltong, O. Bermúdez, J. A. Planell and F. C. M. Driessens, *Compliance of an apatitic calcium phosphate cement with the short-term clinical requirements in bone surgery, orthopaedics and dentistry*. Clin. Mater., **1994**. 17(2): p. 99-104.
357. E. B. W. Giesen, M. Ding, M. Dalstra and T. M. G. J. Van Eijden, *Mechanical properties of cancellous bone in the human mandibular condyle are anisotropic*. J. Biomech., **2001**. 34(6): p. 799-803.
358. C. Du, F. Z. Cui, W. Zhang, Q. L. Feng, X. D. Zhu and K. De Groot, *Formation of calcium phosphate/collagen composites through mineralization of collagen matrix*. J. Biomed. Mater. Res., **2000**. 50(4): p. 518-527.
359. A. T. Neffe, A. Loebus, A. Zaupa, C. Stoetzel, F. A. Müller and A. Lendlein, *Gelatin functionalization with tyrosine derived moieties to increase the interaction with hydroxyapatite fillers*. Acta Biomater., **2011**. 7(4): p. 1693-1701.
360. S. C. Chao, M.-J. Wang, N.-S. Pai and S.-K. Yen, *Preparation and characterization of gelatin–hydroxyapatite composite microspheres for hard tissue repair*. Mater. Sci. Eng., C, **2015**. 57: p. 113-122.
361. J. Li, H. Sun, D. Sun, Y. Yao, F. Yao and K. Yao, *Biomimetic multicomponent polysaccharide/nano-hydroxyapatite composites for bone tissue engineering*. Carbohydr. Polym., **2011**. 85(4): p. 885-894.
362. T. Ichibouji, T. Miyazaki, E. Ishida, A. Sugino and C. Ohtsuki, *Apatite mineralization abilities and mechanical properties of covalently cross-linked pectin hydrogels*. Mater. Sci. Eng., C, **2009**. 29(6): p. 1765-1769.
363. S. A. Hutchens, R. S. Benson, B. R. Evans, H. M. O'Neill and C. J. Rawn, *Biomimetic synthesis of calcium-deficient hydroxyapatite in a natural hydrogel*. Biomaterials, **2006**. 27(26): p. 4661-4670.
364. T. Ogiwara, A. Katsumura, K. Sugimura, Y. Teramoto and Y. Nishio, *Calcium Phosphate Mineralization in Cellulose Derivative/Poly (acrylic acid) Composites Having a Chiral Nematic Mesomorphic Structure*. Biomacromolecules, **2015**. 16(12): p. 3959-3969.
365. C. C. Ribeiro, C. C. Barrias and M. A. Barbosa, *Calcium phosphate-alginate microspheres as enzyme delivery matrices*. Biomaterials, **2004**. 25(18): p. 4363-4373.
366. Z. Li, Y. Su, B. Xie, H. Wang, T. Wen, C. He, H. Shen, D. Wu and D. Wang, *A tough hydrogel–hydroxyapatite bone-like composite fabricated in situ by the electrophoresis approach*. J. Mater. Chem. B, **2013**. 1(12): p. 1755-1764.
367. H. Kobayashi, M. Kato, T. Taguchi, T. Ikoma, H. Miyashita, S. Shimmura, K. Tsubota and J. Tanaka, *Collagen immobilized PVA hydrogel-hydroxyapatite composites*

prepared by kneading methods as a material for peripheral cuff of artificial cornea. Mater. Sci. Eng., C, **2004**. 24(6): p. 729-735.
368. A. Shkilnyy, R. Gräf, B. Hiebl, A. T. Neffe, A. Friedrich, J. Hartmann and A. Taubert, *Unprecedented, low cytotoxicity of spongelike calcium phosphate/poly (ethylene imine) hydrogel composites*. Macromol. Biosci., **2009**. 9(2): p. 179-186.
369. A. Nilson, *Design of concrete structures*. **1997**.
370. M. R. Sherman, D. B. McDonald and D. W. Pfeifer, *Durability aspects of precast prestressed concrete Part 2: Chloride permeability study*. PCI J., **1996**. 41(4): p. 76-95.
371. C. L. Camiré, P. Nevsten, L. Lidgren and I. McCarthy, *The effect of crystallinity on strength development of α-TCP bone substitutes*. J. Biomed. Mater. Res., Part B, **2006**. 79(1): p. 159-165.
372. I. S. Neira, Y. V. Kolen'ko, K. P. Kommareddy, I. Manjubala, M. Yoshimura and F. Guitián, *Reinforcing of a calcium phosphate cement with hydroxyapatite crystals of various morphologies*. ACS Appl. Mater. Interfaces, **2010**. 2(11): p. 3276-3284.
373. A. Ewald, S. K. Glückermann, R. Thull and U. Gbureck, *Antimicrobial titanium/silver PVD coatings on titanium*. Biomed. Eng. Online, **2006**. 5(1): p. 22.
374. F. Tamimi-Marino, J. Mastio, C. Rueda, L. Blanco and E. López-Cabarcos, *Increase of the final setting time of brushite cements by using chondroitin 4-sulfate and silica gel*. J. Mater. Sci.: Mater. Med., **2007**. 18(6): p. 1195-1201.
375. T. Gerber, G. Holzhüter, W. Götz, V. Bienengräber, K.-O. Henkel and E. Rumpel, *Nanostructuring of biomaterials—a pathway to bone grafting substitute*. Eur. J.Trauma, **2006**. 32(2): p. 132-140.
376. M. P. Hofmann, S. N. Nazhat, U. Gbureck and J. E. Barralet, *Real-time monitoring of the setting reaction of brushite-forming cement using isothermal differential scanning calorimetry*. J. Biomed. Mater. Res., Part B, **2006**. 79B(2): p. 360-364.
377. C. J. Brinker and G. W. Scherer, *Sol-gel science: the physics and chemistry of sol-gel processing*. **2013**: Academic press.
378. D. W. Schaefer, *Polymers, fractals, and ceramic materials*. Science, **1989**. 243(4894): p. 1023-1027.
379. D. Zhao, J. Feng, Q. Huo, N. Melosh, G. H. Fredrickson, B. F. Chmelka and G. D. Stucky, *Triblock copolymer syntheses of mesoporous silica with periodic 50 to 300 angstrom pores*. Science, **1998**. 279(5350): p. 548-552.
380. U. Gbureck, E. Vorndran and J. E. Barralet, *Modeling vancomycin release kinetics from microporous calcium phosphate ceramics comparing static and dynamic immersion conditions*. Acta Biomater., **2008**. 4(5): p. 1480-1486.
381. S. Radin, P. Ducheyne, T. Kamplain and B. Tan, *Silica sol-gel for the controlled release of antibiotics. I. Synthesis, characterization, and in vitro release*. J. Biomed. Mater. Res., **2001**. 57(2): p. 313-320.
382. K. Urabe, K. Naruse, H. Hattori, M. Hirano, K. Uchida, K. Onuma, H. J. Park and M. Itoman, *In vitro comparison of elution characteristics of vancomycin from calcium phosphate cement and polymethylmethacrylate*. J. Orthop. Sci., **2009**. 14(6): p. 784-793.
383. U. Gbureck, E. Vorndran, F. A. Müller and J. E. Barralet, *Low temperature direct 3D printed bioceramics and biocomposites as drug release matrices*. J. Controlled Release, **2007**. 122(2): p. 173-180.
384. A. Ewald, K. Helmschrott, G. Knebl, N. Mehrban, L. M. Grover and U. Gbureck, *Effect of cold-setting calcium-and magnesium phosphate matrices on protein expression in osteoblastic cells*. J. Biomed. Mater. Res., Part B, **2011**. 96(2): p. 326-332.
385. T. Yuasa, Y. Miyamoto, K. Ishikawa, M. Takechi, Y. Momota, S. Tatehara and M. Nagayama, *Effects of apatite cements on proliferation and differentiation of human osteoblasts in vitro*. Biomaterials, **2004**. 25(7): p. 1159-1166.
386. M. S. Laranjeira, M. H. Fernandes and F. J. Monteiro, *Innovative macroporous granules of nanostructured-hydroxyapatite agglomerates: Bioactivity and osteoblast-like cell behaviour*. J. Biomed. Mater. Res., Part A, **2010**. 95(3): p. 891-900.

387. M. Hott, C. de Pollak, D. Modrowski and P. J. Marie, *Short-term effects of organic silicon on trabecular bone in mature ovariectomized rats*. Calcif. Tissue Int., **1993**. 53(3): p. 174-179.
388. E. M. Carlisle, *Silicon: a possible factor in bone calcification*. Science, **1970**. 167(3916): p. 279-280.
389. E. M. Carlisle, *Silicon: an essential element for the chick*. Science, **1972**. 178(4061): p. 619-621.
390. A. M. Pietak, J. W. Reid, M. J. Stott and M. Sayer, *Silicon substitution in the calcium phosphate bioceramics*. Biomaterials, **2007**. 28(28): p. 4023-4032.
391. M. Vallet-Regí and D. Arcos, *Silicon substituted hydroxyapatites. A method to upgrade calcium phosphate based implants*. J. Mater. Chem., **2005**. 15(15): p. 1509-1516.
392. M. Bohner, *Silicon-substituted calcium phosphates–a critical view*. Biomaterials, **2009**. 30(32): p. 6403-6406.
393. U. Klammert, E. Vorndran, T. Reuther, F. A. Müller, K. Zorn and U. Gbureck, *Low temperature fabrication of magnesium phosphate cement scaffolds by 3D powder printing*. J. Mater. Sci.: Mater. Med., **2010**. 21(11): p. 2947-2953.
394. S. Wallach, *Effects of magnesium on skeletal metabolism*. Magnesium Trace Elem., **1989**. 9(1): p. 1-14.
395. U. Klammert, T. Reuther, M. Blank, I. Reske, J. E. Barralet, L. M. Grover, A. C. Kübler and U. Gbureck, *Phase composition, mechanical performance and in vitro biocompatibility of hydraulic setting calcium magnesium phosphate cement*. Acta Biomater., **2010**. 6(4): p. 1529-1535.
396. F. Tamimi, D. Le Nihouannen, H. Eimar, Z. Sheikh, S. Komarova and J. E. Barralet, *The effect of autoclaving on the physical and biological properties of dicalcium phosphate dihydrate bioceramics: brushite vs. monetite*. Acta Biomater., **2012**. 8(8): p. 3161-3169.
397. S. Hesaraki and N. Nezafati, *In vitro biocompatibility of chitosan/hyaluronic acid-containing calcium phosphate bone cements*. Bioprocess Biosyst. Eng., **2014**. 37(8): p. 1507-1516.
398. S. Ahmadzadeh-Asl, S. Hesaraki and A. Zamanian, *Preparation and characterisation of calcium phosphate–hyaluronic acid nanocomposite bone cement*. Adv. Appl. Ceram., **2011**. 110(6): p. 340-345.
399. L. Sun, H. H. K. Xu, S. Takagi and L. C. Chow, *Fast setting calcium phosphate cement-chitosan composite: mechanical properties and dissolution rates*. J. Biomater. Appl., **2007**. 21(3): p. 299-315.
400. S. Takagi, L. C. Chow, S. Hirayama and F. C. Eichmiller, *Properties of elastomeric calcium phosphate cement–chitosan composites*. Dent. Mater., **2003**. 19(8): p. 797-804.
401. D. Meng, L. Dong, Y. Wen and Q. Xie, *Effects of adding resorbable chitosan microspheres to calcium phosphate cements for bone regeneration*. Mater. Sci. Eng., C, **2015**. 47: p. 266-272.
402. W.-C. Chen, C.-P. Ju, J.-C. Wang, C.-C. Hung and J.-H. C. Lin, *Brittle and ductile adjustable cement derived from calcium phosphate cement/polyacrylic acid composites*. Dent. Mater., **2008**. 24(12): p. 1616-1622.
403. J. Zhong, M. Ma, W. Li, J. Zhou, Z. Yan and D. He, *Self-assembly of regenerated silk fibroin from random coil nanostructures to antiparallel β-sheet nanostructures*. Biopolymers, **2014**. 101(12): p. 1181-1192.
404. U.-J. Kim, J. Park, C. Li, H.-J. Jin, R. Valluzzi and D. L. Kaplan, *Structure and properties of silk hydrogels*. Biomacromolecules, **2004**. 5(3): p. 786-792.
405. Z. H. Ayub, M. Arai and K. Hirabayashi, *Mechanism of the gelation of fibroin solution*. Biosci., Biotechnol., Biochem., **1993**. 57(11): p. 1910-1912.
406. T. Yucel, P. Cebe and D. L. Kaplan, *Vortex-induced injectable silk fibroin hydrogels*. Biophys. J., **2009**. 97(7): p. 2044-2050.

407. X. Wang, J. A. Kluge, G. G. Leisk and D. L. Kaplan, *Sonication-induced gelation of silk fibroin for cell encapsulation*. Biomaterials, **2008**. 29(8): p. 1054-1064.
408. X. Hu, D. Kaplan and P. Cebe, *Determining beta-sheet crystallinity in fibrous proteins by thermal analysis and infrared spectroscopy*. Macromolecules, **2006**. 39(18): p. 6161-6170.
409. A. Matsumoto, J. Chen, A. L. Collette, U.-J. Kim, G. H. Altman, P. Cebe and D. L. Kaplan, *Mechanisms of silk fibroin sol-gel transitions*. J. Phys. Chem. B, **2006**. 110(43): p. 21630-21638.
410. C. Jiang, X. Wang, R. Gunawidjaja, Y. H. Lin, M. K. Gupta, D. L. Kaplan, R. R. Naik and V. V. Tsukruk, *Mechanical properties of robust ultrathin silk fibroin films*. Adv. Funct. Mater., **2007**. 17(13): p. 2229-2237.
411. C. Vepari and D. L. Kaplan, *Silk as a biomaterial*. Prog. Polym. Sci., **2007**. 32(8): p. 991-1007.
412. X. D. Kong, F. Z. Cui, X. M. Wang, M. Zhang and W. Zhang, *Silk fibroin regulated mineralization of hydroxyapatite nanocrystals*. J. Cryst. Growth, **2004**. 270(1): p. 197-202.
413. S. Bhumiratana, W. L. Grayson, A. Castaneda, D. N. Rockwood, E. S. Gil, D. L. Kaplan and G. Vunjak-Novakovic, *Nucleation and growth of mineralized bone matrix on silk-hydroxyapatite composite scaffolds*. Biomaterials, **2011**. 32(11): p. 2812-2820.
414. J. M. Gosline, P. A. Guerette, C. S. Ortlepp and K. N. Savage, *The mechanical design of spider silks: from fibroin sequence to mechanical function*. J. Exp. Biol., **1999**. 202(23): p. 3295-3303.
415. D. N. Rockwood, R. C. Preda, T. Yücel, X. Wang, M. L. Lovett and D. L. Kaplan, *Materials fabrication from Bombyx mori silk fibroin*. Nat. Protoc., **2011**. 6(10): p. 1612-1631.
416. H. J. Kim, U.-J. Kim, H. S. Kim, C. Li, M. Wada, G. G. Leisk and D. L. Kaplan, *Bone tissue engineering with premineralized silk scaffolds*. Bone, **2008**. 42(6): p. 1226-1234.
417. K. Wei, Y. Li, K. O. Kim, Y. Nakagawa, B. S. Kim, K. Abe, G. Q. Chen and I. S. Kim, *Fabrication of nano-hydroxyapatite on electrospun silk fibroin nanofiber and their effects in osteoblastic behavior*. J. Biomed. Mater. Res., Part A, **2011**. 97(3): p. 272-280.
418. H. Kweon, K.-G. I. Lee, C.-H. Chae, C. Balázsi, S.-K. Min, J.-Y. Kim, J.-Y. Choi and S.-G. Kim, *Development of nano-hydroxyapatite graft with silk fibroin scaffold as a new bone substitute*. J. Oral Maxillofac. Surg., **2011**. 69(6): p. 1578-1586.
419. Y. Zhang, C. Wu, T. Friis and Y. Xiao, *The osteogenic properties of CaP/silk composite scaffolds*. Biomaterials, **2010**. 31(10): p. 2848-2856.
420. S. Pina, J. M. Oliveira and R. L. Reis, *Natural-Based Nanocomposites for Bone Tissue Engineering and Regenerative Medicine: A Review*. Adv. Mater., **2015**. 27(7): p. 1143-1169.
421. L. P. Yan, J. M. Oliveira, A. L. Oliveira and R. L. Reis, *In vitro evaluation of the biological performance of macro/micro-porous silk fibroin and silk-nano calcium phosphate scaffolds*. J. Biomed. Mater. Res., Part B, **2015**. 103(4): p. 888-898.
422. L. Meinel, R. Fajardo, S. Hofmann, R. Langer, J. Chen, B. Snyder, G. Vunjak-Novakovic and D. Kaplan, *Silk implants for the healing of critical size bone defects*. Bone, **2005**. 37(5): p. 688-698.
423. C. Du, J. Jin, Y. Li, X. Kong, K. Wei and J. Yao, *Novel silk fibroin/hydroxyapatite composite films: structure and properties*. Mater. Sci. Eng., C, **2009**. 29(1): p. 62-68.
424. A. M. Collins, N. J. V. Skaer, T. Gheysens, D. Knight, C. Bertram, H. I. Roach, R. O. C. Oreffo, S. Von-Aulock, T. Baris and J. Skinner, *Bone-like Resorbable Silk-based Scaffolds for Load-bearing Osteoregenerative Applications*. Adv. Mater., **2009**. 21(1): p. 75-78.
425. J. Wang, F. Yu, L. Qu, X. Meng and G. Wen, *Study of synthesis of nano-hydroxyapatite using a silk fibroin template*. Biomed. Mater., **2010**. 5(4): p. 041002.

426. X. Kong, X. Sun, F. Cui and C. Ma, *Effect of solute concentration on fibroin regulated biomineralization of calcium phosphate*. Mater. Sci. Eng., C, **2006**. 26(4): p. 639-643.
427. X.-D. Sun, Y.-L. Zhou, J.-Y. Ren and F.-Z. Cui, *Effect of pH on the fibroin regulated mineralization of calcium phosphate*. Curr. Appl. Phy., **2007**. 7: p. e75-e79.
428. Y. Ren, X.-D. Sun, F. Z. Cui and X. Kong, *Effects of pH and initial Ca2+− H2PO4− concentration on fibroin mineralization*. Front. Mater. Sci. China, **2007**. 1(3): p. 258-262.
429. Z. Xia, L. M. Grover, Y. Huang, I. E. Adamopoulos, U. Gbureck, J. T. Triffitt, R. M. Shelton and J. E. Barralet, *In vitro biodegradation of three brushite calcium phosphate cements by a macrophage cell-line*. Biomaterials, **2006**. 27(26): p. 4557-4565.
430. C. Cao, H. Li, J. Li, C. Liu, H. Yang and B. Li, *Mechanical reinforcement of injectable calcium phosphate cement/silk fibroin (SF) composite by mineralized SF*. Ceram. Int., **2014**. 40(9): p. 13987-13993.
431. R. Xie, Q. Deng and H. Zhan, *Preparation of calcium phosphate cement/silk fibroin composite materials*. J. Text. Res., **2009**. 10: p. 002.
432. E. Bini, D. P. Knight and D. L. Kaplan, *Mapping domain structures in silks from insects and spiders related to protein assembly*. J. Mol. Biol., **2004**. 335(1): p. 27-40.
433. T. Asakura, K. Umemura, Y. Nakazawa, H. Hirose, J. Higham and D. Knight, *Some observations on the structure and function of the spinning apparatus in the silkworm Bombyx mori*. Biomacromolecules, **2007**. 8(1): p. 175-181.
434. L. Wang and C. Li, *Preparation and physicochemical properties of a novel hydroxyapatite/chitosan–silk fibroin composite*. Carbohydr. Polym., **2007**. 68(4): p. 740-745.
435. J. Pérez-Rigueiro, C. Viney, J. Llorca and M. Elices, *Mechanical properties of single-brin silkworm silk*. J. Appl. Polym. Sci., **2000**. 75(10): p. 1270-1277.
436. Y. Hirai, J. Ishikuro and T. Nakajima, *Some comments on the penetration of water vapor into regenerated silk fibroin*. Polymer, **2001**. 42(12): p. 5495-5499.
437. J. Aberg, H. Brisby, H. B. Henriksson, A. Lindahl, P. Thomsen and H. Engqvist, *Premixed acidic calcium phosphate cement: characterization of strength and microstructure*. J. Biomed. Mater. Res., Part B, **2010**. 93(2): p. 436-441.
438. M. H. Alkhraisat, C. Moseke, L. Blanco, J. E. Barralet, E. Lopez-Carbacos and U. Gbureck, *Strontium modified biocements with zero order release kinetics*. Biomaterials, **2008**. 29(35): p. 4691-4697.
439. H. J. Jin, J. Park, V. Karageorgiou, U. J. Kim, R. Valluzzi, P. Cebe and D. L. Kaplan, *Water-Stable Silk Films with Reduced β-Sheet Content*. Adv. Funct. Mater., **2005**. 15(8): p. 1241-1247.
440. B. B. Mandal, S. Kapoor and S. C. Kundu, *Silk fibroin/polyacrylamide semi-interpenetrating network hydrogels for controlled drug release*. Biomaterials, **2009**. 30(14): p. 2826-2836.
441. G. Chen, C. Liu, B. Zhang, G. Xu and Y. Huang, *Swelling behaviours of silk fibroin-polyurethane composite hydrogels*. Asian J. Chem., **2014**. 26(5): p. 1533-1536.
442. J.-H. Yeo, K.-G. Lee, Y.-W. Lee and S. Y. Kim, *Simple preparation and characteristics of silk fibroin microsphere*. Eur. Polym. J., **2003**. 39(6): p. 1195-1199.
443. I. C. Um, H. Y. Kweon, Y. H. Park and S. Hudson, *Structural characteristics and properties of the regenerated silk fibroin prepared from formic acid*. Int. J. Biol. Macromol., **2001**. 29(2): p. 91-97.
444. H. Zhu, B. Wu, X. Feng and J. Chen, *Preparation and characterization of bioactive mesoporous calcium silicate–silk fibroin composite films*. J. Biomed. Mater. Res., Part B, **2011**. 98(2): p. 330-341.
445. J.-Y. Kim, J.-Y. Choi, J.-H. Jeong, E.-S. Jang, A.-S. Kim, S.-G. Kim, H. Y. Kweon, Y.-Y. Jo and J.-H. Yeo, *Low molecular weight silk fibroin increases alkaline phosphatase and type I collagen expression in MG63 cells*. BMB Rep., **2010**. 43(1): p. 52-56.

446. Z. Shi, X. Huang, Y. Cai, R. Tang and D. Yang, *Size effect of hydroxyapatite nanoparticles on proliferation and apoptosis of osteoblast-like cells*. Acta Biomater., **2009**. 5(1): p. 338-345.
447. N. Zhang, J. A. Molenda, J. H. Fournelle, W. L. Murphy and N. Sahai, *Effects of pseudowollastonite (CaSiO 3) bioceramic on in vitro activity of human mesenchymal stem cells*. Biomaterials, **2010**. 31(30): p. 7653-7665.
448. Q. Lu, B. Zhang, M. Li, B. Zuo, D. L. Kaplan, Y. Huang and H. Zhu, *Degradation mechanism and control of silk fibroin*. Biomacromolecules, **2011**. 12(4): p. 1080-1086.
449. R. L. Horan, K. Antle, A. L. Collette, Y. Wang, J. Huang, J. E. Moreau, V. Volloch, D. L. Kaplan and G. H. Altman, *In vitro degradation of silk fibroin*. Biomaterials, **2005**. 26(17): p. 3385-3393.
450. U.-J. Kim, J. Park, H. J. Kim, M. Wada and D. L. Kaplan, *Three-dimensional aqueous-derived biomaterial scaffolds from silk fibroin*. Biomaterials, **2005**. 26(15): p. 2775-2785.
451. T. Arai, G. Freddi, R. Innocenti and M. Tsukada, *Biodegradation of Bombyx mori silk fibroin fibers and films*. J. Appl. Polym. Sci., **2004**. 91(4): p. 2383-2390.
452. K. Hurle, T. Christel, U. Gbureck, C. Moseke, J. Neubauer and F. Goetz-Neunhoeffer, *Reaction kinetics of dual setting alpha-tricalcium phosphate cements*. J. Mater. Sci.: Mater. Med., **2016**. 27(1): p. 1.
453. G. H. Altman, F. Diaz, C. Jakuba, T. Calabro, R. L. Horan, J. Chen, H. Lu, J. Richmond and D. L. Kaplan, *Silk-based biomaterials*. Biomaterials, **2003**. 24(3): p. 401-416.
454. L. L. Hench and J. K. West, *The sol-gel process*. Chem. Rev., **1990**. 90(1): p. 33-72.
455. S. Gopi, *Basic Civil Engineering*. **2010**: Pearson Education.
456. J. P. Donegan, *Roller compacted concrete*. ICE Man. Highw. Des. Manage., **2011**. 48: p. 481-485.
457. H. Okamura and M. Ouchi, *Self-compacting concrete*. J. Adv. Concr. Technol., **2003**. 1(1): p. 5-15.
458. D. A. Wicks and Z. W. Wicks Jr, *Blocked isocyanates III: Part A. Mechanisms and chemistry*. Prog. Org. Coat., **1999**. 36(3): p. 148-172.
459. D. A. Wicks and Z. W. Wicks Jr, *Blocked isocyanates III: Part B: Uses and applications of blocked isocyanates*. Prog. Org. Coat., **2001**. 41(1–3): p. 1-83.
460. S. Petersen, *Niedermolekulare Umsetzungsprodukte aliphatischer Diisocyanate 5. Mitteilung über Polyurethane)*. Justus Liebigs Ann. Chem., **1949**. 562(3): p. 205-228.
461. G. B. Guise, M. B. Jackson and J. A. Maclaren, *The reaction of isocyanates with bisulphite salts*. Aust. J. Chem., **1972**. 25(12): p. 2583-2595.
462. K.-D. Vorlop, J. Beyersdorf and A. Muscat, *Gekappte Polyurethan-Präpolymere geringer Toxizität für den Einschluß lebender Zellen*. Chem. Ing. Tech., **1993**. 65(5): p. 554-556.
463. S. Larsson and T. W. Bauer, *Use of injectable calcium phosphate cement for fracture fixation: a review*. Clin. Orthop. Relat. Res., **2002**. 395: p. 23-32.
464. G. S. Hutchinson, D. J. Griffon, A. M. Siegel, G. J. Pijanowski, P. Kurath, J. A. C. Eurell and A. L. Johnson, *Evaluation of an osteoconductive resorbable calcium phosphate cement and polymethylmethacrylate for augmentation of orthopedic screws in the pelvis of canine cadavers*. Am. J. Vet. Res., **2005**. 66(11): p. 1954-1960.
465. S. Heinemann, S. Rössler, M. Lemm, M. Ruhnow and B. Nies, *Properties of injectable ready-to-use calcium phosphate cement based on water-immiscible liquid*. Acta Biomater., **2013**. 9(4): p. 6199-6207.
466. H. H. K. Xu, L. E. Carey, C. G. Simon Jr, S. Takagi and L. C. Chow, *Premixed calcium phosphate cements: Synthesis, physical properties, and cell cytotoxicity*. Dent. Mater., **2007**. 23(4): p. 433-441.
467. B. Han, P.-W. Ma, L.-L. Zhang, Y.-J. Yin, K.-D. Yao, F.-J. Zhang, Y.-D. Zhang, X.-L. Li and W. Nie, *β-TCP/MCPM-based premixed calcium phosphate cements*. Acta Biomater., **2009**. 5(8): p. 3165-3177.

468. L. E. Carey, H. H. Xu, C. G. Simon, Jr., S. Takagi and L. C. Chow, *Premixed rapid-setting calcium phosphate composites for bone repair*. Biomaterials, **2005**. 26(24): p. 5002-14.
469. S. Takagi, L. C. Chow, S. Hirayama and A. Sugawara, *Premixed calcium–phosphate cement pastes*. J. Biomed. Mater. Res., Part B, **2003**. 67(2): p. 689-696.
470. A. Pfister, R. Landers, A. Laib, U. Hübner, R. Schmelzeisen and R. Mülhaupt, *Biofunctional rapid prototyping for tissue-engineering applications: 3D bioplotting versus 3D printing*. J. Polym. Sci., Part A: Polym. Chem., **2004**. 42(3): p. 624-638.
471. D. W. Hutmacher, M. Sittinger and M. V. Risbud, *Scaffold-based tissue engineering: rationale for computer-aided design and solid free-form fabrication systems*. Trends Biotechnol., **2004**. 22(7): p. 354-362.
472. A. R. Akkineni, Y. Luo, M. Schumacher, B. Nies, A. Lode and M. Gelinsky, *3D plotting of growth factor loaded calcium phosphate cement scaffolds*. Acta Biomater, **2015**. 27: p. 264-74.
473. V. Liu Tsang and S. N. Bhatia, *Three-dimensional tissue fabrication*. Adv. Drug Delivery Rev., **2004**. 56(11): p. 1635-1647.
474. R. Landers and R. Mülhaupt, *Desktop manufacturing of complex objects, prototypes and biomedical scaffolds by means of computer-assisted design combined with computer-guided 3D plotting of polymers and reactive oligomers*. Macromol. Mater. Eng., **2000**. 282(1): p. 17-21.
475. A. Lode, K. Meissner, Y. Luo, F. Sonntag, S. Glorius, B. Nies, C. Vater, F. Despang, T. Hanke and M. Gelinsky, *Fabrication of porous scaffolds by three-dimensional plotting of a pasty calcium phosphate bone cement under mild conditions*. J. Tissue. Eng. Regen. Med., **2014**. 8(9): p. 682-93.
476. R. Detsch, I. Dieser, U. Deisinger, F. Uhl, S. Hamisch, G. Ziegler and G. Lipps, *Biofunctionalization of dispense-plotted hydroxyapatite scaffolds with peptides: Quantification and cellular response*. J. Biomed. Mater. Res., Part A, **2010**. 92(2): p. 493-503.
477. S. Das, F. Pati, Y.-J. Choi, G. Rijal, J.-H. Shim, S. W. Kim, A. R. Ray, D.-W. Cho and S. Ghosh, *Bioprintable, cell-laden silk fibroin–gelatin hydrogel supporting multilineage differentiation of stem cells for fabrication of three-dimensional tissue constructs*. Acta Biomater., **2015**. 11: p. 233-246.
478. R. Miano, S. Germani and G. Vespasiani, *Stones and urinary tract infections*. Urol. Int., **2007**. 79(Suppl. 1): p. 32-36.
479. L. S. Burstein, A. L. Boskey, P. J. Tannenbaum, A. S. Posner and I. D. Mandel, *The crystal chemistry of submandibular and parotid salivary gland stones*. J. Oral Pathol. Med., **1979**. 8(5): p. 284-291.
480. G. D. Markham, J. P. Glusker and C. W. Bock, *The arrangement of first-and second-sphere water molecules in divalent magnesium complexes: Results from molecular orbital and density functional theory and from structural crystallography*. J. Phys. Chem. B, **2002**. 106(19): p. 5118-5134.
481. G. Mestres and M.-P. Ginebra, *Novel magnesium phosphate cements with high early strength and antibacterial properties*. Acta Biomater., **2011**. 7(4): p. 1853-1861.
482. M. S. Rahaman, D. S. Mavinic, M. I. H. Bhuiyan and F. A. Koch, *Exploring the determination of struvite solubility product from analytical results*. Environ. Technol., **2006**. 27(9): p. 951-961.
483. J. Lee, M. M. Farag, E. K. Park, J. Lim and H.-S. Yun, *A simultaneous process of 3D magnesium phosphate scaffold fabrication and bioactive substance loading for hard tissue regeneration*. Mater. Sci. Eng., C, **2014**. 36: p. 252-260.
484. J. G. Hardy, L. M. Römer and T. R. Scheibel, *Polymeric materials based on silk proteins*. Polymer, **2008**. 49(20): p. 4309-4327.
485. Y. Zhang and P. S. Cremer, *Interactions between macromolecules and ions: the Hofmeister series*. Curr. Opin. Chem. Biol., **2006**. 10(6): p. 658-663.

486. L. E. Holt, J. A. Pierce and C. N. Kajdi, *The solubility of the phosphates of strontium, barium, and magnesium and their relation to the problem of calcification*. J. Colloid Sci., **1954**. 9(5): p. 409-426.
487. D. Sutor, *The crystal and molecular structure of newberyite, MgHPO4.3H2O*. Acta Crystallogr., **1967**. 23(3): p. 418-422.
488. C. Grossardt, A. Ewald, L. M. Grover, J. E. Barralet and U. Gbureck, *Passive and active in vitro resorption of calcium and magnesium phosphate cements by osteoclastic cells*. Tissue engineering. Part A, **2010**. 16(12): p. 3687-95.
489. F. Wu, J. Wei, H. Guo, F. Chen, H. Hong and C. Liu, *Self-setting bioactive calcium–magnesium phosphate cement with high strength and degradability for bone regeneration*. Acta Biomater., **2008**. 4(6): p. 1873-1884.
490. E. Vorndran, A. Ewald, F. A. Muller, K. Zorn, A. Kufner and U. Gbureck, *Formation and properties of magnesium-ammonium-phosphate hexahydrate biocements in the Ca-Mg-PO4 system*. J. Mater. Sci.: Mater. Med., **2011**. 22(3): p. 429-36.
491. U. Soltmann, B. Nies and H. Böttcher, *Cements with embedded living microorganisms–a new class of biocatalytic composite materials for application in bioremediation, biotechnology*. Adv. Eng. Mater., **2011**. 13(1-2): p. B25-B31.

Danksagung

An dieser Stelle möchte ich mich bei allen Personen und Instituten bedanken, die durch ihre Unterstützung zum Gelingen der vorliegenden Dissertation beigetragen haben.

Herrn Prof. Dr. Jürgen Groll danke ich für die Möglichkeit, meine Dissertation am Lehrstuhl für Funktionswerkstoffe der Medizin und Zahnheilkunde durchzuführen.

Herrn Prof. Dr. Matthias Lehmann danke ich für die Begutachtung meiner Dissertation.

Ein besonderer Dank gilt meinem Doktorvater Herrn Prof. Dr. Uwe Gbureck für die hervorragende Betreuung während meiner Promotion. Vielen Dank für die vielen fachlichen Gespräche und Diskussionen, die ständige Motivation und den Freiraum, meine eigenen Ideen in die Thematiken mit einbringen und verfolgen zu können.

Dem Lehrstuhl für Pharmazeutische Technologie und Biopharmazie an der Universität Würzburg unter der Leitung von Herrn. Prof. Dr. Dr. Lorenz Meinel und im Speziellen Eva Heusler danke ich für die Möglichkeit, die Porositätsmessungen durchführen zu können.

Der Bayrischen Forschungsallianz, Frau Dr. Elke Vorndran und Herrn Prof. Dr. Jake Barralet danke ich, dass sie mir den Forschungsaufenthalt in Montreal, Kanada, an der McGill Universität ermöglichten.

Herrn Dr. Claus Moseke danke ich für die Anfertigung der REM-Aufnahmen und der damit einhergehenden Möglichkeit, neue Erkenntnisse über die entwickelten Materialien zu erlangen.

Frau Dr. Andrea Ewald und Simone Werner danke ich für die Unterstützung bei der biologischen Testung der Materialien.

Herrn Harald Hümpfer und Herrn Anton Hofmann danke ich für die immer hilfsbereite und kompetente Unterstützung bei Reparaturen, werkstattlichen Arbeiten und Computerproblemen.

Danke an alle FMZ-Mitarbeiter für das nette und angenehme Arbeitsklima, für die Hilfe und Unterstützung in allen Fragen und dass aus Kollegen wahre Freunde geworden sind.

Der Deutschen Forschungsgemeinschaft danke ich für die Finanzierung der Forschungsprojekte, was es mir ermöglichte meiner Promotion zu realisieren.

Abschließend möchte ich meinen ganz besonderen Dank an die mir liebsten Menschen richten. Vielen Dank an meine Eltern Uta und Michael Geffers, an meine Brüder Willi und Carl Geffers und an meinen Mann Johannes Schamel. Sie waren stets ein willkommener Zufluchtsort vor dem Arbeitsalltag. Ich konnte jedoch auch immer Thematiken meiner Dissertation mit ihnen diskutieren, wodurch sie mir oft einen neuen Blickpunkt auf die Dinge gaben. Vielen lieben Dank für eure Unterstützung in allen Lebenslagen!